Membrane-based technologies for the production of high-quality water from contaminated sources: from lab experiments to full-scale system design

Doctoral Dissertation
Doctoral Program in Environmental Engineering (32.nd cycle)

Membrane-based technologies for the production of high-quality water from contaminated sources: from lab experiments to full-scale system design

Mattia Giagnorio
* * * * * *

Supervisor
Prof. Alberto Tiraferri, Supervisor

Doctoral Examination Committee:
Prof. Hélix-Nielsen Claus, Referee, Technical University of Denrmark
Prof. Judy Lee, Referee, University of Surrey

Politecnico di Torino
February 13, 2020

I hereby declare that, the contents and organisation of this dissertation constitute my own original work and does not compromise in any way the rights of third parties, including those relating to the security of personal data.

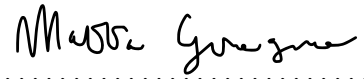

Mattia Giagnorio
Turin, February 13, 2020

Summary

The increasing demand of freshwater worldwide draws research efforts toward the implementation of innovative system processes able to extract high-quality water from contaminated/unconventional water sources. To this purpose, promising results may be achieved by the employment of membrane-based separation technologies, which can help improving the management of water and wastewater streams and a more sustainable human-related water cycle. Within this broad topic, this manuscript presents two case studies in which innovative membrane filtration systems are employed for the recovery of high-quality water from contaminated sources. A methodological approach is presented, where membrane-based solutions are analysed "from lab to full scale" design. In-depth studies of the parameters affecting membrane process performance is first investigated through lab experiments. Consequently, the results obtained in the lab are used to implement and/or evaluate the performance at larger scale, also through system-scale modelling, with the aim to identify the best operating conditions for the final proposal of full-scale designs.

As a first case study, nanofiltration is discussed as a potential technology to produce drinking water from chromium contaminated sources, and sources contaminated by heavy metals in general. Chromium removal is concerning because a new stringent limit was recently adopted in many EU countries. First, three of the most widely used commercial NF membranes are investigated at the lab scale. Overall, laboratory results suggest that tighter NF membranes should be adopted when filtering chromium contaminated waters with significant ions concentration, and in particular divalent cations. Loose NF membranes may instead guarantee higher productivity and adequate Cr rejection in waters with lower salinity or hardness. The influence of the presence of oxidizing agents on membrane performances and their achievable lifetime is also investigated. Promising results are obtained by filtering real well water samples of different chemical compositions, suggesting that nanofiltration is an effective process to extract safe drinking water from chromium-contaminated sources. Based on these results, pilot experiments are discussed with a pilot installed in situ. The denser membranes consistently reject chromium to achieve the desired values in the permeate stream. Finally, a design of a full-scale plant is proposed to treat the contaminated well water, together with the relative

economic and environmental assessments. Guidelines are also presented to perform similar analysis and to help with the choice of the most appropriate nanofiltration membrane, depending on the specifics of water chemistry.

The second case study evaluates the feasibility of a forward osmosis – nanofiltration system to extract high-quality water from brackish groundwater and from wastewater. Through lab experiments, magnesium chloride and sodium sulfate are identified as the most promising draw solutes for this application. High-recovery tests suggest that a feasible recovery larger than 60% may be achieved in the coupled technology by filtering these feed solutions. The diluted draw solutions can be completely regenerated through NF membranes, extracting, at the same time, high-quality water on the permeate side, suitable for beneficial reuse.

An in-depth analysis of fouling phenomena shows that the loss in membrane productivity can be partially recovered through mild physical cleaning, suggesting that fouling would not significantly affect the performance of the system. The higher performance obtained by filtering the real wastewater compared to the brackish water sample suggests that the coupled technology is especially promising for the treatment of water matrices with low salinity and high organic contents. From these results, a system-scale modelling is developed to evaluate the influence of different process parameters, in the case of the FO-NF system applied for the treatment of wastewater. Finally, the design of the full-scale FO-NF plant is presented. Simulations show that the overall system can achieve up to 85% water recovery using Na_2SO_4 or $MgCl_2$ as the draw solute. However, periodical change of the draw solutions should be accounted for.

Overall, the methodological approach presented in this thesis may represent a valuable method to evaluate various membrane-based treatment solutions and their potential full-scale applications.

Acknowledgements

This work was supported financially through the Ph.D. scholarship from MIUR. The case study reported in Chapter 2 was perfomed through the financial support of SMAT SpA, Società Metropolitana Acque Torino, while the case study reported in Chapter 3 was supported by Eni and Syndial S.p.A with the contribution of Compagnia di San paolo through the project "Flowing" to purchase of part of the lab equipment.

To Francesca
& Bianca

Contents

List of Tables

List of Figures

Chapter 1

Introduction

Freshwater represents the fundamental asset to guarantee adequate living standard to people. Many efforts have focused during the last decades to increase water availability and significant breakthroughs were achieved [1]: in 1990 only the 76% of the world's population had access to safe potable water through established drinking-water services. In 2015 this number was 91%. In 2017, the World Health Organization reported that almost 6.9 billion of people used improved water services (with or without restrictions based on the living location). However, the remaining 580 million people still need access to safe potable water today. The goal reported by the Agenda for Sustainable Development is to ensure a safe and unrestricted water service to the whole world's population within 2030 (VI sustainable development goal) [2].

With respect to human activities, the largest fraction of freshwater is required in agriculture and in the food industry, which consume up to 70% of the global freshwater withdrawals [3, 4]. The availability of freshwater, together with energy supply, are considered the most important assets for global development [5]. A strong interdependence exists between the demand of freshwater and the energy consumption, so called "water-energy nexus" [6]. Freshwater indeed must be used to ensure any energy- and raw materials-related operation such as the extraction and conversion of these materials or to provide cleaning and cooling of industrial systems [7]. On the other end, energy is needed not only to operate the industrial processes but also to ensure freshwater extraction and purification, and in the reclamation of contaminated waters.

Considering that only the 2.5% of the water on the Earth is freshwater, with the 68.7% of this fraction being inaccessible [8], freshwater should be accounted as a "limited resource" and its management becomes crucial in global sustainability. Therefore, the engineering approach related to water and wastewater treatment technologies is fundamental for global sustainable development. Nowadays, even if conventional and established technologies are widely employed for water/wastewater treatment, an optimization of the overall "water system" is needed

to face the constant increase of freshwater demand. Efforts are ongoing to study and to develop innovative water/wastewater treatment solutions with the aim to achieve the highest possible recovery rate of the treated water, ensuring an overall high quality of the effluent produced, and possibly extracting other valuable resources from the feed stream. This achievement would translate into a strong reduction of the waste and of the cost associated to wastewater management. The recovery of high-quality water from industrial effluents, contaminated streams or unconventional water sources, would also allow the re-use of water on site, lowering the environmental risks related to wastewater discharge and the pressure on more "noble" freshwater resources. Moreover, in some cases this engineering approach would allow the recovery of valuable resources, such as minerals, ideally achieving the so called "zero liquid discharge".

This thesis is placed within the context described above, presenting two case studies of innovative water treatment solutions for the recovery of high-quality water from contaminated sources. Membrane-based separation technologies were chosen for this specific purpose; this thesis reports a comprehensive overview of the process performance and the results obtained in lab experiments to inform full-scale system design, also discussed herein. Below, a brief summary of the conventional water/wastewater treatment systems is reported followed by an introduction on membrane-based solutions for high-quality water recovery. Finally, the scope of the thesis is described before diving into the details of the two case studies.

1.1 Water and Wastewater treatment systems: an overview

Wastewater Treatment

According to the FAO, wastewater treatment facilities must be employed to treat domestic and industrial effluents before release to the environment without compromising the ecosystems or affecting human health [9]. With the aim to remove particles, organic materials, and nutrients from contaminated streams, conventional wastewater treatment plants (WWTPs) include a series of treatment processes and operations, namely: preliminary treatment, primary treatment, secondary treatment, tertiary and/or advanced treatment, and often disinfection prior to effluent disposal [9, 10, 11, 12]. Preliminary treatment consists of equalization and the use of screens and grids to remove large suspended solids. This step is necessary to guarantee the proper functioning of the overall treatment train [9, 10]. The effluent exiting the preliminary step is usually sent to a sedimentation tank (which commonly represents the primary treatment unit). Here, the aim is to remove all the settleable inorganic and organic particles [9, 10]. Overall, approximately 65% of

the total oil and grease is removed through this step, together with an average 50% to 70% of suspended solids and 25% to 50% of BOD [9, 13]. Secondary treatment usually includes biological treatment units and further sedimentation. Aerobic systems, such as activated sludge, followed by sludge digestion is typically employed for the abatement of organic matter concentration in water [9, 11, 13]. However, in the presence of wastewater constituents, such as nitrogen, phosphorous, heavy metals, or additional suspended solids, physico-chemical treatment (coagulation-flocculation and sedimentation) or anaerobic/anoxic steps may be performed during or following the secondary treatment [9, 14]. Finally, before releasing the effluent into the environment, a disinfection ensures the production of an effluent virtually free from harmful microorganisms [9, 14]. Nevertheless, depending on the characteristics of each wastewater and on contaminant concentrations, the treatment sequence described above may be rearranged and further treatment technologies can be employed. For instance, in the presence of contaminants that may compete with the biological degradation of organic matter, physico-chemical treatments may be used prior to the activated sludge process, thus enhancing the performance of this step and of the subsequent sludge digestion. Depth filtration, instead, can be employed for the abatement of the smallest and not easy settleable suspended particles, while ion exchange resins may be used to further reduce the concentration of heavy metals and dissolved solids from the final effluents [15, 16, 17]. An example of a conventional wastewater treatment train is presented in Figure 1.1.

Conventional wastewater treatment plants are not designed to produce an effluent with a quality suitable for water re-use, such as for further industrial processes or for irrigation. Moreover, emerging contaminants (e.g., micropollutants, biocides/pesticides, surfactants, and heavy metals) produced by anthropic activities are increasingly released into the sewage system but no specific treatment units are included in conventional WWTPs for the abatement of these compounds [18, 19]. For this reason, research is focused on studying innovative treatment technologies or innovative treatment schemes able to guarantee high rate of removal of a wide spectrum of contaminants and consequently to obtain the high recovery of high-quality effluents. This achievement would allow the re-use of the recovered water, thus minimizing the global freshwater withdrawal.

Potable Water Treatment

Drinking water supply represents one of the fundamental assets for all communities. Potable water is commonly produced by different water sources, i.e., ground or surface waters, and different treatment steps are required to ensure a safe effluent. Overall, conventional water treatment facilities comprise different units. Coagulation-flocculation is required to remove natural organic matter, pathogens, and inorganic compounds, such as possible heavy metals, the latter also removable

via oxidation and aeration [14]. Following physico-chemical treatment, sedimentation and depth filtration are usually employed to remove all the remaining suspended compounds, while adsorption and disinfection usually represents the final step to ensure the potability of the treated effluent [20]. An example of conventional water treatment train is presented in Figure 1.1.

Different treatment processes may be employed depending on the water characteristics. For instance, in the presence of a significant concentration of calcium, magnesium or heavy metals, ion exchange resins represent an established technology for their removal [21, 22], while adsorption techniques, such as the use of granular/powder activated carbon, may be applied for the abatement of non-specific organic materials or different inorganic compounds [23]. In the case of seawater exploitation for potable water production, desalination technologies must be employed to ensure the abatement of total dissolved solids (TDS) [24, 25].

However, the increasing demand of freshwater and the risk of pollution due to anthropic activities should draw the research towards studying innovative technologies and innovative treatment schemes able to produce drinking water from less conventional water sources other than ground or surface water bodies. Firstly, innovative treatment solutions should be proposed for the abatement of emerging contaminants from potable sources. In groundwater, which represents the 65% of potable water source for European countries, recent contaminations by nitrates, heavy metals, pesticides or hydrocarbons have been found, while trace of microplastics, micropollutants, and heavy metals have been measured in surface waters in addition to an increase in concentration of organic materials [26, 27, 28, 29]. At the same time, water providers must comply with updating regulation and increasingly more stringent limits for contaminant concentration when delivering potable water [26]. Moreover, within the goal of zero liquid discharge, innovative water treatment solutions should be developed to produce, ideally, potable water directly from wastewater effluents.

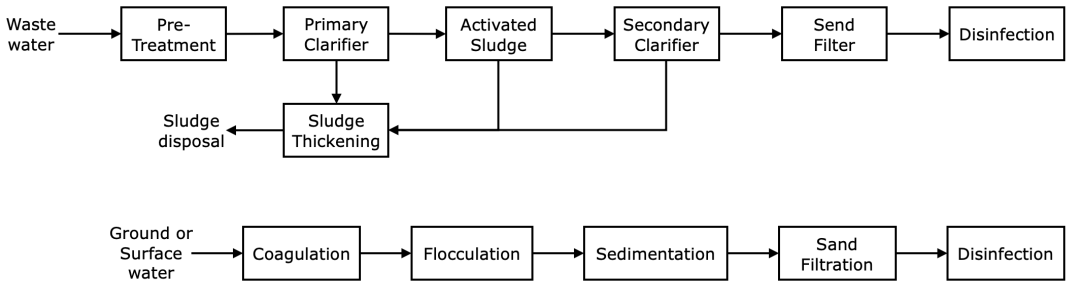

Figure 1.1: *Schematic representation of (a) conventional wastewater and (b) conventional water treatment trains*

1.2 Membrane technologies as innovative solutions for high-quality water recovery from diverse aqueous streams

Some of the most promising engineering solutions for high-quality water recovery from various aqueous streams are membrane-based separation technologies. During the last decades, efforts have focused on studying and implementing membrane filtration solutions for water/wastewater treatment.

The role of reverse osmosis (RO) in the desalination market is well-known. Thanks to its modular configuration, lower energy demand, and easier operation/maintenance, RO units are preferred over traditional thermal desalination technologies [30]. This result was achieved through studies performed towards the implementation of new membrane materials, innovative energy recovery devices, and new membrane module configurations, which have drastically reduced the energy consumed by the reverse osmosis unit and have enhanced the overall membrane performance [31, 32]. Significant research breakthroughs have been achieved: in the 1970s, the water productivity of a seawater RO (SWRO) plant was far from the capacity achievable through an established multi-stage flash (MSF) unit and an average 20 kWh was consumed per cubic meter of water produced. Today, one of the largest desalination plants in the world (Sorek) is working through reverse osmosis membranes producing up to 630,000 m^3 of safe potable water per day with an energy consumption below 3 kWh/m^3.

Like RO, also nanofiltration (NF) represents an established membrane technology for high-quality water production, mostly thanks to the ability of NF membranes to remove contaminants from water up to the ion size with lower energy demand compared to RO [33]. Different types of nanofiltration membranes are available in the market today. Depending on the characteristics of the selective layer used to fabricate the membrane, differences can be observed in perm-selectivity [34]. Overall, NF membranes are characterized by a negative surface charge density, which acts as a barrier to co-ions present in solution (so called Donnan exclusion effect) [35, 36, 37]. However, the density of the active layer placed can vary. Membranes fabricated with a dense active layer (tight NF membranes) would result in high selectivity, with ions separation dominated by steric hindrance [38, 34]. Membranes characterized by a less dense active layer (loose NF membranes) are characterized by higher permeability and lower selectivity compared to denser membranes [38, 34]. Loose or tight NF membranes can be chosen depending on the characteristics of the water to be treated and the productivity/energy/footprint required by the membrane system. Nanofiltration is recognized as a valuable alternative for the recovery of high-quality water from wastewater effluents. In the pulp and paper

industry, NF systems may be employed for the abatement of COD and the removal of multivalent ions, thus being able to recirculate clean water directly inside of the pulp and paper processes [39, 40]. A similar NF application concerns the treatment of wastewaters produced by textile industries, where nanofiltration can reduce the overall freshwater demand through the re-use of the treated effluent, free from dyes, organic matter and with low ion concentration, directly into the fabrics fabrication and handling processes [41, 42]. In both such applications, traditional treatment technologies, such as coagulation, flocculation, or ion exchange resins, would not achieve similar quality effluents due to the influence of the various physico-chemical parameters on process performance [34]. Finally, within the goal of freshwater production, nanofiltration systems may be employed for the recovery of water from municipal wastewater effluents [43, 44]. For instance, the combination of advanced oxidation processes (AOPs) with nanofiltration may allow the extraction of high-quality water (e.g., suitable for irrigation) from municipal wastewaters even in the presence of micropollutants [45].

Among all, nanofiltration may have the potential to produce potable water directly from brackish and other less conventional drinking water sources. Different studies demonstrated that NF may represent a valuable technology for the removal of dissolved minerals, organic components, micropollutants, and for abatement of taste and odours from contaminated waters for drinking water purposes [46, 47, 48, 34]. More and more stringent regulations are imposed worldwide for potable water production, thus requiring technology innovation within the water treatment train to accomplish the new water quality limits, which often cannot be achieved by the traditional treatment processes [34]. Nanofiltration may have a key role in this respect.

To overcome the overall fresh-water demand and with the aim to develop sustainable water production processes, research is also pushing forward towards the implementation of novel membrane-based solutions able to recover water from complex aqueous streams by exploiting low exergy sources. Membrane distillation (MD), a thermally driven membrane process, is one of these promising technologies, with the potential to recover freshwater from hypersaline solutions [49]. Within the zero liquid discharge goal, studies have demonstrated the feasibility to recover high quality water and minerals from concentrated streams produced by RO systems through membrane distillation/crystallization [50, 51]. Membrane distillation may be also employed for the extraction of freshwater from unconventional wastewater sources, such as Oil&Gas produced waters, following their pre-treatment for the removal of oil, surfactants, and volatile compounds [52, 53]. In both applications, conventional treatment technologies cannot achieve similar quality of the product water, due to the extremely high TDS concentrations. Besides, thanks to the low temperatures required to drive the process, achievable through the exploitation of low grade energy sources, membrane distillation may play a key role within the

water-energy nexus [49].

Another recent and novel membrane-based technology for sustainable water production is forward osmosis (FO), in which the driving force is exerted by the osmotic pressure difference between a draw solution and the feed contaminated solution. FO represents a valuable alternative for the recovery of high-quality water from complex water matrices [54, 55]. Thanks to its low fouling propensity, FO may be integrated in membrane bioreactor (MBR) systems, thus providing advanced treatment for the production of high-quality effluents, suitable for irrigation or further industrial processes [56]. MBRs working with micro/ultra-filtration membranes already represents a valuable alternative to conventional technologies, such as biological tanks, sedimentation, clarification or filtration in municipal wastewater facilities. Yet, with FO integrated in it, MBR systems (FO-MBR) can overcome the limitations of MF and UF membranes through the removal of TDS, low molecular weight contaminants, and micropollutants from water, thus achieving higher effluent quality [57, 58, 59]. Studies also investigated the performance of forward osmosis as a feasible technology for the recovery of freshwater from RO brines or Oil&Gas produced waters [60, 61]. Promising draw solutes have been proposed for the treatment of the mentioned hypersaline solutions, such as ammonia/carbon dioxide or sodium propionate, for which membrane distillation was proposed as post-treatment regeneration process [60, 62]. As of today, the two integrated system (FO-MD) represents one of the most promising solution for sustainable water production. However, many efforts are still required to allow the real-scale implementation of these two novel technologies, as individual or as combines processes.

To summarize, the utilization of membrane separation technologies within the water/wastewater treatment trains may provide higher effluent quality with significantly smaller footprint than conventional technologies. Membrane processes present also another significant advantage compared to traditional treatment systems: thanks to their modular composition, membrane units can be easily customized for the specific water volumes and requirements at hand. This characteristic translates into more versatile systems, which may suitable for water recovery *in situ*, i.e., with membrane filtration units directly integrated to, e.g., the drinking water delivery systems, or to recover water in industrial processes [39, 40, 42, 63]. Consequently, the integration of membrane technology would allow an easier water/wastewater management thanks to a reduction of the total water/wastewater volume. Finally, easy operation and maintenance makes membrane-based processes suitable for water/wastewater treatment in remote areas (such as for Oil&Gas offshore facilities), where traditional treatment systems would not achieve the same performance with similar footprint and operational costs.

Many studies have focused on all the different aspects of the above mentioned

membrane-based technologies. An important line of research is dedicated to membrane improvement through the development of novel membrane materials. For instance, efforts have been devoted during the last years to the fabrication of membranes with antifouling properties [64, 65, 66, 67]. Innovative forward osmosis membranes were reported, showing promising enhanced productivity [68, 69]. Omni-phobic and oleophobic membranes were fabricated to overcome the wetting phenomena in membrane distillation [70, 71]. However, few of those innovations were launched on the market and still strong limitations must be addressed to scale-up the proposed fabrication methods. At the same time, research was performed to investigate the mass/contaminant transport theory and the influence of solution chemistry on membrane performance, depending on the driving force of the process and membrane module configurations [72, 73, 74, 75]. Also, research is conducted to evaluate innovative membrane applications at the pilot/large scale. With a view to sustainable water production, studies showed the feasibility to couple renewable energy sources in reverse osmosis units, thus building up more eco-compatible solutions [76, 77]. Other promising results were reported about membrane filtration systems for direct water recovery in different industrial processes [63, 41]. A smaller but good number of pilot scale studies have been carried out to evaluate fouling behaviour and cleaning procedures in various membrane applications, such as in FO-MBR systems [78, 79]. Finally, research is being performed to analyse the economic and environmental potential of full-scale membrane design for the application of novel technologies, such as forward osmosis and membrane distillation [80, 81].

Nevertheless, most of the research performed so far covers only single aspects of specific membrane applications, thus creating a gap between the results obtained at the "micro scale" (lab-scale) and at what is reported at the "macro scale" (pilot/large-scale). Therefore, this thesis aims at partially closing this gap, at least for two specific processes/applications.

1.2.1 Thesis Hypothesis

Two case studies are analysed in which membrane technologies are proposed as treatment processes for the recovery of high-quality water from contaminated sources, reporting a complete and comprehensive overview of each application. A new methodological approach was followed for both the case studies with the aim to evaluate each of the membrane processes or combines processes from the lab to the full-scale application. The methodological approach involved the initial evaluation of the processes in lab experimentation; this phase was followed by a streamlined modelling investigation to evaluate the best operating conditions for the upscaling of the processes; a pilot study then followed for one of the two case studies, which were both completed with a proposal for a full-scale design of the potential treatment

plant, accompanied with some economic and environmental analyses.

In the first case study, nanofiltration is analysed as a potential technology for the production of potable water directly from contaminated groundwater containing hazardous concentrations of chromium(VI). Initial lab-scale identification of suitable membranes and operating conditions is used to inform the operation of a pilot system; the results of its operation are then applied for the proposed design of a full-scale system. In the second case study, a forward osmosis – nanofiltration system is studied and proposed for the recovery of high-quality water from brackish groundwater and from wastewater. Also in this second case, a comprehensive lab experimentation is discussed as a first step for the final design of a potential full-scale system, which is analysed in terms of feasibility and environmental sustainability.

An overview of the lab-to-full-scale approach presented in this dissertation is reported in the following schematic figure, with reference to the main steps developed for each case study.

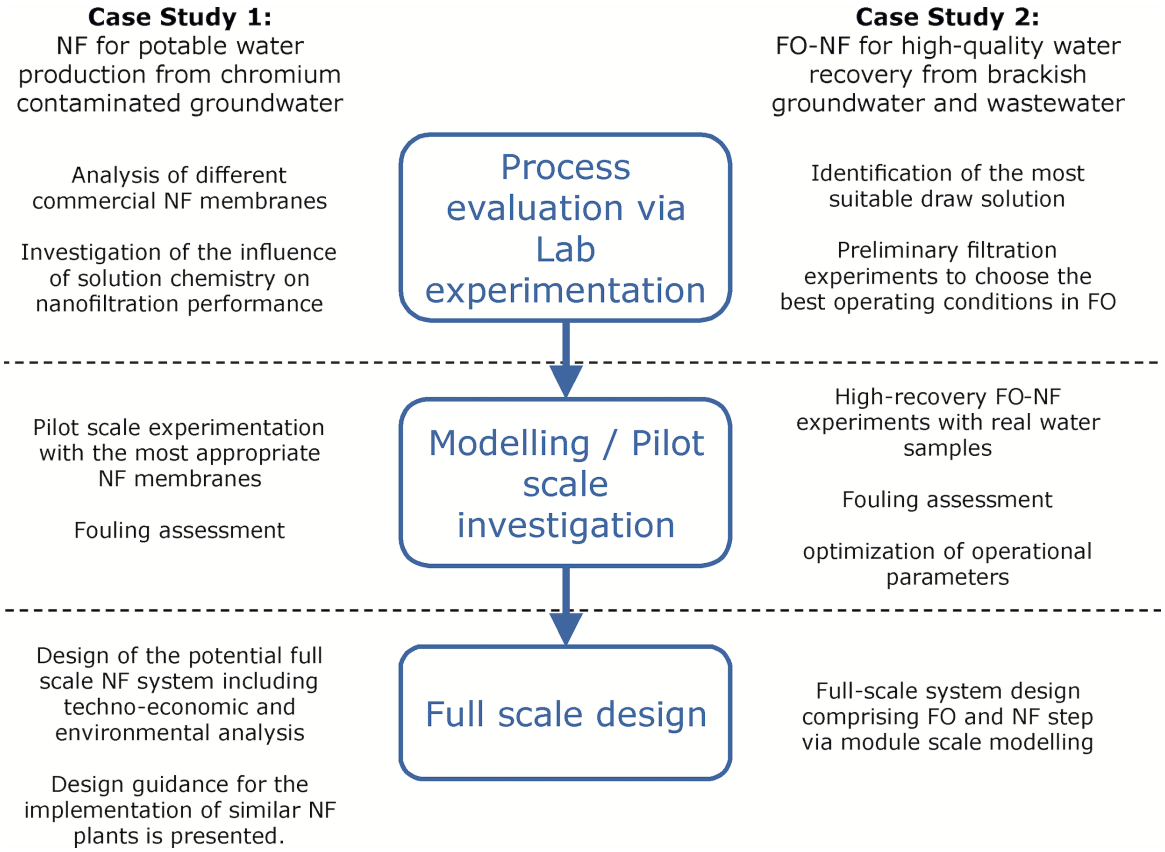

Figure 1.2: *Schematic representation of the lab-to-full-scale approachdiscussed in this manuscript, with reference to the main steps developed for each case study*

Chapter 2

Nanofiltration for the production of drinking water from chromium contaminated source *

2.1 Introduction

Concentration of heavy metals in drinking water must be monitored before delivering this water for drinking purposes. In particular chromium, with the predominance of its hexavalent species in water, is carcinogenic for humans [84, 85]. For this reason, both the European Commission and the World Health Organization (WHO) have imposed a limit of 0.05 mg/L for total chromium concentration in drinking water [86, 87]. In Italy, a decree approved in November 2016 introduced a lower limit of 0.01 mg/L of Cr(VI) in potable water [88]. This provision has recently come into force also in UK and might be soon adopted by the whole European Community [87].

The presence of chromium in water strongly depends on pH, which affects the speciation of this heavy metal: while the neutral H_2CrO_4 species can only be found in strongly acidic environment (pK below 2), the monovalent $HCrO_4^-$ predominates below pH 6.5. Above pH 6.0, chromate CrO_4^{2-} and dichromate $Cr_2O_7^{2-}$ anions represents the major species [89]. CrO_4^{2-} dominates in alkaline conditions and, along with the monovalent $HcrO_4^-$, represent the main source of hexavalent chromium in natural waters [90]. Under the presence of oxidants or in oxygenated drinking water, Cr(VI) species predominates over its trivalent form. Besides, the latter tends to be extremely insoluble between pH 7 and 10, precipitating as solid

*part of the content reported in this chapter, with permissions, has been already published in [82] and [83]

$Cr(OH)_3$.

Nowadays, adsorption, ion exchange resins, and chemical reduction represent the most widely used technologies for chromium removal [91, 92, 93]. However, these processes often cannot guarantee the abatement of Cr(VI) under the new stringent concentration limits. Besides, these technologies are based on the employment of a large amount of chemical compounds needed to enhance the chromium removal from water. A valuable alternative may be represented by membrane-based separation techniques [94]. Promising results have been achieved through the application of reverse osmosis or complexation-ultrafiltration systems [95, 96]. In particular, low-pressure reverse osmosis and micellar/polyelectrolyte-enhanced ultrafiltration were studied as feasible technologies for the abatement of chromium concentration in aqueous streams [97, 98]. Among the various membrane-based solutions, nanofiltration (NF) may actually be the best option to guarantee efficient removal of hexavalent chromium from contaminated water, thanks to its contaminant rejection mechanism based on the combination of size-exclusion and electrostatic effects. Moreover, high filtration performance can be accomplished through the employment of nanofiltration membranes, virtually without the requirement of any chemical compounds or high hydraulic pressures. Nanofiltration technology was proven to be a suitable process for the removal of different heavy metals (e.g., cadmium, copper, manganese, lead) from aqueous solutions [99, 100, 101]. Very few studies reported the effectiveness of NF membranes for the removal of chromium from wastewater [102, 103, 104], and without a wide-range investigation of the influence of physico-chemical characteristics of water or of membrane properties. Even in comprehensive manuals on nanofiltration, no significant references are given about the feasibility of meeting the hexavalent chromium concentration threshold [105].

The most common NF commercial membranes are based on aromatic polyamide selective layers. Even if stable in a wide range of pH, these membranes exhibit poor tolerance to long-term exposure to oxidizing agents, such as chlorine or even mild hypochlorite [106]. This degradation inevitably reduces the service lifetime of the membrane. On the other hand, sulfonated polysulfone membranes have attracted increased interest in recent years being highly resistant to aqueous chlorine over a broad range of pH values [107]. The capability of the membrane to tolerate oxidizing species may be specifically interesting if treating feed solutions relatively rich in Cr(VI), which is intrinsically a strong oxidant.

With respect to potable water production, conventional treatment processes can hardly achieve the increasingly stringent legislative limits applied to ensure high water quality (such as in the case of the new limit imposed for Cr(VI) in drinking water). To reach this goal, nanofiltration may become one of the major technological solutions. NF may be applied for the removal of pesticides, pharmaceuticals,

and for that of a wide range of organic and inorganic compounds from groundwater or surface water [108, 109, 110, 111]. NF is also recognized as a valuable alternative to the more conventional water softening systems [112]. However, there is a lack of data relative to pilot-scale/in situ experiments performed to test the feasibility of NF as a viable technology for drinking water production. Most of the available studies are based on theoretical analyses and comparisons between different water treatment systems or on very specific pilot scale integration (e.g., nanofiltration coupled with renewable energies or ultraviolet photolysis) [113, 114, 115]. Moreover, the results available on the economic assessment of NF systems for drinking water production are usually based only on lab-scale experiments [116].

Overall, there is a lack of studies where nanofiltration is analysed from the "micro" (lab scale) to the "macro" scale (pilot/large scale) with the aim to fully evaluate the feasibility of the technology. Therefore, in this study we evaluate and discuss the nanofiltration as a feasible technology to produce drinking water by purification of chromium contaminated sources. As a first step in this work, three of the most widely used commercial NF membranes are investigated at the lab scale, two based on polyamide chemistry while the third one made of sulfonated polyethersulfone. We provide an investigation of the influence of solution chemistry (i.e., the presence of common salts or variation of pH) on nanofiltration performance, together with specific experiments performed to analyse the separation of the contaminant in relevant solutions, such as tap water and real well water samples. Membrane performance is analysed also in the presence of oxidizing agents in solution, performing filtration experiments with samples after accelerated contact with Cr(VI) and with such oxidizing agents as those typically employed in conventional water treatment plants. Simple correlations are finally proposed to aid with the choice of the most appropriate membrane, based on specific system parameters. As a second step in the work, a pilot scale experimentation is performed with the two most promising NF membranes among those studied during the first phase. The performance of the pilot plant is evaluated and discussed. Based on the results collected, a potential full-scale NF system is designed for the treatment of real well water contaminated by chromium and techno-economic and environmental analyses are included in the discussion. Finally, design guidance for the implementation of similar NF plants are presented.

2.2 Materials and Methods

Laboratory experiments were performed to evaluate the performance of the main representative nanofiltration membranes available commercially for chromium removal from water. After membrane characterization, various set of cross-flow filtration experiments were carried out:

1. Three set of experiments were performed to investigate the influence of physico-chemical parameters of aqueous solution on membrane behaviour and process performances. By changing pH, ions concentration, ionic composition, Cr(III)/Cr(VI) ratio in solution, the variations in terms of productivity and chromium selectivity of each membrane were investigated and discussed together with membrane surface analyses.

2. Preliminary experiments were carried out to evaluate membrane filtration performances by filtering real well water samples (coming from three different location contaminated by chromium) and tap water deliberately contaminated by chromium.

3. A specific set of filtration experiments were performed with membranes exposed to oxidizing agents (such as the Cr(VI) itself and the common chlorinated compounds used for membrane module cleaning in plant) to evaluate the possible membrane degradation and loss of performance due to the presence of such components in solution.

Following lab evaluation, a semi-analytical system-scale analysis was developed to simulate the achievable membrane performance in situ depending on the chemistry of the water sources. Based on the results obtained, pilot investigation was performed with the two most promising commercial NF membranes among those evaluated during the preliminary lab experiments. Firstly, cross-flow filtration tests of real well water samples were performed at lab scale to evaluate in details the characteristics of the permeate products. Pilot tests were performed afterwards, measuring the productivity and chromium selectivity of the membranes studied continuously for 42 days. Based on lab and pilot tests results, a system scale modelling was developed to analyse the different process filtration parameters, ending with the design of the nanofiltration large plant to be potentially installed in the specific location studied. Finally, economic and environmental assessments of the overall filtration unit were carried out, together with modelling analysis developed with the aim to present guidelines for the design of similar NF plants.

The materials and methods reported below in details were already described in previously published papers [82] and [83].

2.2.1 Laboratory facilities and nanofiltration pilot plant

A laboratory membrane filtration unit was assembled to perform the preliminary experiments, while a pilot plant system was installed *in situ* for membrane module performance evaluation. The two membrane systems are described below together with the laboratory facilities used for chromium quantification analysis and characterization of membrane surface potential [82, 83].

Laboratory membrane filtration unit

A cross-flow membrane filtration unit was used to perform the laboratory experiments. The system includes a flat membrane housing cell, a high-pressure pump (Hydra-cell pump, Wanner Engineering, Inc. Minneapolis, MN), feed vessel, temperature control, and data acquisition system. The housing cell is a custom-made rectangular channel with the following dimensions: 7.9 cm long, 2.9 cm wide, and 0.3 cm high. A membrane sample with an active area of 23 cm^2 can be housed in this cell. A computer-interfaced balance was used to measure the permeate flow rate, automatically, every 60 s. The cross-flow rate was instead monitored by a floating disc rotameter. Bypass and back-pressure regulators were adopted to adjust the operating pressure (Swagelok, Solon, OH). The temperature in the feed tank was controlled via a recirculating chiller with a stainless-steel coil immersed in the solution.

Nanofiltration pilot plant

A schematic diagram of the nanofiltration pilot plant is presented in Figure 2.1 while its picture is reported in Figure 2.2. The system was fed with well water through the utilization of a hydraulic pump. A tubular stainless-steel housing was used to accommodate two spiral wound modules in series. Upstream and concentrate valves were used to control the pressure in the unit. Two mechanical flow meters were employed to measure the permeate and concentrate flow rates while a digital manometer measured the pressure at the inlet of the housing. The system was run with an inlet flow rate of 2000 L/h, a cross-flow rate of 26.7 L/min, and a total recovery rate of 20%. Full-fit fiberglass 4040 spiral wound elements were employed in the membrane system. The dimensional characteristics and the intrinsic operating limits for the 4040 module are reported in Table 2.1.

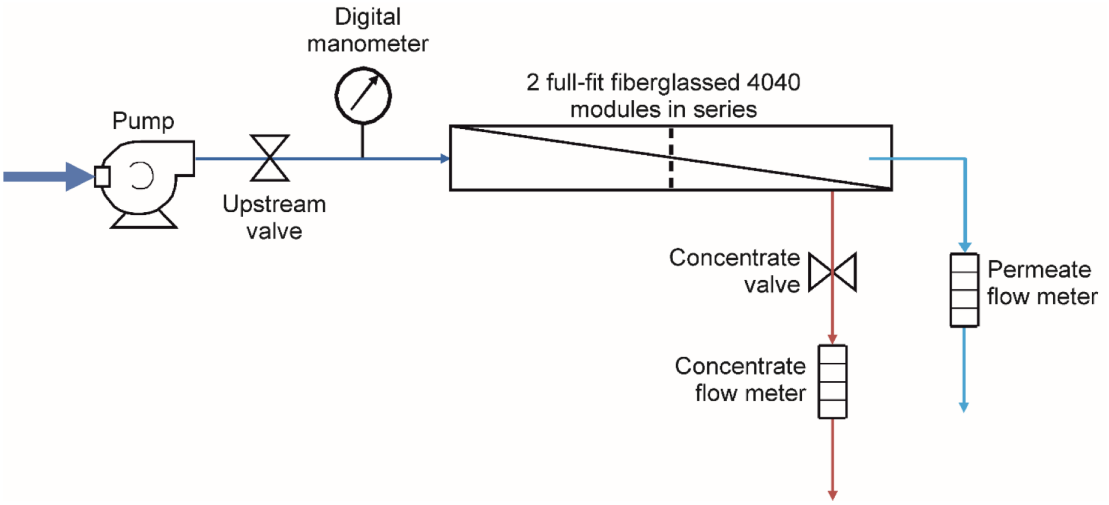

Figure 2.1: *Schematic representation of the NF pilot plant. The plant was designed to operate with two specific membrane modules in series: the NF-4040.*

Figure 2.2: *Picture of the nanofiltration pilot plant used to conduct the field experiments. The system was adapted to work with only one of the three pressure vessels available (stainless steel tubes), thus running each test with two 4040 membrane modules in series.*

Chromium quantification analysis

An inductively coupled plasma optical emission spectrometry (ICP-OES, Perkin Elmer Optima 2000 DV) was used to measure the chromium concentration in the feed and permeate samples collected during the lab experiments. The operating wavelength was 267.716 nm and the detection limit 0.71 μg/L. Determinations were carried out in triplicates in the axial viewing mode.

Table 2.1: *Operating limits and dimensional characteristics of the full-fit fiberglass 4040 spiral wound membrane elements*

Active Area (m^2)	7.6
Length (m)	1.016
Diameter (cm)	99
Maximum Operating Pressure (bar)	41
Maximum Feed Flow Rate (m^3/h)	3.6
Maximum Permeate Flow Rate (m^3/h)	0.325
Minimum Concentrate Flow Rate (m^3/h)	1.4
Maximum element recovery (%)	19

Measurements of membrane surface potential

An electrokinetic analyser (SurPASS 3, Anton Paar, Austria) was used to measure the surface zeta potentials of the membranes immersed in different solutions. Two sample holders were assembled in an adjustable gap cell (20 mm × 10 mm) with membranes taped onto it. The gap height was adjusted to roughly 100 μm. An applied pressure of 200-600 mbar was operated to let the solution flow across the cell, causing electric charge separation. The resulting potential difference was measured and calculated using the Helmholtz-Smoluchowski equation [117].

2.2.2 Preliminary laboratory experiments

The performance of the nanofiltration technology for chromium removal from aqueous solutions were firstly evaluated via lab experiments. A description of the different membranes studied, their characterization and the laboratory tests protocols are reported in the following section [82, 83].

Membranes and their characterization

Three different commercial nanofiltration membranes were studied at the lab scale: NF90, NF270 (Dow Chemical Company, Midland, MI), and HYDRACoRe 70pHT (Hydranautics, Oceanside CA; the name is shortened to Hydra 70 throughout the text), all received as flat sheets and stored dry. These samples are representative of commercial nanofiltration membranes suitable for chromium removal from aqueous mixture. According to the manufacturer, Hydra70 is characterized by a polysulfone support layer with a selective sulfonated polyethersulfone on top of it, whereas the NF270 and NF90 membranes have a polysulfone micro-porous support covered by a semi-aromatic piperazine-based polyamide layer. Under neutral pH conditions, all membranes present a negative surface charge, as measured in this work and also reported in previous studies and by the manufacturers [118, 119].

The intrinsic transport properties were determined by testing samples of all membranes in triplicate. Deionized (DI) water was used to evaluate the permeance of each membrane. The permeate flux was measured at three different applied pressures (100; 150; 200 psi – 6.9; 10.3; 13.8 bar). The solute rejection capabilities instead were evaluated at a single applied pressure of 100 psi (6.9 bar) for different individual compounds with each a nominal concentration of 30 mM in the feed. Before testing the membrane samples, 6 h of membrane compaction at 300 psi (20.7 bar) were performed with a cross-flow rate of 4.5 L/min (cross-flow velocity of 0.85 m/s) and a water temperature of 22 °C (this compaction is performed for all filtration experiments unless otherwise stated). Table 2.2 is reporting the average results obtained for each type of membrane. The lowest water permeance is showed by the Hydra70, while the polyamide-based NF270 is the most permeable one.

Table 2.2: *Characteristics of the membranes used in this study*

Membrane	NF270	NF90	Hydra70
Active layer material	Polyamide	Polyamide	Sulf. Polyethersulfone
Water permeance (LMH/bar)	16.5 ± 1.9	6.9 ± 0.3	4.0 ± 0.3
MgSO4 rejection (%)	98.8 ± 0.3	>99.5	80.9 ± 0.4
MgCl2 rejection (%)	80.8 ± 0.4	99.3 ± 0.3	Not measured
Na2SO4 rejection (%)	98.7 ± 0.5	>99.5	Not measured
Glucose rejection (%)	85.0 ± 0.4	99.4 ± 0.2	Not measured
NaCl rejection (%)		98 ± 0.2	80.2 ± 0.3
Zeta potential[a] (mV)	–23	–17	–29

[a] Measured at pH 7.4 in 10 mM NaCl

Chromium removal experiments

Four sets of cross-flow filtration tests were carried out in order to evaluate the membrane behaviour and performance by changing the physico-chemical characteristics of the feed solution. Two sets of experiments were performed with either a trivalent or a hexavalent chromium solution in DI water, changing (i) the ionic strength of the feed solution through the addition of salts or (ii) the pH conditions. The third series of experiments (iii) was performed with both Cr(III) and Cr(VI) in DI water by varying their relative amount in the feed solution. The (iv) fourth set was conducted by filtering well water samples contaminated by chromium or by filtering tap water from lab spiked with Cr(VI). Well water samples were collected from three different sites in the area around Turin, Italy.

After compaction, tests were carried out at an applied pressure of 100 psi (6.9 bar), with a constant cross-flow rate of 4.5 L/min (cross-flow velocity of 0.85 m/s), and feed water temperature of 22 °C. Rejection values were calculated from concentrations in the feed and permeate sample measured using the ICP described above

(section 2.2.1).

- To achieve a nominal chromium concentration of 5 mg/L, either $K_2Cr_2O_7$ (Alfa Aesar, Karlsruhe) or $Cr(NO_3)_3$ (Acros Organics, New Jersey, US) were added to DI water, once membrane compaction was reached; the pH was then adjusted to 7.6. At this point, either NaCl (Sigma Aldrich, Milano, IT) or $CaCl_2$ (Carlo Erba, Milano, IT) were added individually to the feed reservoir every 45 min thus step-wise increasing the ionic strength (3, 10, 30, 100 mM for NaCl; 3, 9, 30, 90 mM for $CaCl_2$). For each step, one sample of feed solution and three samples of permeate were kept for analysis. The experiment was repeated for each type of membrane studied (i.e. NF270, NF90 and Hydra70).

- Two experiments were carried out changing the pH conditions. In order to understand the removal mechanisms and the possible critical issue related to the filtration of unconventional water sources, tests were performed exploring a wide pH range (even if typical pH of drinking water ranges between 6.5-8.5). The first separation test was performed by increasing the pH from 7.6 to 10 with the utilization of a concentrated NaOH solution (Sigma Aldrich, Milano, IT), while in the second study the pH was decreased step-wise from 7.6 to 4.5 and finally to 3 using HNO_3 (Sigma Aldrich, Milano, IT). In such experiments, either a $Cr(NO_3)_3$ or a $K_2Cr_2O_7$ solution was added to the feed reservoir (pH = 7.6) to achieve 5 mg/L chromium concentration. The pH was then varied every 45 min, collecting one sample of feed solution and three samples of permeate for each step. The experiment was repeated for each type of membrane studied (i.e., NF270, NF90, and Hydra70).

- Three filtration tests were performed varying the amount of trivalent and hexavalent chromium in DI water in the following Cr(III)/Cr(VI) percentage: 80% / 20%, 50% / 50%, and 20% / 80%, respectively. The total nominal concentration of chromium in the solution was always maintained equal to 5 mg/L and the pH was kept at a constant value of 7.6. Prior to each experiment, the membrane was stabilized for 45 min until the permeate flux attained a constant value. At this point, feed and permeate samples were taken for analysis every 15 min. Since the goal of the experiment was to understand the influence of different chromium species during the filtration, the experiment was performed with the two loose nanofiltration membranes (the NF270 and the Hydra70).

- The membranes were tested with tap water spiked with potassium dichromate to obtain a nominal concentration of 5 mg/L. Preliminary experiments were also performed with real well water samples, directly collected from three sites and hence not subjected to any treatment. The main chemical characteristics

of tap water and each sample are reported in Table 2.3. Prior to each experiment, the membrane was stabilized for 45 min in order to reach a constant permeate flux. At this point, feed and permeate samples were collected every 15 min for analysis.

Table 2.3: *Chemical composition of tap and well waters*

	Tap Water	Site A	Site B	Site C
Na^+ (mg/L)	7.5	9	6	1
Ca^{2+} (mg/L)	83.4	107	60	7
Mg^{2+} (mg/L)	14.1	22	19	10
Cl^- (mg/L)	15	14	12	1
$NO_3{}^-$ (mg/L)	30	14	45	2
$SO_4{}^{2-}$ (mg/L)	36	30	31	3
pH	7.5	7.4	8.1	8.1
Total Ionic Strength (mM)	10.6	14.3	9.1	2.3
Total Hardness (mg/L $CaCO_3$ eq.)	260	360	230	60
Cr (µg/L)	5000	23	14.9	14.7

Membrane oxidation procedure

As already stated in the introduction section (section 2.1), the membrane performance can be affected by the presence of oxidizing agents in solutions [106]. To investigate this phenomenon, a specific set of experiments was performed. Three oxidation baths were prepared, each containing 2 L of oxidizing solution. The first and the second baths contained 100 mg/L of NaOCl and $K_2Cr_2O_7$, respectively. The third one was prepared employing a combination of these two oxidizing agents, both at a concentration of 100 mg/L. In each case, the pH was adjusted to 7.6. Three samples of each type of membrane were immersed in each bath for 72 hours and transferred into a 0.1 M NaOH solution afterwards for 24 hours, rinsed thoroughly, and later stored in DI water at 4 °C.

The treated membranes were tested in cross-flow mode, measuring the permeance of DI water as described above in section 2.2.2. Cr(VI) rejection was evaluated by adding potassium dichromate to the feed reservoir in order to achieve a nominal chromium concentration of 5 mg/L. Filtration conditions were kept constant with an applied pressure of 100 psi, the cross-flow rate equal to 4.5 L/min (cross-flow velocity of 0.85 m/s), a pH solution of 7.6, and the feed solution temperature maintained at 22 °C.

2.2.3 In situ pilot investigations

Pilot plant installation site

The pilot plant was installed in the location previously specified as Site A (Table 2.3), since it presents the most difficult well water to be treated among the sites studied, with the highest Cr(VI) concentration, hardness, and ionic strength. The pilot plant was connected directly to the groundwater well. The overall characteristics of the well water are reported in Table 2.4. Before the new legislative limit came into force for the hexavalent chromium (i.e., 0.01 mg/L), an average flow rate of 30 L/s drinking water was delivered from this source to provide water to roughly 13000 residents after a mild disinfection step. However, due to the hexavalent chromium concentration of 0.023 mg/L in solution, this groundwater no longer represents a viable potable water source. To evaluate correctly the filtration experiments *in situ*, both the high hardness and the total ionic strength of 14.3 mM must be taken into account.

Membrane filtration experiments

At this stage of the study, membrane filtration experiments were performed with modules of the two most promising nanofiltration membranes among those evaluated during the preliminary lab experiments. Prior to pilot plant application, a final evaluation of the membrane performance in term of water quality produced was performed through laboratory experiments. Real well water samples coming from the location studied were used as feed solution. Membrane samples were firstly compacted for 14 h at 150 psi (10.3 bar). Tests were then carried out with a constant applied pressure of 100 psi (6.9 bar), a cross-flow velocity of 4.5 L/min, and an average feed solution temperature of 22 °C. Both the concentrate and the permeate streams were recirculated back into the feed reservoir. During the experiments, feed and permeate samples were taken for analysis, performed afterwards by an external accredited company (Eurolab S.r.l., Italy) in order to fully characterize the anions/cations concentration in solution, as well as the content of organic matter and metals.

In situ experiments were performed by running the pilot plant for 42 days with similar applied pressures used during the preliminary lab experiments. The well water described in Table 2.4 was filtered without any pre-treatment. The changes in permeate and concentrate flow rates were recorded over time. Permeate and feed water samples were collected twice per week to measure the chromium concentration. The analyses were performed by SMAT S.p.A, the water utility company owner of the water well, with an inductively coupled plasma optical emission spectrometry. The modules were subjected to a mild physical cleaning performed by increasing the cross-flow velocity to 30 L/min for 1 hour every week. No chemical cleanings were performed during the testing periods.

Table 2.4: *Characteristics of the well water coming from Site A*

pH	7.5
Conductivity (μS/cm)	646
Hardness (°F)	36.8
HCO_3^- (mg/L)	363
Alkalinity (meq/L)	7.24
Aggressive Index	12.6
Ionic Strength (mM)	14.3
Cl^- (mg/L)	9.9
F^- (mg/L)	0.11
PO_4^{3-} (mg/L)	0.03
NO_3^- (mg/L)	7.9
SO_4^{2-} (mg/L)	34
Ca^{2+} (mg/L)	110
Mg^{2+} (mg/L)	23
K^+ (mg/L)	1
Na^+ (mg/L)	11
As (μg/L)	1
B (μg/L)	32
Co (μg/L)	59
Cr (μg/L)	23
Fe (μg/L)	32
Mn (μg/L)	13
Cu (μg/L)	0.12
Se (μg/L)	2.2
Zn (μg/L)	15

2.2.4 Plant design, system scale modelling and Life Cycle Assessment

The following section reports the procedures followed to design the real-scale nanofiltration plant for the specific location studied and to perform the correlated system scale modelling and environmental impact assessment [82, 83].

Plant design and system-scale modelling

Before applying the software, a semi-analytical model was developed to make first estimate of five design parameters of a nanofiltration membrane plant, namely:

- c_f, concentration of pollutant in the feed solution entering the system (Feed)
- c_c, concentration of pollutant in the concentrate exiting the system (Concentrate)
- c_{tw}, concentration of pollutant in the treated water (Permeate)
- *REC*, recovery rate, i.e., the ratio between the flow rate of the treated water and that of feed water
- *Rej*, the observed system rejection, defined as Rej =$(1\text{-}\frac{c_{tw}}{c_f})$

In order to perform the semi-analytical analysis, the membrane system was modelled by a discretization of the control volume from the inlet of the feed stream to the outlet of the concentrate stream. The recovery rate, *REC*, may be considered as the variable describing the spatial or the temporal scale of the system from the inlet to the outlet. In order to simulate the performance that would be obtained by applying membranes with different performance characteristics, the simulation was carried out for several rejection values, *Rej*. For each value of rejection, a series of simulations was performed by varying the initial feed concentration and calculating the permeate and retentate concentrations as a function of recovery rate. These calculations were simply based on mass balances of the substance along the module, some of which is retained in the concentrate stream, some of which passes across the membrane (as a function of rejection). Based on the results from all the simulations, correlations were found between the various parameters, and the best analytical expressions were computed extrapolating the following equations (while these equations do not come from first principles, they are the exact descriptions of the relationships between the various parameters found from the initial simulations):

$$c_c = c_f e^{-Rej \cdot ln(1-REC)} \tag{2.1}$$

$$c_{tw} = c_f[\frac{1}{REC} - (\frac{1}{REC} - 1)e^{-Rej \cdot ln(1-REC)}] \tag{2.2}$$

Therefore, the redundant equation relating c_{tw} to c_c is:

$$c_{tw} = c_c[-(\frac{1}{REC} - 1) + \frac{1}{REC}e^{Rej \cdot ln(1-REC)}] \tag{2.3}$$

This preliminary analysis performed is valid for a system comprising one stage, one pass and no bypass. This means that the concentrate and the permeate stream do not undergo further filtration while the 100% of the feed water is treated, respectively. The analysis is independent of the number of vessels or modules. However, it is assumed that all vessels contain the same number of modules in series. Equations 2.1-2.3 may be employed to conduct a preliminary estimation of the nanofiltration performance in term of concentration of pollutants in the different streams. For example, it can estimate the pollutant concentrations in the final permeate produced by treating feed water with a known level of contamination, using a specific nanofiltration membrane, i.e., a given value of observed rejection, and by simulating different recovery rates for the system studied. Once the main parameters were estimated, these were used as first guess for the following full-scale system design performed using two software programs. WAVE (Dow Water & Process Solutions) was used to design the best module configuration and to simulate the chemical composition of the treated water. AQION was chosen to determine the hydrochemistry and to calculate the Aggressive Index (A.I.) and the Alkalinity of the water streams.

Life Cycle Assessment

Open LCA software was employed to perform the life cycle assessment of the full-scale nanofiltration plant. OpenLCA LCIA method 1.5.7 was used as impact assessment method, with ReCiPe as methodology. Both midpoint and endpoint indicators were considered, the latter presented as normalized values with respect to the total computed endpoint impact. The environmental assessment of the full-scale NF plant was performed considering a specific functional unit: the average daily drinking water demand of the specific location (30 L/s). Attributional LCA was chosen as LCA analysis with hierarchist (H) perspective. The inventory data for the NF system were calculated based on the available literature [120], while the concentrate disposal and the energy requirements were directly imported from the analysis carried out through WAVE. Since previous research showed the negligibility of the burdens related to the disposal of building construction of similar membrane treatment plants [120], the decommissioning of the nanofiltration system was not taken into account in the LCA analysis.

2.3 Results and Discussions

The following section presents the results with the related discussions:

1. In order to choose the appropriate NF membranes for the production of drinking water from chromium contaminated sources, lab experiments were performed first. These tests were conducted to assess the influence of physico-chemical parameters of aqueous solution on membrane filtration performances (i.e. in terms of membrane productivity and chromium selectivity) and to evaluate whether and how the presence of oxidizing agents in solution can affect the membranes behavior.

2. To finalize the membrane performance evaluation at the lab scale, preliminary investigation was also carried out by filtering real well water samples and tap water contaminated by chromium.

3. The achievable membrane performance in situ was evaluated through a semi-analytical system-scale analysis.

4. Based on the results, the two most promising membranes were chosen to perform the pilot scale study in situ, an essential step to analyse membrane module performances and to set up the boundary conditions for the full-scale system modelling and design.

5. Finally, the design of the potential full-scale NF installation is proposed for the specific location studied, together with its economic/environmental analysis. System parameters were also deeply investigated through system-scale analysis in order to present guidelines for the design of similar nanofiltration unit.

What is reported below has been already presented in previously published papers [82] and [83].

2.3.1 Influence of ionic composition, pH, and chromium speciation on membrane flux and Cr(VI) rejection

Ionic Composition

The effect of ionic composition of the feed solution on membrane performance is presented in Figure 2.3. In the case of polyamide membranes, by increasing the ions concentration in solution the permeate flux was significantly reduced. In particular, calcium chloride is affecting the flux more than the other studied compounds (NaCl). Since $CaCl_2$ is rejected at higher rate compared to NaCl by polyamide membranes, as $CaCl_2$ rejection increases, salts accumulate at the solution/membrane interface, thus lowering the driving force to permeation (Figure 2.3a, b). Sulfonated polyethersulfone membrane (Hydra70) showed a low or negligible reduction of flux at increased ionic strength (Figure 2.3c). This observation is a first indication of a different separation mechanism by polyamide and sulfonated membranes, the latter dominated by electrostatic effects. These results are consistent with previous studies, which reported similar separation mechanisms [34].

Accumulation of ions at the membrane/solution interface may reduce the ability of the membranes to reject contaminants through electrostatic effects, causing the screening of the membrane surface charges and compression of the electric double layer. The influence of calcium ions to decrease Cr(VI) rejection was significant with NF270 (Figure 2.3d). The rejection of co-ions at neutral pH ascribable to the Donnan effect is decreased by the presence of higher valence counter-ions shielding the negative charges at the membrane interface. However, the larger effect of calcium compared to sodium at similar ionic strengths is attributed to chemical binding of this divalent cation to the functionalities of the membrane, effectively neutralizing them [121]. The results obtained so far corroborates the hypothesis that the separation mechanism of the NF270 loose nanofiltration membrane is strongly based on Donnan exclusion. Previous studies also highlighted the importance of electrostatic-based separation together with size exclusion, for loose polyamide nanofiltration membranes [118, 119]. On the other hand, the presence of solutes in feed water does not influence negatively the Cr(VI) rejection capabilities of NF90 (Figure2.3e). This result, together with the rejection of different ions presented in Table 2.2, suggests the dominance of size exclusion and solution-diffusion mechanisms for NF90 membranes toward the removal of Cr(VI).

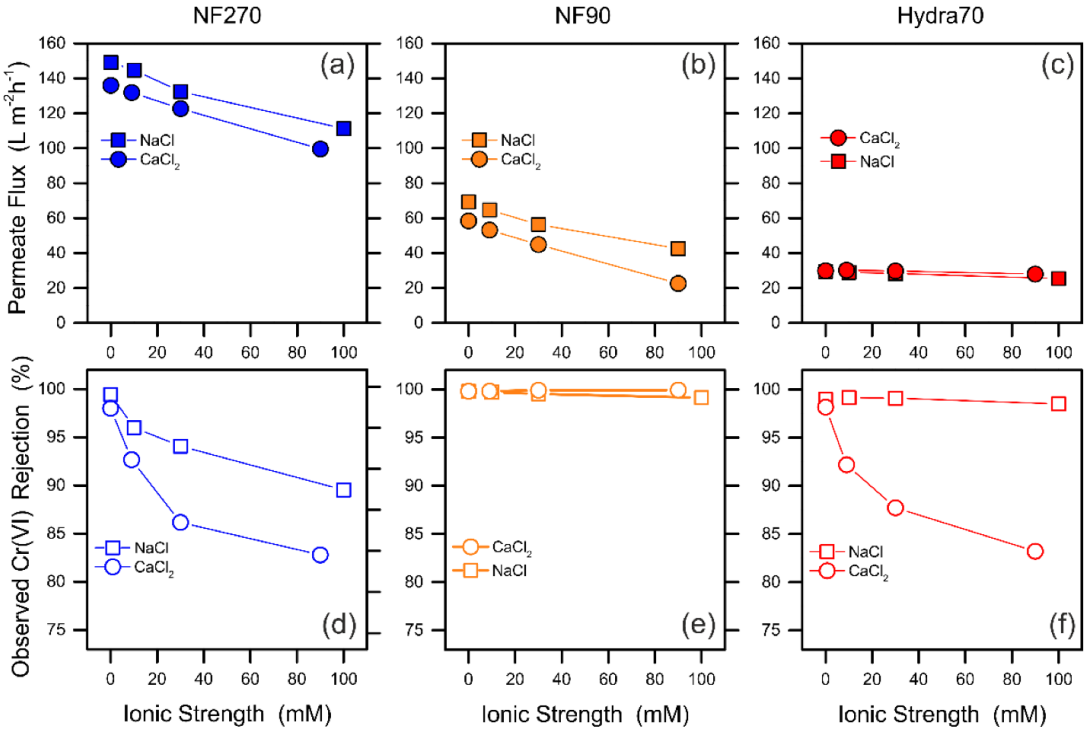

Figure 2.3: *Results of the influence of salt concentrations (expressed as ionic strength) on membrane properties. Experiments performed at pH 7.6. Results refer to Hydra70 (right column, red), NF90 (middle column, orange) and NF270 (left column, blue). (a, b, c) permeate flux; (d, e, f) Cr(VI) observed rejection. Lines are only intended as guide for the eyes.*

Regarding Hydra70 membranes, while the presence of sodium chloride does not affect the Cr(VI) rejection, increasing the $CaCl_2$ concentration in solution would negatively affect hexavalent chromium rejection (Figure 2.3f). In this case, this phenomenon cannot be attributed to concentration polarization, due to the negligible change in water flux observed with the increase of the ionic strength in feed solution. Instead, the hexavalent chromium rejection may be dependent on the membrane-solutes and solutes-solutes interactions. The presence of divalent cations in solution may decrease the efficiency of Donnan exclusion mechanisms by inducing the formation of ion-pairs with the negative functional groups at membrane surface [122], with consequent passage of chromium in the permeate.

To analyse further the importance of the electrostatic effects on membrane selectivity performance, zeta potential measurements were carried out. The overall results are summarized in Figure 2.4. Across the entire pH range, the Hydra70 exhibited the highest magnitude of negative potential among the three membranes, consistent with the nature of its sulfonated moieties; see Figure 2.4a. Polyamide membranes possess instead carboxyl groups at their surface: the looser NF270 membrane had lower (more negative) zeta potential than the denser NF90 membrane and their IEP were roughly 3 and 5, respectively. These results corroborate that electrostatic effects are important separation mechanisms, especially for Hydra70 and NF270 membranes. Zeta potential measurements in solutions of different ionic strengths followed this same trend. Data in Figure 2.4b also suggests that the zeta potential depends not only on the pH value but also on the type and concentration of salt [123]. At neutral pH and with similar ionic strength, the magnitude of the potential was much lower in $CaCl_2$ solution compared with NaCl solutions. This result confirms the hypothesis of specific chemical interactions of calcium with membrane moieties, resulting in charge neutralization and causing the easier passage of hexavalent chromium through membranes governed by Donnan exclusion as separation mechanism [121].

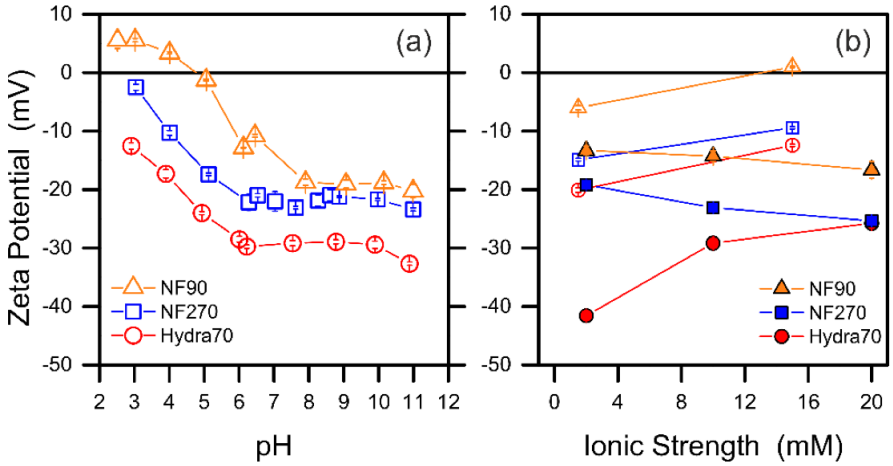

Figure 2.4: *Zeta potential of the membranes as a function of (a) pH in 10 mM NaCl and of (b) ionic strength at a pH value of 7.4 ± 0.5. In (b), empty symbols refer to $CaCl_2$ while solid symbols to NaCl. Experiments were performed at a temperature of 25 ºC, for each of the membranes studied (NF90 represented by orange triangles, NF270 represented by blue squares and Hydra70 represented by red circles). Lines are only intended as guide for the eyes.*

pH and influence of chromium speciation

Figure 2.5 summarizes the effect of pH on the membrane performance. The observed changes in permeate flux (Figure 2.5a) and in Cr(VI) rejection (Figure 2.5b) are reported for all membrane samples. Decreasing the feed solution pH would translate in higher permeate fluxes in the case of the loose polyamide nanofiltration membrane NF270. A shallow maximum is exhibited around the pK of carboxyl groups, in agreement with what reported by other researches, who ascribed this behaviour to two possible factors: (i) a lower osmotic pressure at the membrane surface and (ii) the swelling of the active layer caused by acidic hydrolysis, which would increase the hydrophilic sites in the membrane matrix [119, 124]. An opposite trend was observed for tight polyamide NF membrane (NF90), with flux slightly decreasing at acidic pH. This may be ascribed to the presence of a denser polyamide layer on top of the membrane, less subjected to acid hydrolysis, and a more dominant contribution of concentration polarization.

Nevertheless, at acidic pH, the decrease of the negative charge at the membrane surface would be reflected in a significant drop of Cr(VI) rejection for both the polyamide membranes, mainly due to the consequent decrease in the magnitude of Donnan exclusion mechanism. This is proved also by the measurements of the surface membrane potential, which decreased significantly below pH 5 for both polyamide membranes; see Figure 2.4a. The decrease in chromium rejection at acidic pH is also caused by the speciation of hexavalent chromium itself, no longer present in form of divalent anions that were dominant at neutral pH but as monovalent $HCrO_4^-$. The low $HCrO_4^-$ membrane selectivity may be ascribed to the (i) low valence of this anionic species, which would be translated in a reduction of the overall size of the hydrated ions and (ii) the lower ion charge density compared to the divalent anion found at neutral pH. These two chemical characteristics can enhance the diffusivity of chromium within the polyamide layer and can lower the repulsion of the contaminant by the membrane surface charge, respectively [121].

Hydra70 membrane showed a different behaviour, in accordance with the type of functionalities present at the surface. Figure 2.5a shows a negligible drop in permeate flux with little variation in Cr(VI) rejection with decreasing pH. This result, consistent with previous studies [125], is rationalized with the observed ionized nature of sulfonated groups in the entire pH range (Figure 2.4a), corroborating the importance of electrostatic effects for the rejection of contaminants with like charges [126, 127].

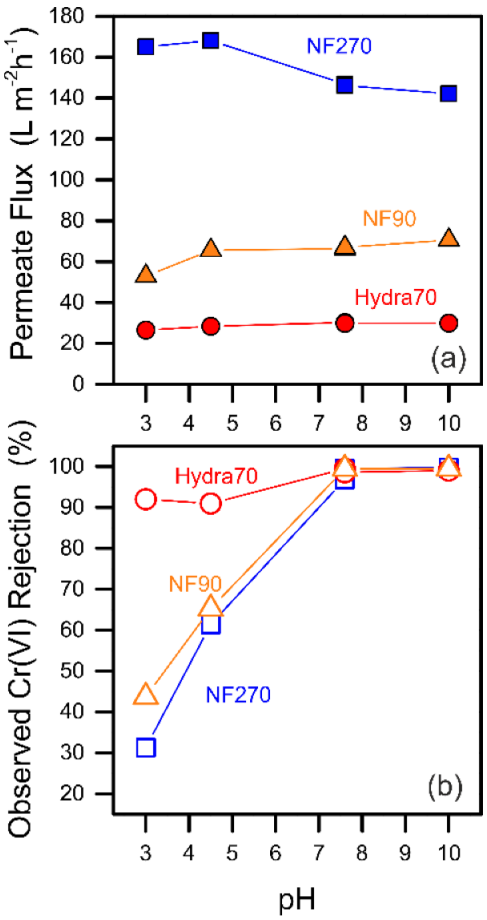

Figure 2.5: *Results of the tests performed at different pH of the feed solution. (a) Permeate flux; (b) Cr(VI) observed rejection. Results are reported for polyamide NF270 (blue squares), polyamide NF90 (orange triangles), and sulfonated polyethersulfone Hydra70 (red circles) membranes. Lines are only intended as guide for the eyes.*

The results obtained varying the relative amount of trivalent and hexavalent chromium in DI water are presented in Figure 2.6. An increase in Cr(III) concentration produced a decrease in the permeate flux and a simultaneous increase in the total chromium rejection by membranes. This result is rationalized with the presence of sparingly soluble $Cr(OH)_3$ in water at neutral pH. The uncharged species might be removed by size exclusion by the membrane and deposit onto its surface, thus enhancing the overall rejection of the heavy metal. A further proof of this deposition mechanism is given by the decrease of total chromium concentration in the feed water, which was observed in time during the separation tests (not reported here). Hydra70 showed the same behaviour as NF270 when the 50%/50% ratio of Cr(VI)/Cr(III) was employed. As expected, the membrane material had negligible influence on the deposition of suspended and sparely insoluble $Cr(OH)_3$.

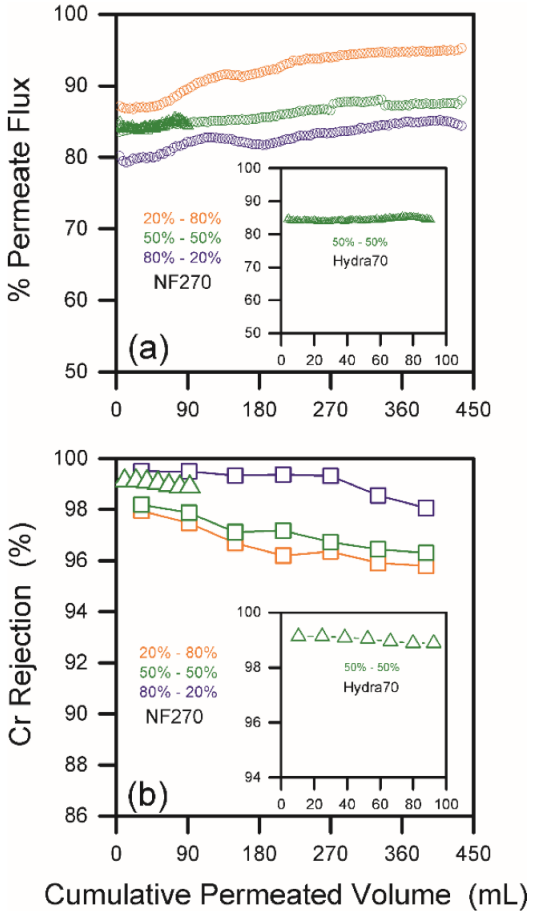

Figure 2.6: *Results of the tests performed by varying the relative amount of trivalent and hexavalent chromium in DI water. The results are presented for the different Cr(III)/Cr(VI) percentage 20% - 80% (orange points), 50% - 50% (green pont), and 80% - 20% (blue points). Results are reported for both NF270 and Hydra70, showing the trend of (a) permeate fluxes and (b) chromium rejection as a function of the cumulative permeated volume.*

Summary

Results obtained by varying chemical composition of feed waters have important implications for the deployment of commercial membranes in water treatment plants. Each type of membrane showed high values of Cr rejection at near neutral pH or above. However, the presence of divalent cations negatively affected the Cr(VI) rejection, mostly in the case of loose nanofiltration membranes where Donnan exclusion represents the main separation mechanism. Tight NF membrane instead, such as the NF90, exhibited high Cr(VI) rejection with high ionic strength solutions, ascribable to the denser nature of the selective layer. Therefore, hardness is an important parameter to consider when designing a nanofiltration system for chromium removal from aqueous mixtures. Specifically, results were schematically

depicted in Figure 2.7 and may be summarized as follows: (i) under typical surface or well water conditions, NF270 should provide adequate rejection mostly by electrostatic effects while guaranteeing the largest permeate fluxes; (ii) however, for feed water containing a greater amount of solutes or hardness, NF90 may be needed, which can provide consistently high Cr(VI) removal by size-based mechanisms, although at the expense of system productivity. (iii) Sulfonated polysulfone has lower permeability and is affected by divalent cations, while it is robust across a wide pH range and at high concentration of monovalent ions.

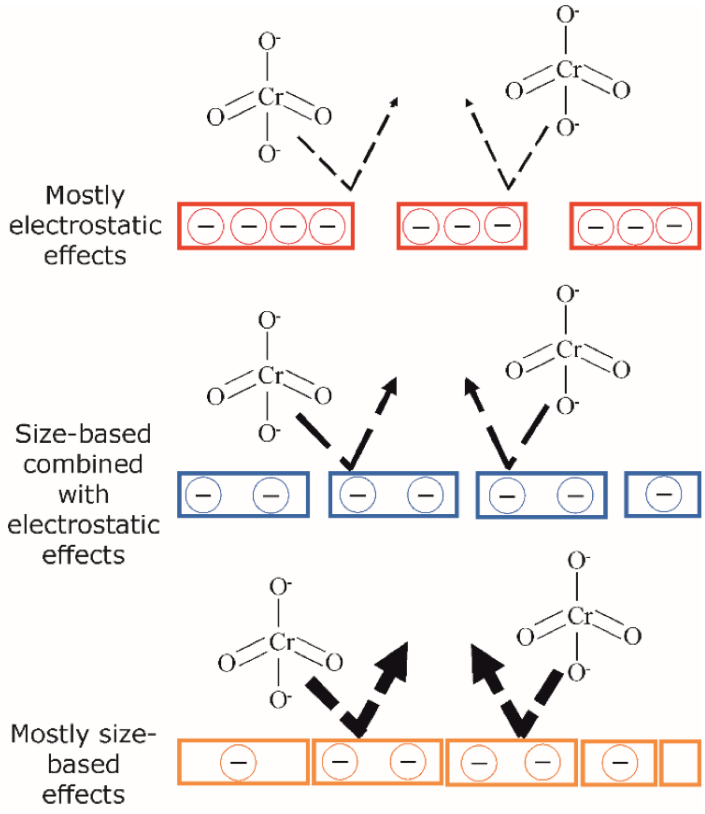

Figure 2.7: *Schematic representation of the mechanisms involved in Cr(VI) rejection and consequent extent of removal by nanofiltration membranes as a function of active layer density and surface charge.*

2.3.2 Performance of oxidized membranes

The membrane performance before and after exposure to oxidizing agents (concentrated hypochlorite and/or highly concentrated hexavalent chromium solutions) are presented in Figure 2.8 for both (a) NF270, (b) NF90, and (c) Hydra70. Overall, the NF270 performance might be strongly affected by the presence of oxidizing agents in solution. Namely, a 1.5 fold increase in permeate flux was observed after exposure to solutions of Cr(VI) alone, whereas the effect of hypochlorite and of combined Cr(VI)/NaOCl was less severe. The enhancement of water passage through the membrane may be ascribed to the degradation of polyamide, which would eventually result in loss of membrane integrity and irreversible damage to the polymeric matrix. Several studies have investigated the mechanism of chlorine attack on polyamide and a so-called "Orton re-arrangement" has been suggested [106]. Even if the mechanism is still uncertain, the proposed pathway involves the substitution of hydrogen on the amide nitrogen by chlorine followed by ring chlorination via an intramolecular rearrangement. Polyamide damage by hexavalent chromium has not been reported so far. However, some studies highlighted the role of transition metal ions in catalyzing polymer degradation processes [128]. Results also suggests that selectivity of the loose polyamide nanofiltration membrane (NF270) can be strongly affected by the presence of oxidizing agents in solution. In the case of NF270 membrane samples treated in the hexavalent chromium solution at high concentration, roughly a 10-time increase in Cr(VI) passage was observed during filtration (Figure 2.8d). Permeance of the tight polyamide nanofiltration membrane (NF90) was also affected by oxidation treatment. Enhancements of water passage were observed in the case of samples treated with either Cr(VI) or NaOCl, while lower permeance was measured for membranes treated with both Cr(VI) and hypochlorite, but variability among samples increased significantly. However, the NF90 showed high rejection of Cr(VI) (>99%) after a 72-hour exposure to all the oxidizing agents investigated. Finally, Hydra70 did not exhibit significant changes in permeate water flux upon exposure to oxidizing agents and only a slight decrease in selectivity to Cr(VI) following contact with a solution containing both oxidizing agents. This result confirms that sulfonated polyethersulfone possesses an adequate chemical stability. The results are in accordance with other recent studies [129] and can be attributed to the lack of chlorine-sensitive amide group in the membrane matrix.

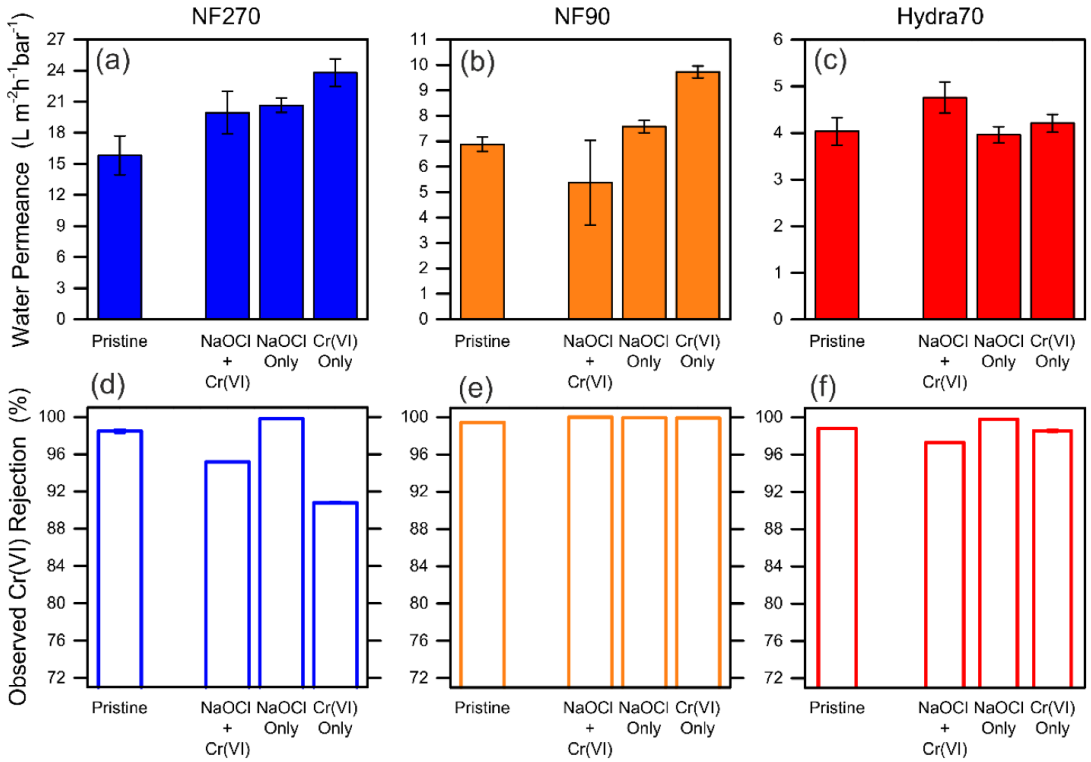

Figure 2.8: *Results of the experimental tests performed on membranes exposed to oxidizing agents. (a, b, c) Permeance values and (d, e, f) observed chromium(VI) rejection percentages are reported as filled and empty bars, respectively: (a, d) blue bars in the left column for NF270, (b, e) orange bars in the middle column for NF90, (c, f) and red bars in the right column for Hydra70. Results are presented for pristine membranes as well as for samples after accelerated contact with hexavalent chromium, sodium hypochlorite, or a mixture of the two agents.*

Based on the results discussed above, it can be stated that:

- NF270 performance are mostly affected by contact with hexavalent chromium
- Selectivity of tight polyamide nanofiltration membrane (NF90) to chromium is not negatively influenced by the exposure to oxidizing agents
- The presence of both Cr(VI) and hypochlorite can affect the performance of sulfonated polyethersulfone membranes (Hydra70)

Taking into account the experimental results obtained by oxidized membranes, a performance analysis is reported for both NF270 and Hydra70 to describe the behavior of the membranes at increasing exposure times to oxidizing agents. In particular, the time required to increase the Cr(VI) concentration in the permeate stream upon contact with the most sensitive oxidizers or mixture of oxidizers was calculated for each type of membrane. To conduct the analysis, it was assumed

that the rate of change in relative concentration of the permeate stream (due to membrane oxidation) is proportional to the concentration of oxidizing agents in solution, $[OX]^{FEED}$, which is constant in time,

$$t : \frac{d(\frac{[Cr(VI))]^{PERM}}{Cr(VI)_0^{PERM}})}{dt} = k_{ox}[OX]^{FEED} \tag{2.4}$$

The above equation yields, upon integration:

$$\frac{[Cr(VI]_t^{PERM}}{[Cr(VI)]_0^{PERM}} = 1 + k_{ox}[OX]^{FEED}t \tag{2.5}$$

where $[Cr(VI)]_0{}^{PERM}$ is the concentration of Cr(VI) in the permeate stream at time zero, and k_{ox} is the kinetics constant of material degradation calculated for each membrane-oxidant combination from the results presented in Figure 2.8. As expected from the results shown in Figure 2.8, concentration of the contaminant in the permeate would increase faster for NF270 than for Hydra70 following membrane degradation; see Figure 2.9. For example, Figure 2.9a suggests an increase in Cr(VI) concentration in the permeate of 10% (i.e., 1.1 of the initial value) after only 2 years of operation, with a Cr(VI) feed concentration of 20 μg/L. Roughly the same degradation of Hydra70 would be reached upon a 3-year contact with both NaOCl and Cr(VI) at concentrations of 100 μg/L.

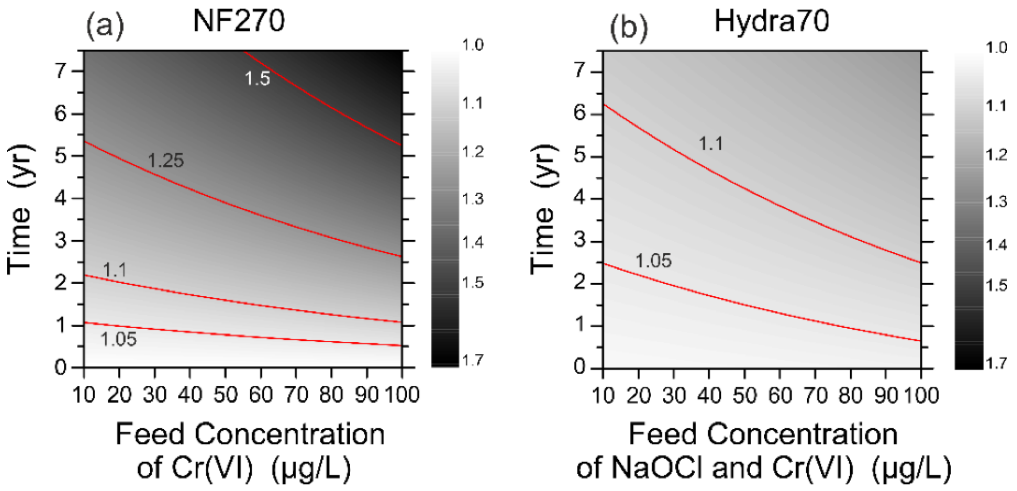

Figure 2.9: *Effect of membrane active film degradation upon exposure to oxidizing agents. Red isolines represent specific values of permeate Cr(VI) concentration normalized by the value of permeate concentration at initial time obtained with the pristine membrane. This analysis was conducted for (a) NF270 in contact with solutions of Cr(VI) and for (b) Hydra70 in contact with feed waters containing both Cr(VI) and NaOCl.*

2.3.3 Treatment of contaminated real water samples

Specific filtration experiments were performed with tap water spiked with Cr(VI) and real well water as feed solutions. Figure 2.10 presents the results from these tests. NF270 and Hydra70 showed high removal rates of chromium (> 85%) by filtering contaminated tap water; due to the results obtained with loose nanofiltration membranes, experiments with tight NF were not performed, since NF90 may thus be oversized for this feed solution. With higher rejection rate and an average permeate flux four times larger, the performance of the NF270 overcome those observed for the Hydra70. This is in agreement with the results discussed in previous sections. Since the tap water contains a medium ionic strength and hardness (see Table 2.3), the loose NF membranes are suitable for adequate Cr(VI) removal, while guaranteeing high permeate fluxes.

The results also suggest that the NF270 membrane may guarantee suitable quality of the product water with each of the three well waters, considering their Cr(VI) levels (Table 2.3). However, compared to the tests performed with tap water, important reductions of permeate flux was observed even in the case of real aqueous streams characterized by low total hardness (Figure 2.10). Since the well water samples were used as drawn from the well and without any pre-treatment, a strong influence on membrane performance may be given by the presence of trace of organic contaminants. In accordance with the results obtained with synthetic waters, the loss in Cr(VI) rejection was strongly influenced by the increase of ionic strength and total hardness of the feed solution. The loose NF membrane showed high rejection of chromium in the case of treatment of water samples coming from site B and site C, achieving a chromium concentration in the permeate stream close to 1 μg/L. The performance of the loose NF membrane was lower (with lower Cr(VI) selectivity) by treating the water samples coming from the Site A, which contain highest hardness, ionic strength, and Cr(VI) concentration compared to the other samples. A 6 μg/L of Cr(VI) concentration in the permeate was obtained by treating the water from Site A, which might be considered a threshold value for a large installation plant, taking into account a concentration safety factor for the heavy metal and possible loss in performance of the membrane in time. Therefore, it is important to further investigate the performance of the loose NF membrane with *in situ* pilot plant through long-term filtration experiments. Oppositely, tight nanofiltration membrane (NF90) showed an appropriately low concentration of hexavalent chromium in the permeate stream (0.3 μg/L) with a relatively high permeate flux when waters from site A were filtered. Considering the mentioned performance, the NF90 might be the most suitable membrane option to produce potable water from this specific site. Considering the results, the pilot plant investigation was performed also with NF90 membrane modules.

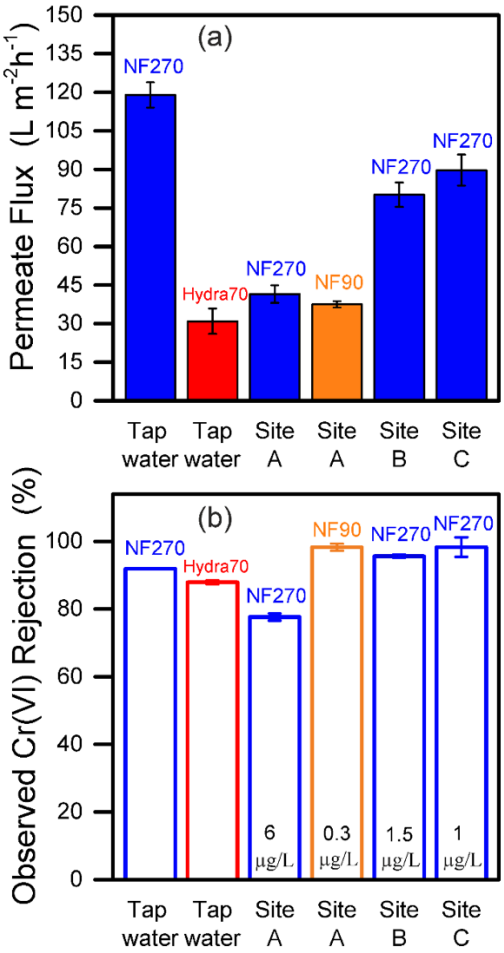

Figure 2.10: *Results of the experiments performed with tap and well water samples. (a) Permeate flux (solid bars) at an applied pressure of 100 psi (6.9 bar) and (b) chromium(VI) observed rejection (empty bars). Values of final total chromium concentration in the permeate samples are also reported inside the respective bars, for the experiments performed with well waters as feed solutions. Results for the NF270, NF90, and Hydra70 are presented in blue, orange, and red, respectively.*

2.3.4 From lab experiments to pilot plant study: choice of appropriate membranes

Table 2.5 summarizes the overall membrane behaviour discussed so far considering the results obtained with synthetic feed water. In particular, the table can be used as a first tool for the choice of the appropriate nanofiltration membrane for *in situ* application, depending on the chemistry of the source water.

The semi-analytical system-scale analysis (equations 2.1, 2.2 and 2.3) was applied to evaluate the achievable NF membrane performance for the abatement of

Table 2.5: *Summary of the behaviour and Cr(VI) removal observed with the different membranes.*

Membrane	**Cr(VI) separation mechanism**	**Influence of feed solution composition**	**Influence of oxidants in contact with the membrane**	**Observed range of Cr(VI) rejection in different waters at neutral pH**
NF270 High Permeability	Size-based and electrostatic effects	Decreased Cr(VI) rejection in solutions with medium-high ionic strength or low-medium hardness	Reduced performance upon contact with hexavalent chromium and/or hypochlorite	75-97%
NF90 Medium Permeability	Mostly size-based effects	Little influence of ionic strength or hardness	Little effect of oxidants	>98%
Hydra70 Low Permeability	Mostly electrostatic effects	Decreased Cr(VI) rejection in the presence of calcium	Slow degradation only when hexavalent chromium and hypochlorite are both present	80-98%

Cr(VI) from potable water in situ. The system-scale analysis was carried out considering the target Cr(VI) concentration in the product water and the variability of the following parameters:

- The Cr(VI) concentration in the feed water
- The feasible recovery rate of the system (i.e. the production of water with respect to the total water flow rate of the feed)
- The membrane rejection

Calculations were made by considering the increase in Cr(VI) concentration along the modules, due to accumulation in the retentate as a function of recovery rate. Figure 2.11 presents the results obtained for four specific recovery rate and for a wide range of feed and permeate concentrations of hexavalent chromium. The results reported in the graphs may be used to estimate the concentration of Cr(VI) in the product water given a certain combination of membrane properties and recovery rate, or to select a membrane (rejection) given a specific goal of product water quality. The system analysis was made considering the observed and not the real rejection of the contaminant. In other words, if users want to take advantage of this analysis, preliminary experiments (such as those reported in the previous section 2.3.3) need to be conducted to evaluate the membrane rejection with each site-specific feed water under conditions similar to those of the real system.

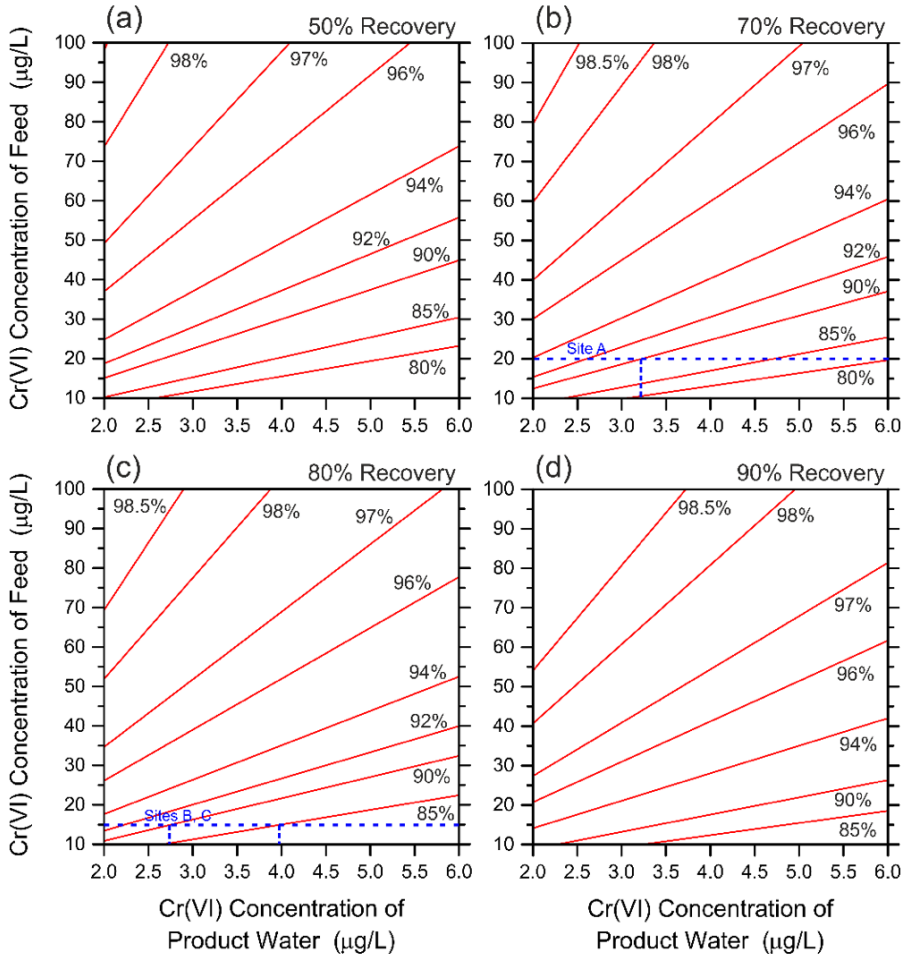

Figure 2.11: *Analysis for the selection of the membrane with appropriate observed rejection of Cr(VI) as a function of system recovery rate and Cr(VI) concentrations in the feed and in the product streams. Recovery rates of (a) 50%, (b) 70%, (c) 80%, and (d) 90%. Red lines represent different observed Cr(VI) rejection of the membrane. Range of concentrations: feed stream 10-100 µg/L, product water 2-6 µg/L of Cr(VI). This graph may be used to estimate the concentration of Cr(VI) in the product water given a certain combination of membrane properties and recovery rate, or to select a membrane (rejection) given a specific goal of product water quality.*

2.3.5 Pilot plant study: results and discussions

Given the results presented in the sections above, the most promising nanofiltration membranes to deploy for chromium abatement in well water from Site A would be the loose and tight polyamide membranes, i.e., the NF270 and NF90. The sulfonated polyethersulfone Hydra 70 indeed would not be suitable for the specific location studied, considering the productivity needed and the behavior/performance of the membrane. Therefore, only the two polyamide membranes were deployed for the pilot plant study, thus evaluating their performance *in situ*.

First, a detailed analysis of the membrane selectivity was carried out, filtering real well water samples from Site A in lab. The results are reported in Figure 2.12 for both the NF270 and NF90, showing the rejection of different inorganic compounds from the well water. As expected, NF90 presented higher selectivity than NF270, with a rejection above 80% for most of the elements or ions. Consistent with literature reports, boron was the only element removed at low rate [130, 131]. Indeed, nanofiltration membranes cannot achieve significant rejection of boron from water at neutral pH, due to the predominance of its uncharged specie (i.e. boric acid), which is not rejected neither by size exclusion, nor by the electrostatic effects. Multivalent anions, together with cobalt, iron, manganese, and selenium were almost completely rejected by both membranes. Zinc removal is instead strongly dependent on the nature of the associated ions, as already reported in previous studies [132]. However, lower selectivity was observed for all the cationic elements in solution by the NF270. This is clearly due to its main separation mechanism, strongly based on Donnan exclusion [82]. These results suggest the feasibility to reduce the concentration of chromium in potable water with both membranes. Indeed, the divalent chromate anion CrO_4^{2-}, which is the predominant chromium specie in drinking water, may be removed from water through the combination of electrostatic repulsions (thanks to the presence of negative surface on the membranes) and size-exclusion mechanism [82]. Specifically, NF270 and NF90 samples had a chromium removal of 78% and 98%, respectively. Monovalent ions, such as fluoride, chloride, and nitrate are mainly removed by size exclusion. This is in accordance with our results, showing significantly higher rejection by the NF90 compared to the NF270. The presence of other compounds in solution can thus influence negatively the electrostatic repulsions of monovalent anions by nanofiltration [133]. Table 2.6 is presenting the characteristics of the permeates produced by both membranes. All the concentrations of ions were well below the limits imposed by the Italian legislation. In term of water productivity instead, the looser NF270 showed only slightly higher values (40.3 $L\,m^{-2}\,h^{-1}$) compared to the tighter NF90 (37.5 $L\,m^{-2}\,h^{-1}$) at equivalent applied pressure.

Performance of the nanofiltration pilot plant

The pilot plant schematically described in Figure 2.1 was employed to perform two field experiments, aiming at evaluating the nanofiltration as a feasible technology for drinking water production from waters contaminated with chromium. The results of both tests are presented in Figure 2.13. Tests were conducted with an applied pressure of 5.25 bar (76 psi) for NF270, and 5.75 bar (84 psi) for NF90. The permeate flux started at roughly 480 L/h, in agreement with the values measured in preliminary lab experiments, expected as 480 L/h and 475 L/h for NF270 and NF90, respectively.

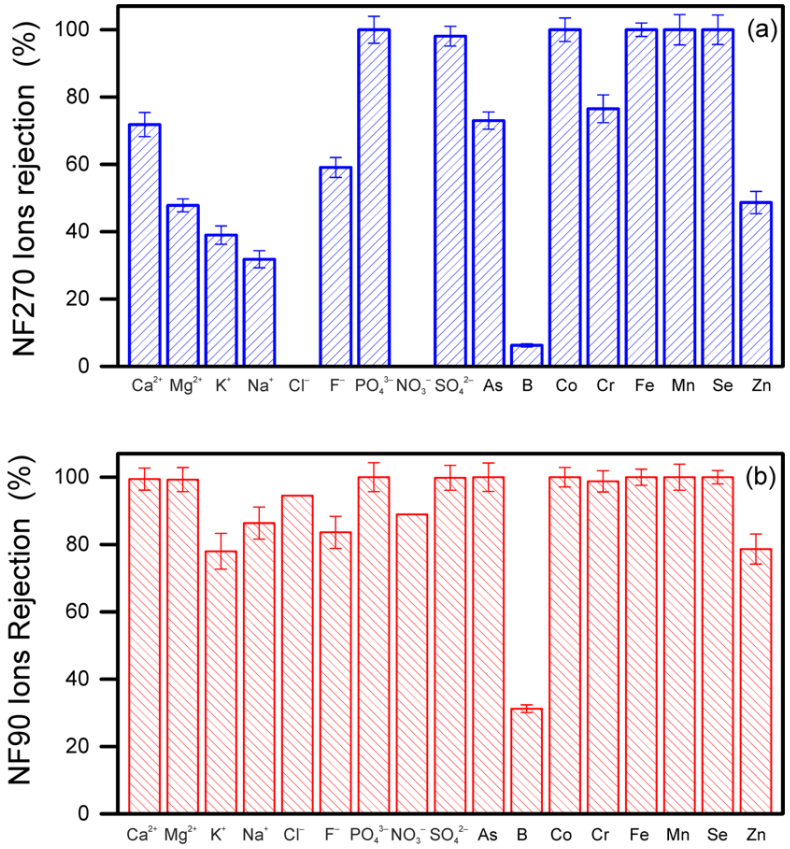

Figure 2.12: *Rejection of the most common cations, anions and metals from the well water described in Table 2.4 for both a) the NF270 and b) NF90.*

During the 42 days of experiment, both membranes showed significant flux decline, likely due to organic fouling and to the precipitation of metals and carbonate species onto the membrane surface. This result is in accordance with previous studies, performed to evaluate fouling and scaling on the membrane surface with similar feed water [134, 135]. The larger operating pressure and the higher selectivity of the membrane causes a slightly more pronounced decline of water flux in the case of NF90 modules compared to the NF270. It must be considered that only a very mild physical cleaning (running the feed water at higher flow rate 1 hour per week) of the membranes was performed and no chemical cleanings were carried out during the tests. No significant recovery of permeate flux was observed by restoring the operating parameters (the applied pressure) after the physical cleaning. The flux trends presented here can hence be considered as the worst possible scenario (i.e., the most conservative case, for such a system), since the flux decline in real application would be significantly lower with proper management system.

Table 2.6: *Concentration of the different elements in the product water produced by the NF270 and the NF90 membranes and comparison with the Italian legislation limits and the characteristics of the well water (Site A).*

Composition	Legislation Limit	Well Water (Site A)	NF270 Permeate	NF90 Permeate
pH	6.5 < pH < 9.5	7.5	8.3	7
Conductivity (μS/cm)	2500	646	256	12.8
Hardness (°F)	15 < °F < 50	36.8	22	15
Cl^- (mg/L)	< 250	9.9	13	0.54
F^- (mg/L)	< 1.5	0.11	0.045	0.018
PO_4^{3-} (mg/L)	/	0.03	0	0
NO_3^- (mg/L)	< 50	7.9	8.3	0.87
SO_4^{2-} (mg/L)	< 250	34	0.65	0.056
Ca^{2+} (mg/L)	/	110	31	0.61
Mg^{2+} (mg/L)	/	23	12	0.16
K^+ (mg/L)	/	1	0.61	0.22
Na^+ (mg/L)	< 200	11	7.5	1.5
As (μg/L)	< 10	1	0.27	0
B (μg/L)	< 1000	32	30	22
Co (μg/L)	/	59	0	0
Cr (μg/L)	< 10 [as Cr(VI)]	23	5.4	0.28
Fe (μg/L)	< 200	32	0	0
Mn (μg/L)	< 50	13	0	0
Cu (μg/L)	< 1000	0.12	0.22	0.23
Se (μg/L)	< 10	2.2	0	0
Zn (μg/L)	/	15	7.7	3.2

Chromium rejection and chromium concentration values in the permeates are shown in Figure 2.13b and 2.13c, respectively. The tight nanofiltration membrane NF90 was able to maintain a constant Cr concentration in the treated water below 0.5 μg/L, with a consequent Cr rejection of roughly 98% during the entire test. The loose nanofiltration NF270, on the other hand, was characterized by a gradual decrease of chromium rejection from 95% to 70% during the 42 days of operation. This result can be ascribed to the influence of fouling, scaling, and fouling-enhanced concentration polarization on membrane performance, which can neutralize and/or shield the negative surface charges of the membrane, thus lowering the effect of Donnan potential for chromium removal. Chromate anion (CrO_4^{2-}) is indeed the major chromium species in natural waters. On the contrary, the size-based rejection mechanism of the tight NF90 is less affected by the influence of fouling, scaling, and fouling-enhanced concentration polarization, showing a constant high removal rate of the contaminant.

The overall chromium selectivity observed in the pilot study was in accordance with the results obtained in lab experiments, where an average chromium rejection of 98.8% and 76.5% was estimated for the NF270 and the NF90 membrane, respectively. Given the results obtained so far, it can be stated that preliminary lab experiments represented a strong initial support to the pilot plant study, providing

representative results of *in situ* application. In particular, the permeate flux obtained in the lab may be regarded as the initial permeate flux for field application, or the flux that would be observed in real application for clean membranes. As for chromium removal, the rejection values measured in the lab were representative of the values observed during the pilot tests once steady-state conditions were reached.

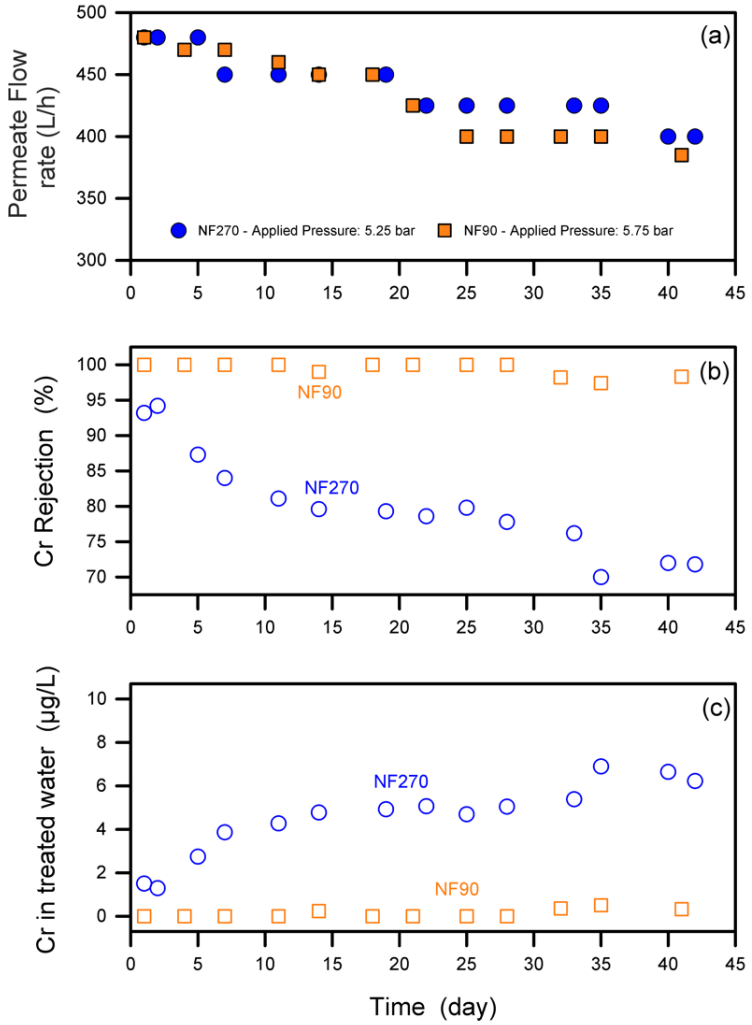

Figure 2.13: *Performance of the nanofiltration pilot plant. a) Permeate flow rate, b) Total chromium observed rejection, and c) Chromium concentration measured in the treated water. Results are presented for NF270 (blue circles) and NF90 (orange squares) for a test period of 42 days. Those represented are point-values measured day by day, therefore reported without any standard deviation. Physical cleaning was performed every week by increasing the cross-flow velocity to 30 L/min for 1 h*

2.3.6 Design of the full-scale nanofiltration plant

A full-scale NF plant was designed for the specific location studied (Site A). Given the promising results obtained during the pilot tests, the proposed configuration was set up to work with the tight nanofiltration membrane, NF90. Overall, even if the system designed is site-specific, it provides (i) an idea of the needs, performance, and cost of plants with similar size (i.e., feed flow rate of tens of L/s), and (ii) an overview of the feasibility of the application of nanofiltration for chromium / heavy metals removal in general.

The design simulation was performed taking into account (i) the drinking water demand of the specific location (30 L/s of potable water must be delivered to the surrounding area) and (ii) a target value of 80% for the recovery of the filtration unit. Based on the results obtained during the field experiments, the membrane system was designed to work with NF90-400/34i modules, characterized by an active area of 37.2 m^2. The dimensional characteristics and the operating limits of this module type are reported below in Table 2.7.

Table 2.7: *Dimensional characteristics and operating limits of the NF90-400/34i modules.*

Active Area (m^2)	37.2
Length (m)	1.016
Diameter (cm)	201
Maximum Operating Pressure (bar)	41
Maximum Feed Flow Rate (m^3/h)	17.03
Maximum Permeate Flow Rate (m^3/h)	1.43
Minimum Concentrate Flow Rate (m^3/h)	2.95
Maximum element recovery (%)	19

The best configuration designed for the NF plant is depicted in Figure 2.14. The system was modelled accounting for (i) the best operating conditions (with the aim to reduce the overall membrane area and the amount of energy to be supplied) and (ii) the quality of the product water. The system comprises two stages operated with nine and six vessels, respectively. Well water is pumped to Stage 1 and the concentrate from this stage is then processed by Stage 2. A percentage of the well water is bypassed and mixed with the permeate produced by the system, in order to ensure the potability of the final produced water (i.e., with appropriate mixture of ions). In particular, the membrane configuration described in Figure 2.14 would allow a range of bypass values between 0% and 30%. Concentrate is instead designed to be disposed of in the sewage system.

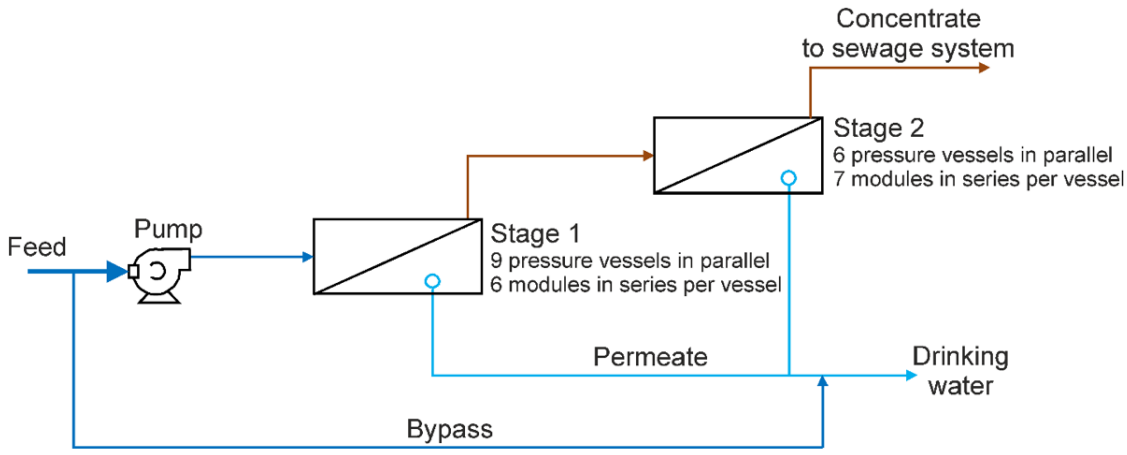

Figure 2.14: *Design of the nanofiltration pilot plant. Two stages are included. Stage 1 designed with 9 pressure vessels and 6 modules per vessel. Stage 2 designed with 6 pressure vessels and 7 modules per vessel.*

Results of the simulations performed based on the full-scale design represented in Figure 2.14 are reported in Figure 2.15a. The chromium concentration and the aggressive index (A.I.) of the produced water are plotted as a function of percentage of feed bypass. In practice, with larger bypasses, a lower proportion of demineralized water is mixed in the final produced water. This entails an increase of both chromium concentration and aggressive index, as expected. In particular, taking into account a safety/maximum chromium concentration of 5 μg/L in the product water and a minimum A.I. of 10, the suitable configurations for the NF system would be characterized by a bypass in the range of 10-15%. Below this range, the product water would be too aggressive, while above, it would contain a concentration of Cr too close to the limit of 10 μg/L.

A system analysis was also performed by applying equations 2.1-2.3. This analysis was here conducted specifically for chromium but it can be applied to analyse nanofiltration systems working for the abatement of any contaminants of interest. In particular, this analysis provides an estimation of the concentration of a specific substance in the streams entering and exiting the membrane plant as a function of recovery and system rejection rate. The overall results are presented in Figure 2.15b-d. Figure 2.15b shows the trend of chromium concentration in the final concentrate stream by varying the chosen recovery system and the Cr concentration in the feed water, at a specific observed system rejection of 98%, i.e., the Cr removal rate of NF90. Feed Cr concentration and recovery are represented on a linear scale on the left vertical and bottom horizontal axes, respectively. Dotted lines are drawn in the graph to exemplify the case of the NF plant designed for the specific location considered in this study. This graph can be used to estimate the largest possible recovery resulting in Cr concentration in the retentate that meets the limits for the

disposal of this stream in the sewage system. In our case, with a Cr concentration in well water of 23 μg Cr/L and a NF plant recovery rate of 80%, the concentrate would contain about 100 μg Cr/L of Cr. This value is below the legislative limit for the disposal of this stream in the sewage system as ruled by the Italian law, i.e., 200 μg/L.

Figure 2.15c is reporting a more detailed analysis, always accounting for a specific value of observed Cr rejection of 98%. This graph shows the highest recovery rates achievable, above which the chromium concentration would exceed 5 μg/L in the treated water and 200 μg/L in the concentrate stream. We can hence infer that the most relevant design parameter when tight NF membranes are deployed is the concentration of Cr in the retentate, as this boundary (blue line connecting squares) sits below that related to the permeate concentration (red line connecting circles), i.e., designing a plant with higher recovery would guarantee the safety of the treated water but impossibility to discharge the concentrate at low costs in the sewage system. The case of the employment of loose nanofiltration membranes is completely different. In this case, the system configuration and the recovery rate is limited by the Cr concentration reached in the product water (red line connecting circles). This can be observed in Figure 2.16 where similar analyses were performed with lower observed system rejections of 75%; 85%; 90%, or 95%. When decreasing the rejection capabilities (i.e., looser NF membranes), the permeate value becomes the more stringent parameters, with the two boundaries first overlapping and then crossing each other. Finally, the last modelling analysis is reported in figure 2.15d where the trend of Cr concentration in both the treated water (right axes) and the retentate stream (left axis) is plotted as a function of recovery rate for four specific chromium concentrations in the feed solution. While the models described in figure 2.15d were obtained for specific concentration ranges relevant for this present study, the overall analysis can be extended to wider concentration ranges. Figure 2.17 is an example. Overall, chromium concentration can vary significantly in the permeate (solid lines) and concentrate streams (dashed lines) by increasing the recovery rate of the system and with both loose and tight nanofiltration membranes.

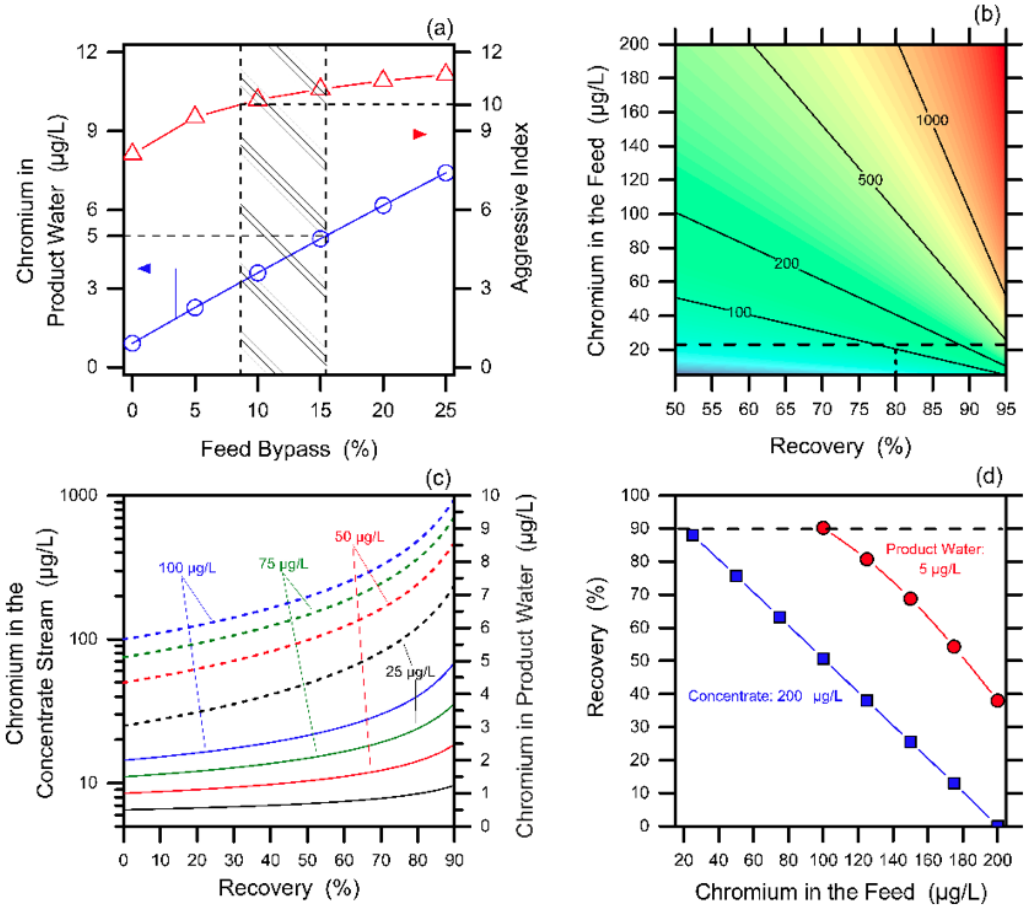

Figure 2.15: *Results of the system modelling and performance of the NF full-scale plant. a) Chromium concentration and aggressive index of the product water, as a function of the percentage of feed bypass, for the full-scale NF configuration of Figure 2.14 using NF90 modules, with the portion of feed bypass to apply to the final system configuration in order to respect the limits for Cr concentration in product water and for A.I. b) Chromium concentration in the concentrate stream as a function of recovery rate and Cr concentration in the feed stream, at a system rejection of 98%. Solid lines represent the different level of chromium concentration in µg/L in the concentrate stream. c) Chromium concentrations in the product water and in the concentrate stream as a function of the recovery rate for four values of Cr concentration in the feed water for a system rejection of 98%. Trend of chromium concentration in the product and concentrate stream represented by solid and dashed lines, respectively. d) Maximum recovery rate as a function of Cr concentration in the feed stream to obtain a Cr concentration in the treated water of 5 µg/L (red circles) and a Cr concentration in the concentrate stream of 200 µg/L (blue squares), for a system rejection of 98%.*

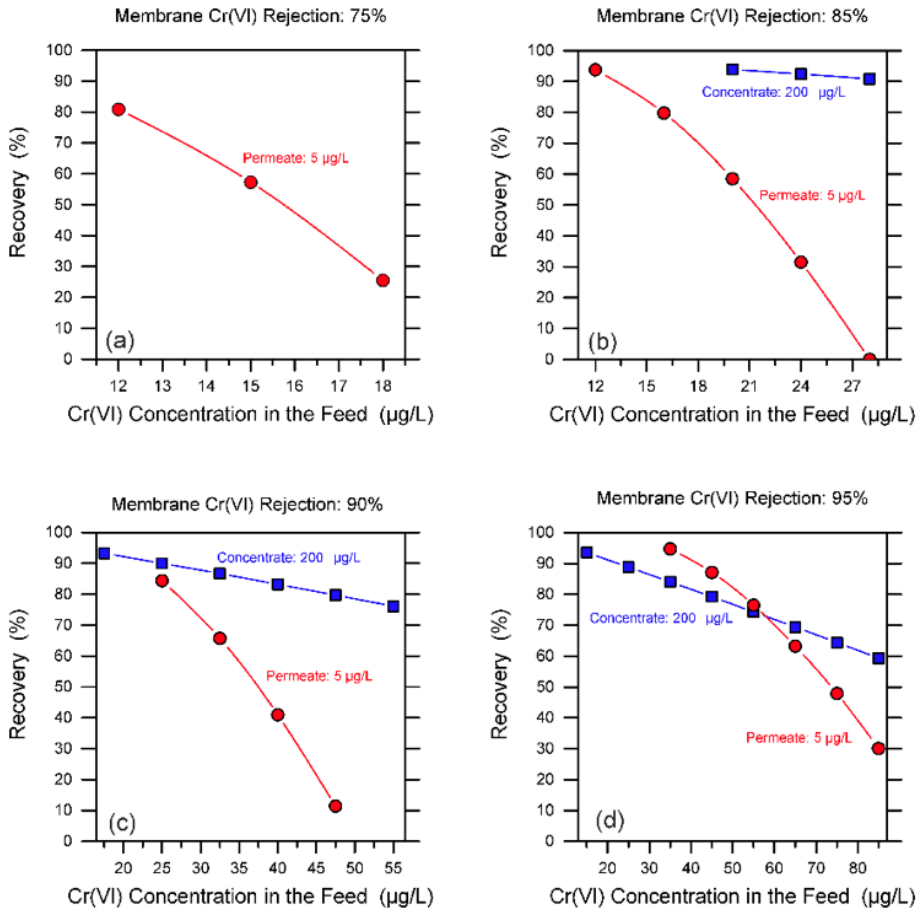

Figure 2.16: *Maximum recovery rate as a function of Cr concentration in the feed stream. Red line connecting circles represents the boundary for chromium concentration in the treated water (5 µg/L) while blue line connecting squares represents the boundary for chromium concentration in the concentrate stream (200 µg/L). Analysis was performed by changing the feasible membrane characteristics, i.e., for a system with observed rejection of a) 75%, b) 85%, c) 90% and d) 95%.*

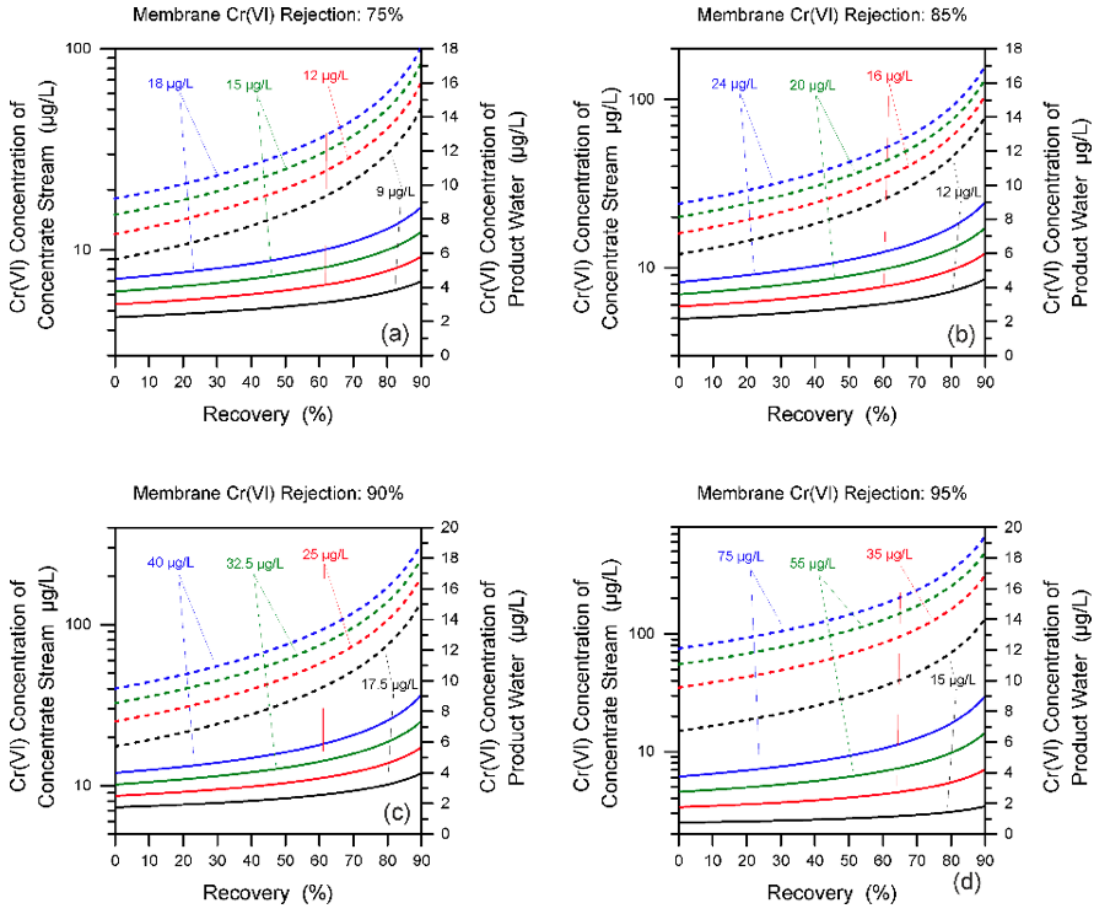

Figure 2.17: *Chromium concentrations in the product water and in the concentrate stream as a function of the recovery rate for various values of Cr concentration in the feed water for a system with observed rejection of a) 75%, b) 85%, c) 90% and d) 95%. Trend of chromium concentration in the product and concentrate stream represented by solid and dashed lines, respectively.*

2.3.7 Economic assessment

The economic assessment was performed on the full scale nanofiltration plant reported in Figure 2.14. Capital costs were estimated based on the economic assessment performed by Samhaber et al, in which the trend for installation and equipment costs for nanofiltration plants in tubular, plate & frame, and spiral modules is reported as a function of the product flow rate of water [[136]. In particular, authors estimated an exponential decrease of the Specific Equipment Cost (SEC) by increasing the number of modules required, reaching a plateau with an average cost of around 360 €/m^2 for plant designed to work with an overall membrane area larger than 500 m^2. A membrane replacement cost of €0.017 for each m^3 of product water was estimated based on a membrane lifetime of 5 years and a cost

of about €800 for each membrane module. Schafer et al. have estimated a similar cost for NF membranes applied to remove organic matter from water [137]. A 0.15 €/kWh was accounted for the energy system requirement, based on the selected geographical region. At the same time, a 0.31 €/m^3 was considered as cost for concentrate disposal into the sewage system. A cost of €0.01 for each m^3 of water produced was considered for membrane cleaning, taking into account the chemicals suggested by the membrane manufacturers for conventional cleaning-in-process operation [45, 116].

The computed capital and operating costs are presented in Table 2.8, together with a summary of the operating parameters for the NF plant designed. Overall, the plant was designed to work with 96 NF90-400/34i membrane modules (i.e., a total membrane area of 3568 m^2) in order to supply 2593 m^3/day of drinking water. The overall calculations were performed based on a feed bypass of 12.5% and an ideal recovery rate of 80%. In accordance with the results presented in figure 2.15a, this configuration allows the abatement of chromium in potable water below 4.3 μg/L, keeping an overall aggressive index of the product water above 10. The concentrated stream would result in 112 μg/L of chromium concentration, entirely disposable toward the wastewater treatment facility. The installation cost for the nanofiltration plant was estimated around 1.3 million euro and a total daily cost of €586 was calculated accounting for (i) a lifetime of 10 years for the membrane filtration plant and (ii) the amount of water to be produced per day. It can be observed that the cost of energy and those related to the concentrate disposal strongly affect the economic assessment of the NF plant accounting for 17% and 24% of the total daily cost, respectively. In accordance with previous studies, the cost of membrane replacement and chemicals are negligible compared to other items [45, 116]. Therefore, there would not be any essential cost abatement by the improvement of specific cleaning procedures or cleaning solutions. On the other hand, coupling the NF system with renewable energy sources would results in overall economic benefits.

Table 2.8: *Economic assessment of the nanofiltration plant designed.*

Operating Parameters	
Drinking water supply (m^3/day)	2593
Total well water (m^3/day)	3142
Bypass water (m^3/day)	393
Feed water to NF (m^3/day)	2749
Permeate water produced (m^3/day)	2200
Concentrate water produced (m^3/day)	549
Cr concentration in the product water (µg/L)	4.26
Cr concentration in the concentrate stream (µg/L)	112
Aggressive index of produce water	10.4
Total membrane area (m^2)	3568
Feed Pressure (bar)	6.56
Specific energy (kWh/m^3 of pumped water)	0.29
Total installation cost of the plant (€)	1,296,000
Cost per m3 of potable water provided (€)	
Capital costs (depreciation, lifetime 10 years)	0.14
Energy	0.046
Concentrate disposal	0.066
Chemicals	0.009
Membrane replacement	0.01
TOTAL	0.271

2.3.8 Environmental Impact Assessment of the full-scale NF plant

An analysis was performed to understand the process phases or the plant issues that would have the largest impacts on the environment. Figure 2.18 presents the results of the LCA analysis performed on the full-scale NF plant reported in figure 2.14, with the endpoints indicators summarized in Figure 2.18a. The power supply needed to pump well water in the NF system at the desired hydraulic pressure and necessary to heat up the cleaning solution is significantly higher than the other environmental burdens related to both concentrate treatment and to the installation and operation of the membrane plant, i.e., building construction, membrane modules, and cleaning agents. This result is in accordance with previous studies, which underlined the need to improve the operating phases of membrane systems to achieve lower environmental impacts [120, 138].

The results at the midpoint level is reported in figure 2.19. Again, power supply represents the most impactful item on all the midpoint parameters, except for freshwater and marine eutrophication. Figure 2.18b-d present the absolute impact

values related to both these parameters, as well as to climate change. Due to the large amount of freshwater necessary for building construction, membrane modules fabrication, and cleaning agents, freshwater eutrophication is a critical effect. This result is in accordance with others from previous studies analysing the overall impacts of ultrafiltration plants [63]. When dealing with marine eutrophication, the most important factors increasing it are the concentrate stream treatment and power supply, the latter burden also having the largest impact on CO_2 emissions.

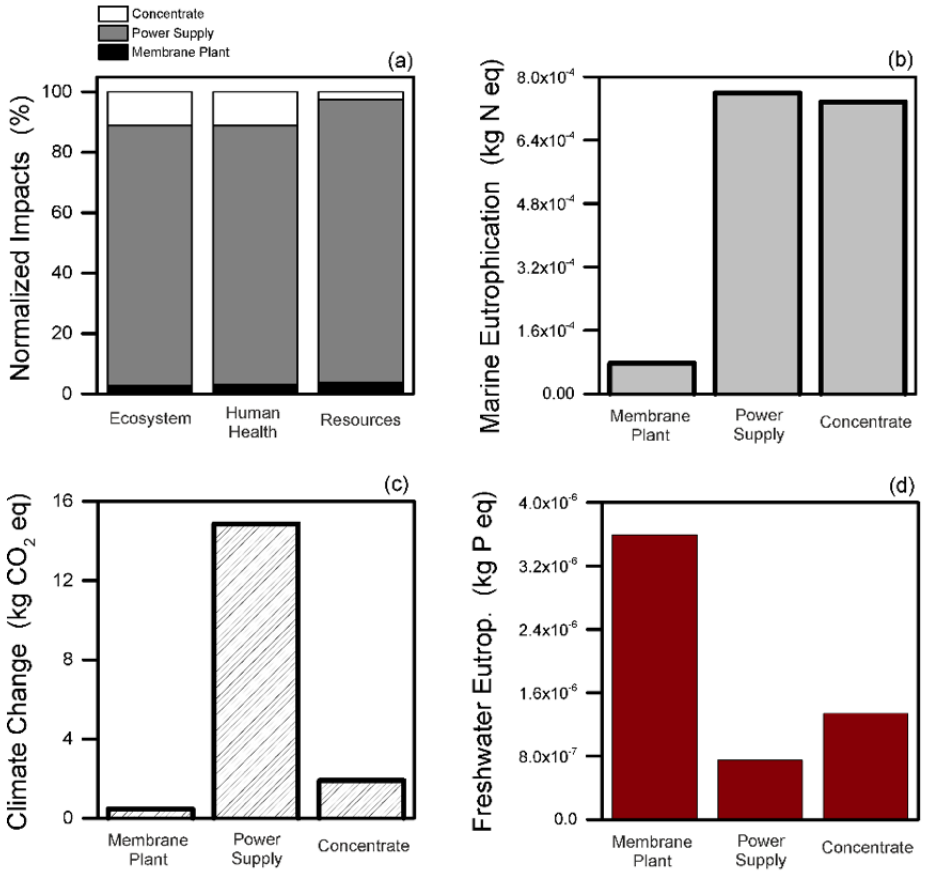

Figure 2.18: *Environmental impacts of the full-scale NF plant. a) Results obtained through endpoint analysis, presented as normalized values of the overall impact computed for membrane plant, power demand, and concentrate treatment. b-d) Results obtained for three representative midpoint indicators.*

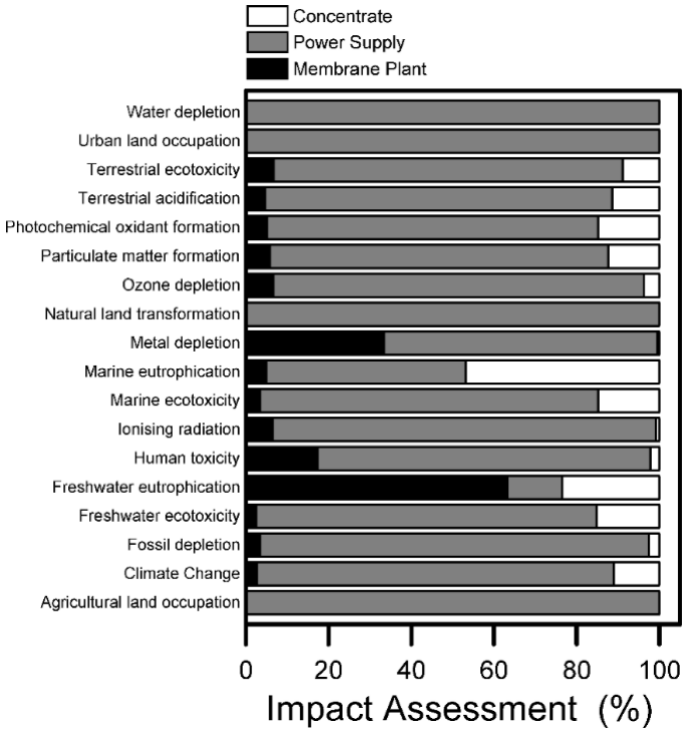

Figure 2.19: *Environmental impacts of the full scale NF plant evaluated at the midpoint indicators. Results are presented as relative impacts related to the various materials and processes involved in the process. Functional unit is the daily drinking water demand for the specific location studied (30 L/s).*

2.4 Conslusion

This study is exemplary of the research pathway to follow in order to analyse a specific process/application of a membrane-based separation technology from the "micro" to the "macro" scale (lab-to-full scale approach). In this study, through the combination of laboratory experiments, pilot-scale field tests, and system design, the applicability of nanofiltration to produce safe potable water was demonstrated for groundwaters containing heavy metals, and specifically chromium(VI). The study focused on the removal of chromium from water with the aim to achieve the new stringent limit of 0.01 mg/L of Cr(VI) in potable water. From laboratory experiments, we can conclude that Cr(VI) rejection is strongly influenced by chromium speciation, the chemistry of the feed solution, and the separation mechanism of the different membranes. Cr(VI) rejection increased when the feed pH was varied from acidic to neutral. These trends were caused by speciation of chromium and its interaction with the charged membrane surface. The presence of salts in the feed solution also affected the performance of two of the membranes analysed:

NF270 and Hydra70. The most negative effect was observed in the presence of calcium ions in solution, which can neutralize the active film charges of the membranes. NF90 can instead maintain very high contaminant rejections even in the presence of hard water, thanks to its intrinsic higher selectivity due to size exclusion. Looking at the results obtained during filtrations performed on oxidized membrane samples, the degradation of the polyamide selective layer was observed in some cases. In contrast, Hydra70 suffered little loss of selectivity. Overall, the results suggest that all the membranes investigated here may reach the new stringent limits for hexavalent chromium in drinking water when treating sources contaminated by this metal. However, the chemistry of the feed water governs the selection of the most appropriate membranes.

The results obtained at the pilot scale suggested that the choice of the suitable NF membrane is essential to overcome inefficiencies related to fouling and to the impairment of system performance during operation. For the specific location investigated in this study, the utilization of NF membranes with medium-high selectivity was indispensable to meet the requirements in terms of drinking water quality and specifically of chromium concentration. Moreover, the results obtained with the pilot unit were very consistent with those observed at the lab scale, entailing the importance of performing preliminary lab investigation prior to pilot studies and full-scale system design, to gain a reliable insight into the membrane performance and behaviour in situ. A potential design for a full-scale NF plant for chromium removal was also presented, based on the data available for the location studied, i.e., flow rate and chromium concentration in the feed stream. Two stages and a feed bypass of roughly 15% would allow the production of safe potable water with (i) an aggressive index higher than 10 and (ii) a chromium concentration lower than 5 μg/L. This design may be generalized for plants of similar size and it can be used as a preliminary estimation of the plant requirements for a variety of NF applications. This generalization may be carried out also thanks to a proposed system scale analysis, able to provide preliminary guidelines for the design of generic nanofiltration systems. Specifically, at high recovery rates, the main design parameter of NF plants treating waters contaminated by toxic metals may be the composition of the final retentate stream, which needs proper management also owing to the resulting high concentration levels of the target toxic metal.

Techno-economic and environmental assessments were performed for the potential full-scale plant, to understand the real feasibility of NF implementation for drinking water applications. The results showed a total cost of < 0.3 €/m^3 for the product water. The total installation cost for the NF plant was estimated to be €1.3 million, while concentrate disposal and energy requirement would represent the costliest operating parameters. Power supply would also be the most impactful item for the environment based on the LCA analysis performed for the installation and for the operation of the NF plant.

To conclude, a brief discussion of the possible advantages and drawbacks of the nanofiltration application studied and developed in this chapter should be presented. Overall, the results showed that nanofiltration may represent a valuable alternative to conventional treatment train for potable water production from groundwater contaminated by heavy metals. NF systems can be easily adapted and designed based on the characteristics of each specific location and feed water. Different membranes are available commercially and can be employed to perform an in-depth analysis of the system performance before pilot installation. Moreover, the final membrane configuration can be designed to work with low footprint. Thanks to the modular configuration, and the requirement of the only pumping system for the filtration process, the nanofiltration can be also considered one of the best treatment technologies for potable water production in relatively remote areas. However, fouling may be the bottleneck of the application and it should be analysed deeply to design a Cleaning In Place (CIP) system able to maximize the membrane performance and lifetime. In some cases, depending on the feed water characteristics, a pre-filtration or pre-treatment process may be advantageous. Besides, the membrane system should be designed to simplify the wastewater effluent disposal. In the specific application reported in this study, the system was designed to produce a wastewater effluent suitable for discharge into the sewage system, without pre-treatment or further costs to be considered. However, in real operation, the wastewater effluent characteristics should be analysed constantly to verify that the contaminant concentrations are indeed below the limit imposed for the discharge.

Chapter 3

FO-NF system to reclaim high-quality water from brackish groundwater and wastewater *

3.1 Introduction

At present, groundwater and seawater represent two of the main sources of freshwater. However, aquifers are being depleted due to their widespread exploitation [141], while seawater requires energy intensive technologies (e.g., reverse osmosis or thermal desalination units) to remove the large concentration of salts and contaminants [142]. Therefore, mid-salinity waters, such as brackish groundwater or wastewater, are becoming valuable alternatives for freshwater supply.

In recent years, the treatment of wastewater and brackish groundwater has been studied by applying different technologies [143, 144], with membrane filtration among the most promising options. Research has shown the feasibility to produce high-quality water by treating wastewaters with membrane bio-reactors (MBR) or membrane steps coupled with advanced oxidation processes [145, 45, 146]. Nanofiltration (NF) and low-pressure reverse osmosis have been instead proposed as feasible technologies for the purification of brackish groundwater sources, thanks to their high removal rate of TDS [147]. However, fouling would affect severely the lifetime of the membranes involved in pressure-driven filtration processes, with a consequent increase of the overall cost of the system [148]. For this reason, current research is focused on the evaluation of innovative membrane technologies or treatment scheme based on different driving forces.

*part of the content reported in this chapter, with permissions, has been already published in [139] and [140]

Thanks to its low fouling propensity, forward osmosis (FO) was reported as one of the most promising solutions in the case of treatment of complex water sources, such as drilling mug, liquid foodstuffs ,or fracturing flowback water [55, 149, 150, 151, 54]. So far, most of the research was focused on membrane development, module design, and identification of the most suitable draw solutions [152, 153, 154]. Different membrane materials were proposed to enhance membrane performance and to reduce the detrimental effect of internal concentration polarization [155, 156]. Comprehensive studies were reported to assess the behavior of different draw solutes [157, 158]. Phuntsho et al. have studied fertilizers as DS for the treatment of brackish groundwater [157], while Achilli et al. have reported a comprehensive overview of the most commercially available inorganic draw solutes [158]. All these studies have increased the understanding of the FO process and promoted its rapid development, but mainly focusing on the optimization of specific sections of the FO technology, e.g., the membrane or the draw solute. Few studies were carried out to evaluate the FO performance in combination with feasible post-treatment processes, such as other established membrane filtration systems (RO, NF) [159, 160]. Some researchers investigated FO coupled with RO or NF to treat wastewater effluents and promising results were also reported for a forward osmosis – nanofiltration system applied for the treatment of brackish water [161, 162, 159]. However, these studies lack data related to the feasibility of draw solution recovery and on the quality of the final product water.

The literature also provides theoretical calculations strengthening the economic and environmental potential of full-scale FO-based systems [163, 80, 81, 164, 165], but very few experimental reports exist on these issues. Some modelling-based research was carried out to study the possible module designs and to compare feasible configurations, e.g., co-current vs counter-current, but focusing only on mass transfer mechanisms and without looking at the overall system process [75, 166, 167, 168, 156]. Ali et al. have also developed a software tool to optimize the performance of full-scale FO system based on the utilization of innovative spiral wound elements [169]. This represents a useful tool but it comprises only the FO step, without accounting for the recovery process and without considerations related to performance reduction due to fouling.

Overall, these studies have increased the understanding of the FO process and promoted its rapid development, but they do not yet address some of the most important parameters affecting the process performance, i.e., (i) the feasibility of achieving high-recovery rate, (ii) the optimal operating conditions when FO is coupled to the draw solute recovery step, and (iii) the quality of both the recovered draw solution and the final water product. Moreover, most of the systems were investigated only at the lab scale and literature lacks research aiming at the implementation of full-scale systems. Besides, when forward osmosis is applied to produce high-quality water, it must be coupled with a downstream step of draw

solution recovery and water purification. The effective design of the entire treatment scheme requires that the parameters and operational condition of both steps are optimized together, as optimization of one step alone may be not ideal, or even detrimental, for the performance of the other. Therefore, there is need of implementing research from the "micro" (lab scale) to the "macro" scale (full plant design) with the aim to deeply investigate the possible advantages and drawbacks related to an innovative membrane technology such as forward osmosis.

In this study, a forward osmosis – nanofiltration system is evaluated as a feasible technology to produce high-quality water from real brackish groundwater and from real wastewater. In the first part of the work, different draw solutions are assessed in lab tests in order to identify the most promising ones for these specific FO applications. Preliminary filtration experiments are performed to choose the best operating conditions in FO. Afterwards, high-recovery tests are carried out with the two real contaminated waters followed by post-regeneration process of the diluted draw solutions through NF and consequent extraction of the high-quality water. The quality of the various aqueous streams involved in the filtration experiments are analyzed and the overall performance of the coupling technology is discussed. As second step of this work, a full-scale system design comprising both the FO and the NF step is presented for the most promising applications, heavily based on the results obtained in the first phase of the study. The previous experimental analysis is integrated with module-scale modelling and with a deeper study of fouling behavior in FO. An optimization of the most important operational parameters (i.e., the net driving force represented by the osmotic pressure of the draw solution, the flow rate of the draw solution itself, and the recovery target) for the potential coupling system is presented. Complete systems with numbers of total membrane area, flow rates, and energy supply are reported. Finally, the forward osmosis is analyzed in co-current and counter-current mode to discuss the best possible operating configuration.

3.2 Materials and Methods

Laboratory experiments were performed to assess the feasibility of the coupling technology (FO-NF) for the production of high-quality water from brackish groundwater and wastewater. Following the characterization of the FO membrane, specific filtration experiments were performed to evaluate the various draw solutions and the feasibility of their post-recovery process through nanofiltration. Once the most promising DS were identified, high-recovery FO-NF tests were performed with real water samples as feed solution, with the aim to assess the overall performance of the system (in terms of productivity, recovery, and selectivity of the FO and NF step together with quality assessment of the final product water and of the regenerated draw solutions). Moreover, to evaluate the fouling propensity in forward osmosis, specific FO fouling experiments were carried out with real brackish groundwater and wastewater samples as feed solution and different ionic composition in the draw solution. To isolate the effect of fouling, the experimental results were coupled with the modelling analysis of the water flux across the FO membrane. Based on the results obtained during the lab experiments, a system-scale modelling was developed to evaluate the best FO-NF configurations. FO-NF process parameters were first analyzed through system-scale modelling, followed by the design of the full-scale plants. The section below describes the laboratory set up, the experimental procedures, and the system modelling. The materials and methods reported below in details were already described in previously published papers [139] and [140].

3.2.1 Laboratory facilities and experiments

Lab filtration setups

Nanofiltration experiments were performed with the same cross-flow lab plant described in the previous chapter (section 2.2.1). The FO setup was purchased from Sterlitech Corporation (Kent, WA, USA). It comprises two reservoirs for feed and draw solutions, two variable gear pumps (Cole-Parmer, Vernon Hills, IL), a flat custom-made membrane cell, and a programmable logic controller (PLC) for data acquisition. In particular, the custom-made membrane cell consists of a rectangular channel with the following dimensions: 146 mm (5.75 inches) length, 94.5 mm (3.72 inches) width, and 1.5 mm (0.059 inches) height. A membrane with an active area of 140 cm^2 (21.7 in^2) can be allocated in it. The cross-flow rate can be adjusted manually and it was set to 1.8 L/min (0.34 m/s cross-flow velocity) for each experiment. Temperature and conductivity were recorded through the PLC. A computer-interfaced balance was used to measure the water flux across the membrane, recording the change of volume in the feed reservoir in time. Feed and draw solutions were always recirculated back to the respective tanks, thus performing all the experiments in batch. All the tests were conducted with the

membrane in FO configuration, i.e., active layer facing the feed solution, in co-current mode, and at a temperature of 23 °C.

Membranes and draw solutes

Two commercial nanofiltration membranes were acquired from Dow Chemical (Dow Chemical Company, Midland, MI) for NF experiments, i.e., the tighter NF90 and the looser NF270. Forward osmosis membrane was acquired from a commercial company, fabricated in TFC mode with a polyamide selective layer on top. Each membrane was received as flat sheet samples and stored dry. The FO membrane was characterized following the protocol reported by Tiraferri et al. [72]. Values of the active layer water permeance, A, of the NaCl permeability coefficient, B^{NaCl}, and of the support layer structural parameter are reported in the table below (Table 3.1).

Table 3.1: *Characteristics of the Porifera's forward osmosis membrane. Characterization was performed experimentally following the protocol reported by Tiraferri et al. [72]*

A ($L\,m^{-2}\,h^{-1}\,bar^{-1}$)	B^{NaCl} ($L\,m^{-2}\,h^{-1}$)	S μm
2.75 ± 0.50	0.94 ± 0.25	427 ± 19

With a draw solution of 485 mM NaCl and a feed solution of deionized water, a water flux of roughly 15 $L\,m^{-2}\,h^{-1}$ was obtained together with an approximately value of 0.09 $mol\,m^{-2}\,h^{-1}$ (5 $g\,m^{-2}\,h^{-1}$) for the reverse salt flux. Three different inorganic salts and one organic compound were evaluated as possible draw solutes for this specific research study: magnesium chloride, magnesium sulfate, sodium sulfate, and glucose were all purchased from Carlo Erba (Milan, Italy). These solutes were chosen because of the possibility to regenerate the related draw solutions using nanofiltration, which is an established technology with already robust operational standards.

Feed water samples

Real water samples were collected from two separate treatment plants located in Italy. The first one, referred to as "Site A", is treating brackish groundwater while the second plant, "Site B", is treating a mixture of industrial and civil wastewater. As reported in Figure 3.1, samples of the effluent coming from the secondary sedimentation were collected from both sites. Figure 3.1 is also reporting the current treatment trains operated in both locations and the novel alternative technology proposed. The scope of the project is to assess the possibility to substitute the treatment steps following the secondary sedimentation with a coupled FO-NF system, with the aim to obtain water for high-end uses. It can be stated that in the case of site B, however, the FO-NF system would require an overall higher energy

input compared to the current configuration, but in contrast it would promote the beneficial reuse of this wastewater. The main characteristics of the effluents samples (used as feed water in our FO system) are reported in Table 3.2 together with the respective osmotic pressures calculated with OLI System software.

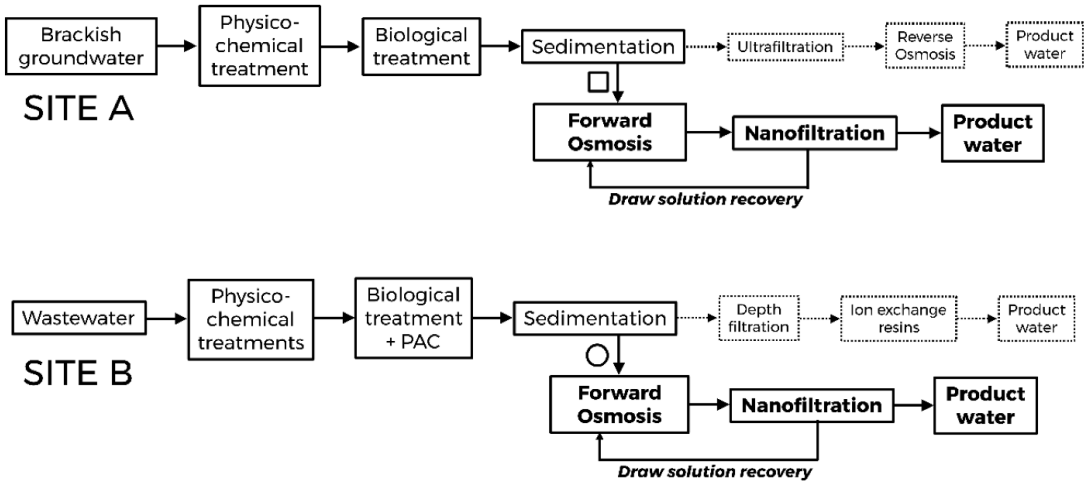

Figure 3.1: *Current and envisioned treatment trains for (top) site A and (bottom) site B. Scheme represents the main water line. In site A (square data points in the manuscript), the FO+NF system replaces ultrafiltration and reverse osmosis. In site B (circle data points), the FO+NF system replaces sand- and resin-based filtration steps.*

Table 3.2: *Characterization of water samples coming from Site A and Site B.*

Parameter	Site A	Site B
Organic carbon (mg/L)	TOC: 4.4	DOC[a]: 22
pH	7.8	8
Cl^- (mg/L)	2000	100
F^- (mg/L)	2.5	0.1
${PO_4}^{3-}$ (mg/L)	2.5	1.5
${NO_3}^-$ (mg/L)	49	2.2
${SO_4}^{2-}$ (mg/L)	290	250
$N-NH_4$ (mg/L)	0.01	0.004
Ca^{2+} (mg/L)	160	31
Mg^{2+} (mg/L)	90	13
K^+ (mg/L)	45	15
Na^+ (mg/L)	1200	120
Al (mg/L)	n.d.	70
As (mg/L)	n.d.	4.2
Cr (mg/L)	n.d.	1.3
Fe (mg/L)	n.d.	16
Ni (mg/L)	n.d.	3.7
Conductivity (μS/cm	6400	1100
TDS (mg/L)	3900	540
Osmotic Pressure (bar)	3	0.5

n.d. not detected or below detection limit
[a] Measured following microfiltration (0.45 µm pores)

Tests for DS evaluation and preliminary FO experiments

Forward osmosis experiments were performed with each draw solution, varying the osmotic pressure of the draw stream and using deionized water on the feed side. The draw osmotic pressure was varied in five consecutive steps with bulk osmotic pressures ($\pi_{B,DS}$) of 4, 8, 12, 16, and 20 bar, respectively. Permeate and reverse salt fluxes were measured during the whole experiment. The experiments were run with same volumes of DS and FS (1.5 L) and in co-current mode (feed and draw solutions entering and exiting from same sides in the membrane cell). To verify the feasibility of recovering the different draw solutions through nanofiltration, NF experiments were performed afterwards by filtering different synthetic draw solutions, separately (i.e., feed solutions of salts dissolved in deionized water with analogous characteristics of each draw solution analyzed in FO). Taking into account the intrinsic bulk osmotic pressure of the feed solution ($\pi_{B,DS}$), a hydraulic pressure equal to $\pi_{B,DS}$ +4 bar was applied to the cross-flow system while maintaining a cross-flow rate of 4.5 L/min (cross-flow velocity of 0.85 m/s) and a water

temperature of 22°C. The permeate fluxes and salt rejections were measured during the whole experiment. Permeate and concentrate streams were continuously recirculated back to the feed reservoir while permeate samples were collected for ions selectivity measurement during the filtration stage. At the end of these tests, the best draw solutions were chosen upon evaluation of the measured fluxes obtained in FO and in NF, the reverse salt fluxes, and the rejections observed in FO and NF experiments. Based on the results, $MgCl_2$ and Na_2SO_4 were chosen as the most promising draw solutions among those studied. A second set of forward osmosis experiments was then conducted with either of these two salts used separately as draw stream to filter feed solutions composed by real water samples from site A or B. These tests were analogous to those described previously and comprised measurements of the permeate fluxes for five steps with varying driving force.

Forward osmosis fouling experiments

Feed solutions of real water samples coming from Site A or Site B were used to perform FO fouling experiments, always run in co-current mode with a volume of 1.5 L for both the draw and feed side. Tests were carried out with Na_2SO_4 or $MgCl_2$ as draw solute, with a salt concentration suitable to achieve an initial flux of approximately 13-14 ($L\,m^{-2}\,h^{-1}$). In these 8-h long fouling tests, additions of appropriate volumes of a stock draw solution (in the draw tank) and of deionized water (in the feed tank) were carried out every 30 min to keep the nominal driving force constant. Some fouling experiments with the wastewater sample from site B also comprised physical cleaning steps to promote a larger shear stress at the membrane/solution interface, without backwashing: every 2 h, the cross-flow velocity was increased and a cleaning solution of 4.5 mM of Na_2SO_4 or 1 mM of $MgCl_2$ was used both on the draw and on the feed side. A larger flow rate would result in a more significant pressure drops within the channels of the membrane module with a consequent increase in the energy requirements for pumping; in this study, the cross-flow velocity was only increased by 30% (to 0.45 m/s) during cleaning, representative of a mild process that would minimize the energy needs. After 20 min, the cleaning streams were replaced with previous draw and feed solutions and the fouling experiments carried on.

Additional fouling experiments with wastewater from Site B as feed solution were further performed. In this case, different draw solutions were used in order to evaluate the influence of different ions on membrane fouling: magnesium chloride, magnesium sulfate, sodium chloride, sodium sulfate, and calcium chloride (always purchased from Carlo Erba, Milan, Italy). Each experiment was performed with a fixed osmotic pressure of 18.4 bar, achieved by appropriate concentrations of each draw solution and calculated by OLI System Software, corresponding to 0.262 M for $MgCl_2$, 0.796 M for $MgSO_4$, 0.406 M for NaCl, 0.308 M for Na_2SO_4, and 0.279 M for $CaCl_2$. Differently from those described previously, these fouling experiments were

performed by keeping constant the nominal driving for the first 8 h of experiment and without making any additions/adjustments for the rest of the test. No physical or chemical cleaning was performed, and experiments were carried out in duplicates or triplicates for each draw solution.

3.2.2 High-recovery forward osmosis and nanofiltration tests

Magnesium chloride and sodium sulfate were used individually as draw solution for high-recovery forward osmosis tests, with (i) an initial osmotic pressure of 15 bar (0.304/0.218 M of Na_2SO_4/$MgCl_2$) in the case of treating the brackish groundwater from site A, and (ii) 12 bar (0.238/0.178 M of Na_2SO_4/$MgCl_2$) when filtering the wastewater effluent from site B. An initial volume of 3.5 L of draw solution and real water samples was used to fill up the draw and feed reservoir, respectively. The tests were prolonged until roughly 65% of solution, i.e., 2.3 L, permeated from the feed to the draw side, while permeate flux across the membrane was measured every 10 min. At the end of each FO test, the diluted draw solution was processed in NF. Taking into account (i) the separation mechanisms of the nanofiltration membranes, based on a combination of size exclusion and electrostatic effects, and (ii) the valence of the ions in solution, a looser NF270 and a denser NF90 membranes may be employed to re-concentrate Na_2SO_4 and $MgCl_2$, respectively, and to produce high-quality permeate water. NF experiments were performed by keeping a constant applied pressure of 20 bar and 16 bar to regenerate the DS coming from the treatment of the brackish groundwater (site A) and the wastewater effluent (site B), respectively. The applied pressure in NF needs to be at least equal or higher than the osmotic pressure of the feed solution at the end of the test, i.e., 15 and 12 bar, respectively. The NF tests were prolonged until a relative recovery rate of 100% was achieved, i.e., 2.3 L of solution permeated from the feed side to the permeate side. Samples of the FO draw solution, FO concentrate stream, as well as NF permeate and feed were collected at the end of each experiment and analyzed by an external accredited lab (Eurolab, Turin, Italy).

3.2.3 Modeling of the forward osmosis - nanofiltration fluxes

Simulation of FO permeate flux, Jw, and reverse salt flux, Js, were performed by application of the following equations [72]:

$$J_w = A\left(\frac{\pi_D exp(-\frac{J_w S}{D}) - \pi_F exp(-\frac{J_w}{k})}{1 - \frac{B}{J_w}[exp(\frac{J_w}{k}) - exp(-\frac{J_w S}{D})]}\right) \tag{3.1}$$

$$J_s = B\left(\frac{C_D exp(-\frac{J_w S}{D}) - C_F exp(-\frac{J_w}{k})}{1 - \frac{B}{J_w}[exp(\frac{J_w}{k}) - exp(-\frac{J_w S}{D})]}\right) \tag{3.2}$$

where A, D, B and S are the active layer water permeance, the diffusion coefficient of the draw solute in water, the salt permeability coefficient, and the support layer structural parameter, respectively. These are parameters intrinsic to the membrane characteristics (A and S) or to the draw solute (B and D. Table 3.3 shows these values for each of the draw solutes involved in this study [72, 158]). In the equations, CD / π_D and CF / π_F represent the draw and feed concentrations / osmotic pressures, respectively, while the exponential terms account for both the internal ($-(J_w S)/D$) and external (J_w/k) concentration polarizations. Finally, k represents the mass transfer coefficient at the active layer-solution interface, function of the hydrodynamics in the membrane flow cell and maintained equal to 68 $L\,m^{-2}\,h^{-1}$ for all the simulations [72, 170]. If the loss of draw solute due to reverse salt flux is negligible, the two equations 3.1 and 3.2 can be simulated separately.

Table 3.3: *B and D of the draw solutes [72, 158].*

Draw Solute	B (LMH)	D (m^2/s)
Na_2SO_4	0.06	$7.6x10^{-10}$
$MgCl_2$	0.07	$1.1x10^{-9}$
NaCl	0.94	$1.5x10^{-9}$
$MgSO_4$	0.39	$4.3x10^{-10}$
$CaCl_2$	0.16	$1.1x10^{-9}$

Simulations of the water flux across the membrane were performed (i) to isolate the effect of fouling on FO filtration (Case 1) and (ii) to perform a system-scale analysis of the forward osmosis-nanofiltration hybrid system (Case 2). The wastewater feed was simulated without considering any foulants concentration and by simplifying the mixture of ionic species with an equivalent NaCl concentration providing the same overall osmotic pressure, i.e., 0.5 bar.

Case 1: Simulation of the water flux across the FO membrane during fouling experiments

In Case 1, equation 3.1 was applied to model the flux reduction due only to the loss of driving force during fouling experiments. Information related to the effect of fouling were hence inferred by comparing the modeled flux reduction with the observed trend of water flux. For each of the draw solution studied ($MgCl_2$, Na_2SO_4, $MgSO_4$, NaCl, and $CaCl_2$), a model was performed calculating the trend of the water flux from the actual values of DS/FS osmotic pressures at any given time, known based on their dilution/concentration during the tests.

Case 2: System-scale analysis and design of the forward-osmosis nanofiltration system

In this case, a system-scale analysis and design of the forward osmosis stage was developed through the application of equations 3.1 and 3.2. Given the results obtained during lab experiments (reported in the following sections), the analysis was performed only for the treatment of the wastewater from Site B, thus accounting for an inlet flow rate of 76 m^3/h in the FO system. The water flux across the membrane in a hypothetical FO plant working in cross-flow mode (either with spiral-wound or tubular modules), would vary along the length of the membrane module. In particular, the overall water flux, recovery, and required membrane area in the FO system would be strongly influenced by three main parameters:

1. the influent draw solution to feed solution flow rate ratio, DS:FS
2. the initial (influent) DS osmotic pressure (π_D)
3. the module configuration, i.e., co- vs. counter-current

Firstly, a series of simulations were hence performed in co-current mode analyzing different combinations of influent DS osmotic pressure and DS:FS. For each simulation, the water flux was modeled through the discretization of the control volume (i.e., the theoretical length of the membrane module), followed by calculation of the associated recovery and of the required membrane area. Based on the obtained results, a system-scale analysis conducted to study the FO performance in counter-current mode was developed, by keeping the same boundary conditions, that is, the same DS:FS ratio and influent draw solution osmotic pressure. While equations 3.1 and 3.2 were used to design the forward osmosis stage of the full-scale system, Wave software (DuPont) was instead employed to simulate the nanofiltration stage. Based on the results obtained through lab experiments and high-recovery FO-NF tests [139], the membrane system was designed to be operated with either sodium sulfate or magnesium chloride as draw solute.

3.3 Results and Discussion

The following section presents the results obtained during the study with the related discussions:

1. The coupling technology was firstly evaluated at the lab scale, in order to investigate the feasibility of the entire process FO-NF. After the identification of the most promising draw solution and of the best operating conditions.

2. High-recovery tests were performed to evaluate (i) the FO performances by filtering real water samples and (ii) the feasibility to extract high-quality water while reconcentrating the diluted DS in nanofiltration. The overall results are reported below together with the assessment of the quality of the product water and of the reconcentrated DS.

3. To finalize the forward osmosis performance evaluation, an in-depth study of fouling propensity was carried out where different DS were tested to assess whether different reverse salt fluxes may affect fouling behavior. Lab scale analysis was essential for the preliminary assessment of the coupling technology and the results obtained were fundamental to set up the boundary conditions for the full-scale design.

4. A system scale modelling was developed based on the experimental results obtained, with the aim to evaluate the influence of different process parameters on FO-NF performances. In particular, the forward osmosis step was deeply studied to analyze the feasible configurations.

5. Finally, the full-scale design of the coupling technology has been developed and reported in the section below with discussion.

What is reported below has been already presented in previously published papers [139] and [140].

3.3.1 Choice of the draw solutes and of the operating conditions

The first set of experiments aimed to select the most appropriate draw solutes. Four candidate compounds were evaluated, namely, magnesium sulfate, magnesium chloride, glucose, and sodium sulfate. The choice was based on previous research [158, 171], which has reported promising results when applying these compounds as draw solutes in forward osmosis. Moreover, they are all widely available and inexpensive compounds, with the possibility to be effectively recovered in nanofiltration (NF). The results of the first set of tests are reported in Figure 3.2. Based on the calculation performed through OLI System, magnesium chloride, $MgCl_2$, and

sodium sulfate, Na_2SO_4, have the largest osmolality among the four compounds (Fig 3.2a). These two inorganic compounds showed the highest fluxes (Fig 3.2b) and the lowest specific reverse salt fluxes (Fig 3.2c) in forward osmosis (FO) when DI water is used as feed solution. The results obtained in nanofiltration ensure the feasibility to effectively recover the two inorganic salts in the NF post-recovery process, with salts rejected at high rate with suitably high fluxes in NF. In particular, in order to maximize the productivity in nanofiltration, the denser NF90 and the looser NF270 can be employed to separate the $MgCl_2$ and Na_2SO_4, respectively (Fig 3.2d, e).

Once the two most promising draw solutes were identified, preliminary low-recovery FO experiments were performed with real water samples as feed solutions. The purpose of these tests was to choose the concentration of both magnesium chloride and sodium sulfate to be later applied in high-recovery tests. Experiments were performed with the two waters from site A and B as feed solutions while fluxes across the membrane were monitored as a function of bulk osmotic pressure of the draw solution. The results are presented in Figure 3.3. The trends of water fluxes are consistent with theoretical expectations [72, 154]. The two draw solutes showed similar FO fluxes. Higher productivity was observed when the less saline water was used as the feed solution, especially in the lower range of nominal osmotic driving force. The combined effects of concentration polarization and reverse salt flux [172] strongly influenced the FO performances at high values of draw bulk osmotic pressure, showing similar flux trends with both the two feed solutions. In particular, dilutive internal concentration polarization is more pronounced at higher flux rate, thus affecting the membrane performance. Finally, it is important to consider that the choice of the concentration of the draw solution for high-recovery tests should be based on a compromise between the expected FO productivity and the external hydraulic pressure to be employed in NF to restore the initial concentration value. Therefore, based on the profiles shown in Figure 3.3, draw osmotic pressures of 15 bar and 12 bar were selected for subsequent high-recovery experiments with water samples from site A and B, respectively.

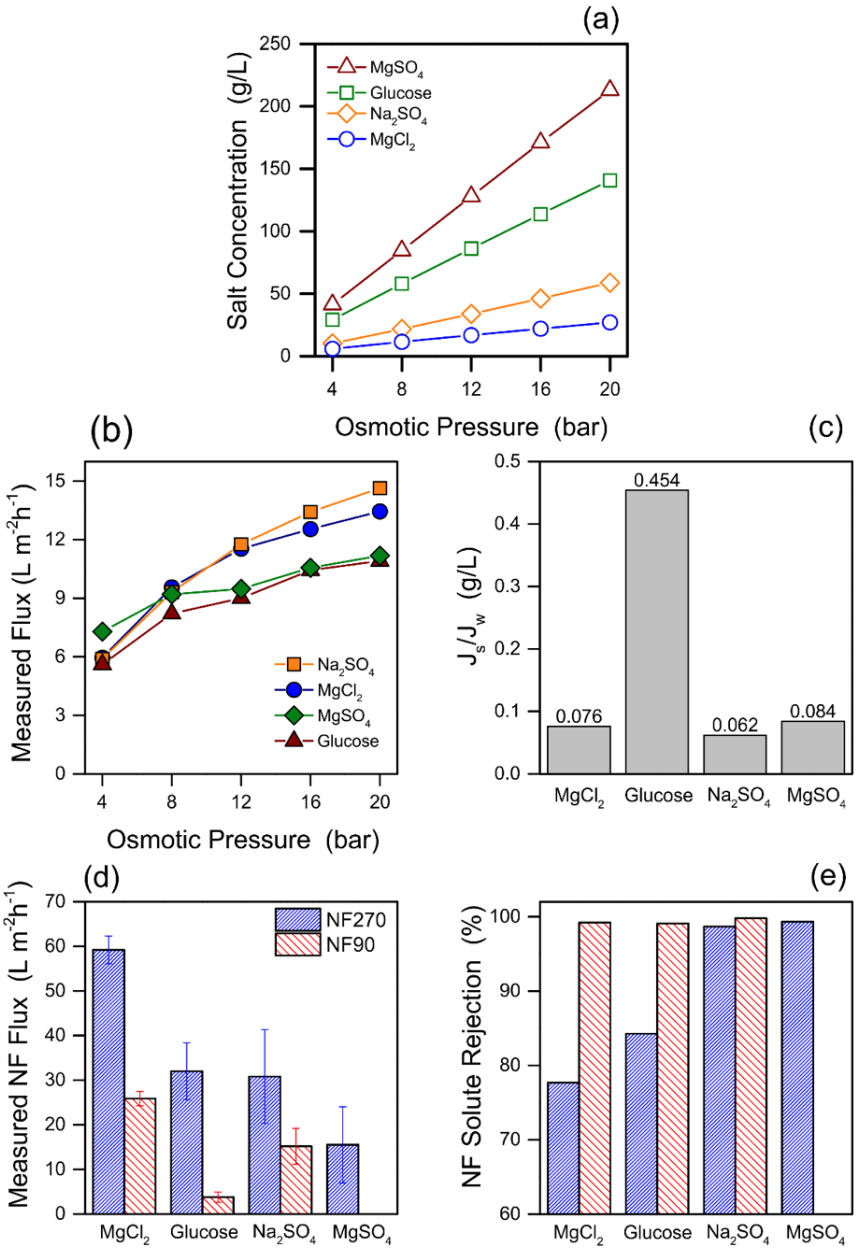

Figure 3.2: *Choice of the most appropriate draw solutions among the four options investigated in this study. (a) Salt concentration as a function of osmotic pressure (modelled through OLI System software). (b, c) Flux and specific reverse salt flux observed in forward osmosis. (d, e) Flux and rejection observed in nanofiltration.*

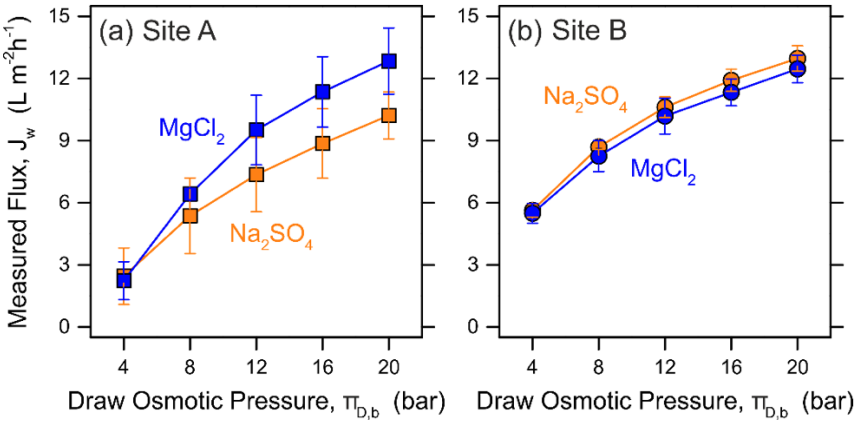

Figure 3.3: *Fluxes measured in forward osmosis as a function of osmotic pressure of the bulk draw solution. The feed solution is (a: left) real brackish groundwater from site A and (b: right) real wastewater secondary effluent from site B. Blue and orange points depict data obtained with $MgCl_2$ and Na_2SO_4 as draw solutes, respectively. Average and standard deviation of two separate tests are shown. Lines are only intended as guide for the eyes.*

3.3.2 Evaluation of the coupled FO-NF system

Productivity of the coupled FO-NF system

Firstly, magnesium chloride and sodium sulfate were used as draw solutions to filter the two contaminated waters from site A and B in forward osmosis high-recovery tests. These experiments were run until a recovery of roughly 65% was achieved. Subsequently, nanofiltration tests were performed with the diluted draw solutions as feed streams, with the aim to produce 100% of the dilution volume (i.e., the permeated volume during the respective previous FO test) on the permeate side. As a result, the draw solution was virtually completely regenerated and high-quality water was produced, the latter amounting to 65% of the volume of the initial feed of the FO test.

The results of the high-recovery FO experiments are reported in Figure 3.4a and Figure 3.4b showing the water fluxes across the membrane as a function of recovery, at the initial draw osmotic pressures indicated in each graph. Fouling and reduction of the driving force caused the gradually decrease of the permeate flux in time (FO tests were indeed carried out in batch mode). In order to have a validation of the experimental results, duplicates were performed, showing high reproducibility of the overall process (figure A1 reported in the Appendix). A large difference can be noticed in terms of productivity in forward osmosis when treating the two real waters: the average fluxes across the membrane were significantly larger when filtering the wastewater effluent from site B, compared to those measured during the tests performed with brackish water from site A. This is in accordance with data displayed in Figure 3.3. Also, using sodium sulfate as draw solute instead

of magnesium chloride resulted in slightly higher fluxes, possibly due to a more pronounced reverse salt diffusion of the latter salt [158]. Specifically, the average fluxes were 6.4 $L\,m^{-2}\,h^{-1}$ and 5.2 $L\,m^{-2}\,h^{-1}$ for brackish groundwater (site A) and 11.1 $L\,m^{-2}\,h^{-1}$ and 9.7 $L\,m^{-2}\,h^{-1}$ for the secondary wastewater effluent (site B). An important implication can be inferred from the results obtained in high recovery FO tests: by treating wastewaters similar to those from site B, it could be possible to reach significantly larger recovery values (up to 80%) compared to those achievable by filtering higher saline feed waters. In the latter case indeed, a lower recovery goals may be necessary to maintain high fluxes in the FO unit.

The results of the high recovery NF experiments are reported in Figure 3.4c and 3.4d. The measured fluxes in nanofiltration were significantly larger than those observed in forward osmosis, owing to the different transport mechanisms and driving force involved in the two processes. For each experiment, permeate flux decreased in time as function of the recovery rate, which may be ascribed to the loss of driving force as the feed solution become more concentrated. The looser NF270 showed higher productivity compared to the denser NF90, as expected from the intrinsic properties of the active materials characterizing the two NF membranes. Average fluxes were calculated simply by dividing the total cumulative permeated volumes by the duration of each respective test, computing values of 86.2 $L\,m^{-2}\,h^{-1}$ and 54.9 $L\,m^{-2}\,h^{-1}$ to recover the draw solution used to treat samples from site A (applied hydraulic pressure of 20 bar), and 69.9 $L\,m^{-2}\,h^{-1}$ and 50.8 $L\,m^{-2}\,h^{-1}$ in the case of site B (applied hydraulic pressure of 16 bar).

It is important to consider that while in the laboratory the filtration process is operated in batch and the recovery increases with time, in real plant, recovery increases with space along the membrane module. Therefore, the recovery can be considered as the parameter to tie the two modes of operation [165]. A FO-NF plant operating at the equivalent recovery rate of lab tests and in co-current mode may hence show the same fluxes discussed so far and presented in Figure 3.4. It can be also stated that the capital costs of installation of the FO plant would be larger than for the associated NF plant, owing to the lower FO productivity compared to the NF productivity. Based on the data showed in Figure 3.3, it would be possible to work with a larger initial DS osmotic pressure to maximize the productivity of the FO step while maintaining the same applied pressure in NF, thus reducing capital costs related to FO installation. Conversely, the nanofiltration system may be configured to operate at lower applied pressure, resulting in energy savings for the overall system. There are other possible options to optimize the filtration system. For instance, (i) working in counter-current mode in the forward osmosis stage or (ii) working with larger flow rates of the draw solution compared to the feed solution, which would result in a lower dilution rate of the DS at equivalent recovery. In this case, the excess flow of the draw would be treated in NF at higher fluxes compared to FO, thus producing larger volumes of high-quality water without greatly increasing the size of the plant. Clearly, it is important to accomplish a

simultaneous optimization of both FO and NF steps in order to achieve an optimal design of the overall system. A deeper analysis has been performed in this sense, by modelling the forward osmosis – nanofiltration system. Results are reported in the following sections.

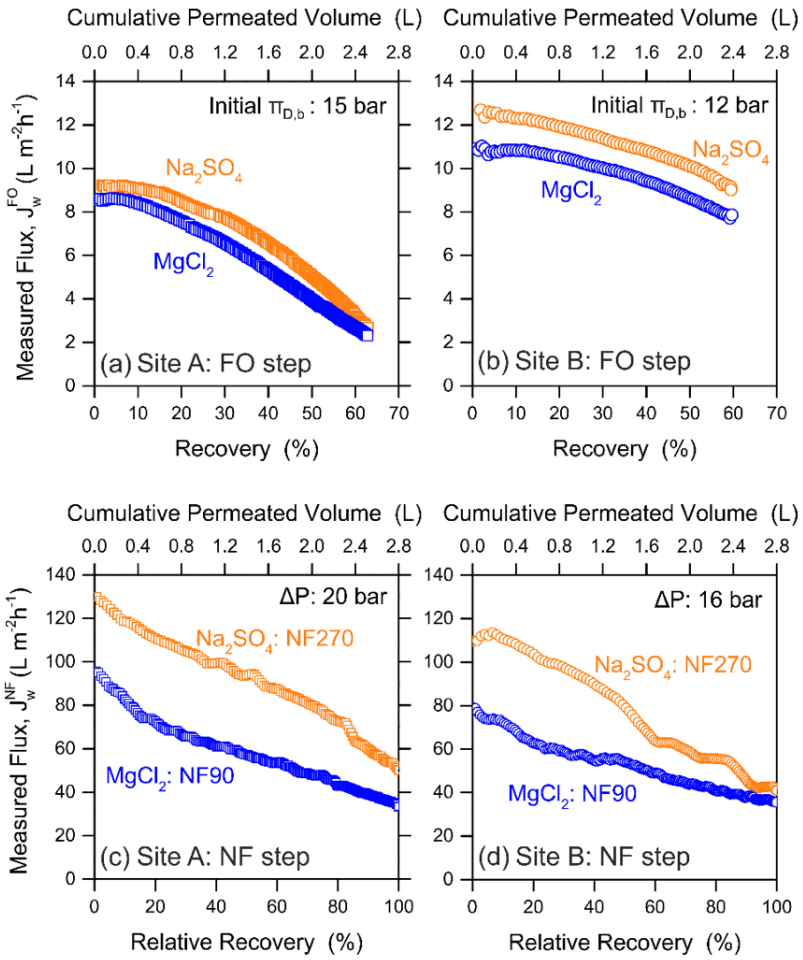

Figure 3.4: *Fluxes measured in the two treatment steps comprising the coupled system. (a, b: top row) Fluxes in batch forward osmosis as a function of absolute recovery: data points are average values of duplicate experiments. The draw solution bulk osmotic pressure in the beginning of the test was 15 bar for site A and 12 bar for site B. (c, d: bottom row) Fluxes in batch nanofiltration as a function of relative recovery, i.e., the amount of cumulative permeated volume relative to the amount of solution recovered in the previous FO step. $MgCl_2$ and Na_2SO_4 draw solutions were recovered in nanofiltration with NF90 and NF270 TFC membranes. The applied pressure was 20 and 16 bar (290 and 232 psi), respectively, for draw solutions obtained treating waters from site A and B, respectively.*

Quality of the product waters, draw solution regeneration, and feasibility of the process

There are three main issues to be addressed when analyzing the feasibility of the coupled system in terms of quality of the various streams:

1. **the management of the FO concentrate**
2. **the end uses of the product, i.e., the NF permeate**
3. **the regeneration of the draw solution, i.e., the NF retentate stream**

For this reason, chemical analyses were performed to characterize the composition of all the streams entering and exiting both the FO and the NF systems in terms of ionic species, organic carbon, and heavy metal concentrations.

Management of the FO concentrate

The composition of the retentate streams produced at the end of the high recovery FO steps is summarized in the Table 3.4 and Table 3.5. The scope of the following discussion does not encompass the treatment of the FO retentates, but some suggestions may be drawn for their potential management strategy. It can be stated hence that:

- the correct management of the concentrated brackish groundwaters (site A) may involve further concentration to recover salts or other resources, and for a more facile disposal, thus exploiting its medium-high salinity (close to 10 g/L; see Table 3.4)
- the correct management of the concentrated secondary effluent (site B) may comprise its partially recirculation within the treatment train. Thanks to its relatively low salinity and large amount of organics (which would be even larger at higher advised recovery rates; see Table 3.5) it would be easily treated within the biological section, already present in site B, without specific problematic issues related to other nutrients, such as nitrogen or phosphorous

Table 3.4: *Characteristics of the final concentrate produced in forward osmosis pilot tests treating the groundwater samples from Site A. The results are presented for the tests performed with both sodium sulfate and magnesium chloride as draw solutes.*

	Draw Solution: Na_2SO_4	**Draw Solution: $MgCl_2$**
TOC (mg/L)	**9.1**	**9.4**
pH	8.1	8.1
Cl^- (mg/L)	4900	5000
F^- (mg/L)	0.8	n.d.
PO_4^{3-} (mg/L)	n.d.	n.d.
NO_3^- (mg/L)	110	70
SO_4^{2-} (mg/L)	1100	970
$N-NH_4$ (mg/L)	n.d.	0.11
Ca^{2+} (mg/L)	360	400
Mg^{2+} (mg/L)	290	400
K^+ (mg/L)	39	100
Na^+ (mg/L)	2900	2800
Conductivity (μS/cm	14360	15000
TDS (mg/L)	**9700**	**9740**

n.d. not detected or below detection limit

Table 3.5: *Characteristics of the final concentrate produced in forward osmosis pilot tests treating the wastewater samples from Site B. The results are presented for the tests performed with both sodium sulfate and magnesium chloride*

	Draw Solution: Na_2SO_4	**Draw Solution: $MgCl_2$**
DOC (mg/L)	**27**	**27**
pH	8.2	8.4
Cl^- (mg/L)	62	260
F^- (mg/L)	n.d.	n.d.
PO_4^{3-} (mg/L)	n.d.	n.d.
NO_3^- (mg/L)	n.d	n.d.
SO_4^{2-} (mg/L)	520	490
$N-NH_4$ (mg/L)	0.062	0.036
Ca^{2+} (mg/L)	51	83
Mg^{2+} (mg/L)	n.d.	51
K^+ (mg/L)	5.3	64
Na^+ (mg/L)	360	280
Conductivity (μS/cm	2000	2460
TDS (mg/L)	**998**	**1228**

n.d. not detected or below detection limit

End uses of the product

Table 3.6 and Table 3.7 show the chemical composition of the product waters, in the case of the treatment of feed waters from site A and B, respectively. Promising results were obtained with high quality levels reached for both the product waters generated by the coupled FO-NF technology (i.e., the permeate produced by the nanofiltration step). This demonstrates the ability of the coupled system to desalinate brackish groundwater and to treat secondary effluents for high-end uses. In particular, one of the four product streams could be used directly as source of drinking water. The permeates produced by the FO-NF system running with $MgCl_2$ as draw solution may be readily employed as source for irrigation, without restrictions, thanks to the low SAR value (lower than 3), which makes the two product waters compatible with the most sensitive crops. On the other hand, the value of aggressive index slightly below 10 for the product waters from site B (Table 3.7) may be addressed by operating with a small bypass to mix the NF permeate with untreated water, still guaranteeing high quality of the final product. No significant concentrations of heavy metals were detected, with values always below detection limit or at least one order of magnitude lower than the limits for potable water. Overall, these results are only partly surprising, as the initial feed stream was treated by two highly selective membranes in series, the first FO and the second NF membrane. Only in the case of the product waters produced with

Na_2SO_4 as draw solute, the values of SAR were relatively high, resulting in limitation for irrigation. Moreover, the NF permeates generated by the treatment of brackish water showed a final concentration of sodium and sulfate of 250 mg/L and 270 mg/L, respectively (Table 3.6), being larger than the limit value for potable water in Italy. In this case, a second pass for only part of the NF permeate can be performed to readily resolved these issues. Preliminary tests showed that similar product qualities may be obtained by directly applying significantly denser nanofiltration membranes, e.g., XLE membranes (Dow), to treat the influent feed waters. Comparable recovery rates and permeate fluxes to those observed in this study may be achieved by working at lower applied pressures (10-15 bar), but with more considerable concerns related to fouling. The choice between the implementation of a coupled FO-NF system and a stand-alone NF system would require pilot-scale tests and evaluation of the various trade-offs of the two alternatives. Moreover, a system consisting of NF only would comprise only one high-selectivity barrier, while the coupled FO-NF is a two-barrier system that would potentially allow higher removal rates also of small organic compounds and micropollutants.

Table 3.6: *Characterization of the final product water obtained through the treatment of the brackish groundwater coming from Site A. Two replicate experiments were performed, showing comparable results. Here, we report data from one of the two replicates.*

	Draw Solution: Na_2SO_4	**Draw Solution: $MgCl_2$**	**Limits for use as irrigation water** [a]	**Limits for use as drinking water** [a]
TOC (mg/L)	0.60	0.50		10
pH	8.5	9.2	5.5 - 9	6.5 - 9.5
Cl^- (mg/L)	140	110	200	250
F^- (mg/L)	n.d.	n.d.	1	1.5
PO_4^{3-} (mg/L)	n.d.	n.d.	30	
NO_3^- (mg/L)	15	n.d.	50	50
SO_4^{2-} (mg/L)	270	0.04	2500	250
$N–NH_4$ (mg/L)	n.d.	n.d.		0.5
Ca^{2+} (mg/L)	2.5	9.6	150	
Mg^{2+} (mg/L)	0.35	13	35	
K^+ (mg/L)	0.64	5		
Na^+ (mg/L)	250	40	180	200
Conductivity (μS/cm	1100	380	2500	2500
TDS (mg/L)	680	180	2000	
Hardness (mg $CaCO_3$/L)	69	78		500
Alkalinity	62	16		
Aggressive Index	11.4	11.5		>10
SAR of irrigation water	39	1.98	Depends on crops	

n.d. not detected or below detection limit

[a] Limits for Italy

Table 3.7: *Characterization of the final product water obtained through the treatment of the secondary wastewater effluent coming from Site B. Two replicate experiments were performed, showing comparable results. Here, we report data from one of the two replicates.*

	Draw Solution: Na_2SO_4	**Draw Solution: $MgCl_2$**	**Limits for use as irrigation water** [a]	**Limits for use as drinking water** [a]
TOC (mg/L)	1.1	0.33		10
pH	9.8	7.2	5.5 - 9	6.5 - 9.5
Cl^- (mg/L)	7.4	55	200	250
F^- (mg/L)	n.d.	n.d.	1	1.5
PO_4^{3-} (mg/L)	n.d.	n.d.	30	
NO_3^- (mg/L)	0.24	n.d.	50	50
SO_4^{2-} (mg/L)	110	0.21	2500	250
$N–NH_4$ (mg/L)	0.022	0.0024		0.5
Ca^{2+} (mg/L)	0.7	3.5	150	
Mg^{2+} (mg/L)	0.065	16	35	
K^+ (mg/L)	0.16	2.5		
Na^+ (mg/L)	75	3.7	180	200
Conductivity (μS/cm	350	190	2500	2500
TDS (mg/L)	190	80	2000	
Hardness (mg $CaCO_3$/L)	43	83		500
Alkalinity	40	8		
Aggressive Index	12.3	9.3		>10
SAR of irrigation water	23	0.2	Depends on crops	

n.d. not detected or below detection limit

[a] Limits for Italy

Regeneration of the draw solution

The third issue concerns the quality of the regenerated draw solutions, which should be ideally equivalent to the initial draw solution applied in the FO step, at least in terms of osmotic pressure. Table 3.8 and Table 3.9 presents a comparison of the composition of the initial and regenerated draw streams. At the end of the coupling technology, the regenerated draw solutions contained between 87% and 97% of the original TDS, vastly provided by the respective draw solutes, with only traces of different ions. The reduction of the amount of salinity translates into a nearly proportional loss of osmotic pressure for the regenerated draw solutions, compared to that of the initial DS. The change in composition and the decrease of TDS is attributed to possible phenomena of scaling, reverse salt flux in FO, and to incomplete (<100%) salt rejection by nanofiltration [82]. A larger relative loss of total dissolved solids was observed when treating wastewater from site B; in this case, the osmotic pressure of the regenerated draw solution (i.e., the NF retentate stream) was roughly 10.5 bar instead of 12 bar. This result may be rationalized

considering the largest salt gradient across the membrane during the FO treatment step, which would generate a larger net reverse salt flux to the feed stream. This phenomenon may be accentuated in the case of treatment of low-salinity feed (such as the wastewater from site B), compared to the filtration of brackish waters (e.g., water from site A). Overall, a larger relative loss of osmotic pressure was observed with $MgCl_2$. The issue discussed so far may be addressed in real operation by adopting one of the following expedients:

- adding solute continuously to the draw stream, thus keeping constant the osmotic pressure of the draw solution entering the FO system
- reaching a relative recovery rates larger than 100% in the nanofiltration step. This would also increase the overall system recovery. However, a certain amount of draw solution still should have to be supplemented in order to maintain the flow balance at the entrance of the FO unit.

Another important aspect to be addressed is the composition of the regenerated draw solution in terms of molar ratio of its constituting ions. The $Na^+/{SO_4}^{2-}$ ratios of the NF concentrates were 1.87 and 1.98 (nominal ratio is 2) following the treatment of the brackish groundwater from site A and the wastewater from site B, respectively. The Cl^-/Mg^{2+} ratios were 2.08 and 2.04, respectively. These data imply larger loss of cations compared to each respective anion in the system. This result is rationalized with exchange mechanisms between draw and feed solutes in FO and with bidirectional and coupled ion transport across the FO and the NF membranes. The complex mixture of species present in feed waters may induce a departure of the draw solutions from the initial compositions. Further impairment of the draw solutions may be caused by the possible contamination of micropollutants and other undesired substances. This aspect was not observed in this study, but it may have a significant impact on the performance of the filtration process mostly in the case of coupling the FO treatment step with an even more selective draw regeneration technology (e.g., dense RO membranes), which rejects at high rates all the species that pass through the FO membrane. In the case of nanofiltration as post-regeneration process, this phenomenon should be thwarted but still providing the advantages of a dual barrier system to contaminants (hence, providing high-quality product waters). It is important to mention that in real operation, the continuous alteration in the composition of the recirculated draw solution would imply different actions than the simple additions of solutes to the draw stream. Periodically, it may involve partial or complete replacement of the draw solution. In this sense, research should be focused on developing ideally more selective FO membranes, capable of providing high fluxes using lower draw solute concentrations. This would represent a step forward to address issues related to loss of osmotic pressure and alteration of draw solutions during operation.

Table 3.8: *Characteristics of the final concentrate produced in nanofiltration pilot tests used to recover the draw solutions used in FO to treat the samples coming from Site A. The results are presented for the tests performed with both sodium sulfate and magnesium chloride.*

	Draw Solution: Na_2SO_4	**Draw Solution: $MgCl_2$**
TOC (mg/L)	2.5	3.5
pH	9.2	8
Cl^- (mg/L)	92	**14000 (ideally 15456)**
F^- (mg/L)	n.d.	5.5
PO_4^{3-} (mg/L)	n.d.	n.d.
NO_3^- (mg/L)	n.d.	n.d.
SO_4^{2-} (mg/L)	**29000 (ideally 29215)**	16
$N-NH_4$ (mg/L)	n.d	0.1
Ca^{2+} (mg/L)	29	92
Mg^{2+} (mg/L)	6.1	**4600 (ideally 5297)**
K^+ (mg/L)	39	8.6
Na^+ (mg/L)	**13000 (ideally 13984)**	150
Conductivity (μS/cm	33600	28400
TDS (mg/L)	42166	18872
Osmotic Pressure (bar)	**14.5 (ideally 15)**	**13.4 (ideally (15)**

n.d. not detected or below detection limit

3.3.3 Evaluation of fouling in forward osmosis

Preliminary fouling results

The results of the preliminary fouling experiments are reported in figure 3.5, showing the trends of water fluxes across the membrane in FO. Since the driving force was kept constant during all the tests, the progressive reduction in productivity observed was due solely to fouling-related effects. Looking at the experiments performed with brackish groundwater as feed solution, the flux decline was moderate with $MgCl_2$ and very low with Na_2SO_4, both used as draw solution. This difference may be rationalized with the negative effect of magnesium, which enhances foulant deposition at the membrane/solution interface as it diffused to the feed side [173]. This phenomenon also explains the slight dissimilarity of the data from high-recovery experiments with the same feed water from site A (Fig 3.4a). However, it must be considered that the use of sulfate in draw solution may necessitate additions of anti-scalants in real operation.

Table 3.9: *Characteristics of the final concentrate produced in nanofiltration pilot tests used to recover the draw solutions used in FO to treat the samples coming from Site B. The results are presented for the tests performed with both sodium sulfate and magnesium chloride.*

	Draw Solution: Na_2SO_4	**Draw Solution: $MgCl_2$**
TOC (mg/L)	2.1	2.9
pH	9	8.1
Cl^- (mg/L)	n.d.	**11000 (ideally 12620)**
F^- (mg/L)	n.d.	n.d.
PO_4^{3-} (mg/L)	n.d.	n.d.
NO_3^- (mg/L)	n.d.	n.d.
SO_4^{2-} (mg/L)	**20000 (ideally 22870)**	n.d.
$N-NH_4$ (mg/L)	0.031	0.052
Ca^{2+} (mg/L)	34	50
Mg^{2+} (mg/L)	n.d.	**3700 (ideally 4325)**
K^+ (mg/L)	29	n.d.
Na^+ (mg/L)	**9500 (ideally 10950)**	n.d.
Conductivity (μS/cm	27600	24700
TDS (mg/L)	29563	14750
Osmotic Pressure (bar)	**10.6 (ideally 12)**	**10.4 (ideally (12)**

n.d. not detected or below detection limit

Fouling was more pronounced when the secondary effluents was used as feed solution, compared to the treatment of brackish groundwater. This is somewhat expected due to the larger amount of organic molecules dissolved in the wastewater samples (Table 3.2). In particular, the water fluxes measured after 8 h of filtration test with samples from site B were 75-80% of the initial flux, regardless of the nature of the draw solution. This is one of the major differences when filtering the two real waters: when brackish water from site A was used as feed stream, fouling is promoted mostly by using magnesium chloride as draw solution. However, fouling from the feed stream from site B is less affected by the nature of the draw solute. This observation may be rationalized with larger magnesium flux into the feed in the case of site A, which may interact with some of the components of the brackish water. The passage of magnesium ion through the membrane may be caused by bidirectional ion transport mechanisms and exchanges with sodium ions contained at higher levels in water A compared to water B.

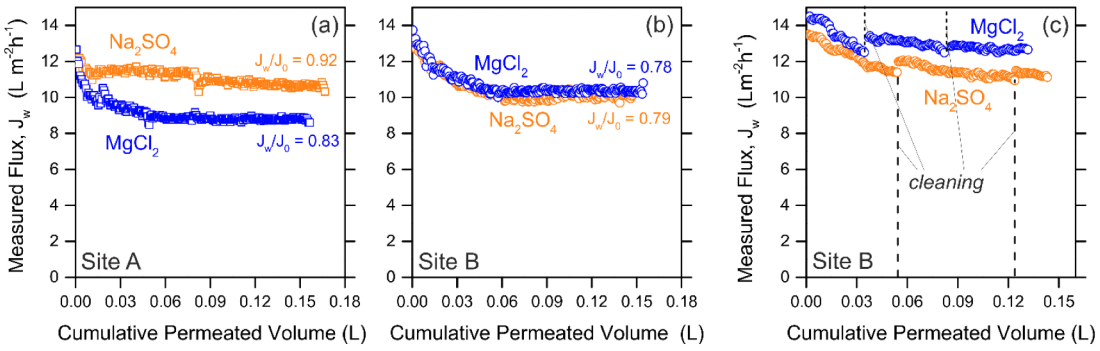

Figure 3.5: *Flux profile in forward osmosis fouling tests as a function of cumulative permeated volume with imposed initial flux of 13-14 L m^{-2} h^{-1}. Flux decline observed with the feed solution from (a) site A and (b) site B. (c) Flux decline and recovery following cleaning with the wastewater effluent from site B; cleaning times are indicated by dash lines. Blue and orange points depict data obtained with $MgCl_2$ and Na_2SO_4 as draw solutes, respectively. The value of flux at the end of the test, divided by the initial flux, J_w/J_0, is also reported near each curve. In these tests, the driving force was kept constant by addition of a concentrated draw solution and DI water in the draw and feed container, respectively.*

It should be considered that the results observed in Figure 3.5 overestimate the true prevalence of flux decline due to fouling. No provision was taken to minimize fouling during lab tests, viz., spacers were not used, the cross-flow velocity was relatively low, and the initial flux, which is an important parameter correlated to the extent of fouling [174], was intentionally in the higher range of typical FO fluxes. In order to have a better understanding of the real influence of fouling on FO performance, simple and mild physical cleaning was performed in the case of wastewater from site B used as feed solution. Beneficial effects were observed when physical cleaning was adopted, with partial recovery of the flux previously loss. Moreover, water fluxes were generally higher compared to the experiments performed without cleaning, regardless of the nature of the draw solution. Similar results were observed in previous studies, where researchers verified the possibility to partially recover the previously lost water flux thanks to physical cleaning using pure water [174, 175]. If the cross-velocity is increased at larger rates during real operation, even more important effects of cleaning are expected, at the expense of some energy costs. Additional observations can be made from the data in Figure 3.5. Firstly, the observed decrease in flux at the onset of the tests may be also partly attributed to system equilibrium. Moreover, all the fluxes shown in the three graphs tended to stabilize within roughly one third of the experiment duration, suggesting that fouling may be minimal during operation after an initial influence on productivity.

Fouling propensity and behavior

In order to analyze even more in detail the fouling behavior in forward osmosis in the light of a full-scale design, further experiments were performed with wastewater from site B used as feed solution and for longer filtration times. The purpose is to evaluate the FO flux decline and its potential discrepancy with respect to the water flux modeled through equation 3.1 used for the design of the FO plant in the coupled system. Experimentally, each test was carried out in two phases, i.e., by keeping constant the nominal driving force for the first 8 h of operation and without making any additions/adjustments for the rest of the test. To emphasize the detrimental effect of fouling, each experiment was performed in a very challenging condition in terms of hydrodynamics, viz., a low Reynolds number, no spacers used, and an initial water flux was always higher than the highest values simulated for each respective draw solute. Experiments were performed not only with $MgCl_2$ and Na_2SO_4, but also with $MgSO_4$, $CaCl_2$, and NaCl as draw solutions in order to evaluate the influence of different ionic species on the fouling behavior. Results are presented in Figure 3.6 where, for each draw solute, the experimental flux decline is compared to the modeled one, the latter representing the change in water flux in time due to solely the loss of driving force. The real contribution to flux decline due to fouling can hence be inferred from the difference between the two profiles.

Looking at the profiles presented in each graph in Figure 3.6, it can be stated that the model strongly agrees with the initial experimental water flux values for all the draw solutions. The model does not include any adjustable parameter and represents the development of equation 3.1, accounting for the measured and known values of mass transfer coefficients and membrane transport properties. With a fixed initial osmotic pressure, the FO flux varied significantly depending on the draw solute employed. Each draw solute indeed presents different characteristics, due to differences in B and D values [158, 176]. NaCl produced the largest initial flux, mostly attributed to its high diffusion coefficient in water, which thwarts the effects of internal concentration polarization. In general, it can be stated that the initial water flux has some influence on the extent of fouling, as a larger value of initial flux implies a larger flux reduction. However, this is not the only factor at play. Comparing the results obtained with draw solutions composed by same anion species, it can be observed that:

1. $MgSO_4$ caused more fouling-related flux reduction compared to Na_2SO_4, despite the latter producing a higher initial flux

2. $MgCl_2$ and NaCl showed similar fouling propensity even if NaCl resulted in significantly larger values of initial FO flux

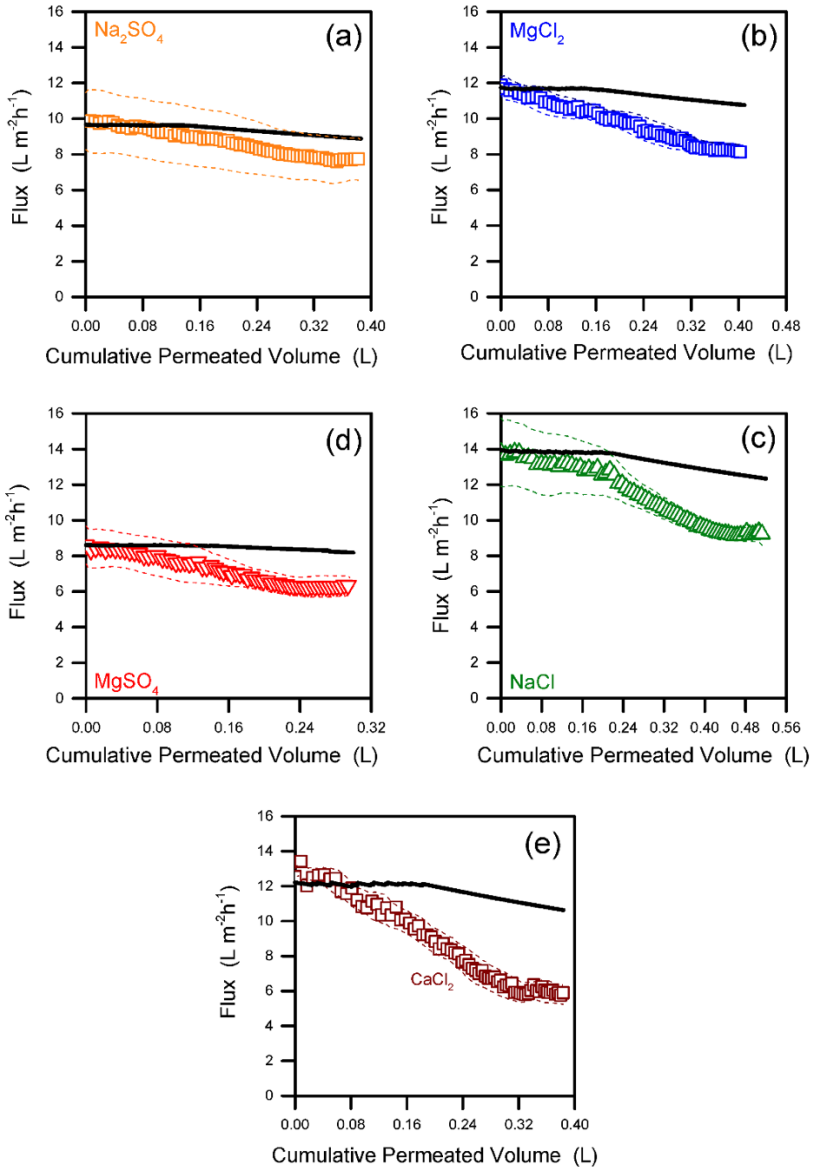

Figure 3.6: *Results of the fouling experiments performed with (a) sodium sulfate, (b) magnesium chloride, (c) sodium chloride, (d) magnesium sulfate and (e) calcium chloride as draw solutes, at initial draw osmotic pressure of 18.4 bar. The open points represent the average values of flux from duplicate or triplicate experiments. The dashed lines are the flux values with addition and subtraction of the standard deviation. The black lines depict the modelled fluxes, computed considering the sole reduction due to the loss of driving force in the batch tests, i.e., dilution of the draw and concentration of the feed solutions following water permeation.*

Overall, the results suggest that chloride ions have a greater influence on flux decline compared to sulfate ions. This can be rationalized considering the more accentuated tendency of chloride to diffuse into the feed solution. This facilitates

the formation of a denser cake [177]. Also, magnesium is much more prone to produce flux decline than sodium. This is also in accordance with literature reports, discussing the role of Mg^{2+} in increasing the attachment of organic compounds to the membrane [178, 179]. Moreover, due to their ability to interact with negatively charged species, multivalent cations are known to enhance the membrane fouling propensity [180]. A definite proof of this phenomenon is clearly visible for tests comprising $CaCl_2$ as draw solute, associated with very large flux declines ($> 50\%$), as presented in figure 3.6e [180, 181].

Another interesting observation can be made looking at the results: a near stable flux was achieved around the end of the tests performed with three out of the four draw solutes, suggesting the possible existence of a critical, sustainable or threshold flux, as in accordance with previous authors [182, 183, 184, 185, 186]. The mechanism underlying this phenomenon is constantly under debate among researchers. However, the flux stabilization suggests that there may be a limitation factor that slows down or nearly prevents further fouling after a certain point. This phenomenon may be rationalized considering the kinetics of foulant deposition onto a pre-deposited foulant layer which may be related to a constraint in building up the foulant cake layer above a certain thickness or due to foulant-foulant interactions. This observation is quite noteworthy, implying that the water flux may be trusted not to cross below a threshold value, which is most likely related to the complex system consisting of the membrane, the draw solute, the hydrodynamics, and the feed composition. Based on our results, the minimum flux with Na_2SO_4 may be only about 10% lower than the modelled flux (Figure 3.6a). Overall, the effect of fouling was not overly harsh, also considering that, as stated by the results reported before (section 3.3.3), simple physical cleanings allowed the recovery of the near totality of the initial flux. Certainly, the overall results reported so far suggest the interesting behaviour of the forward osmosis process in terms of fouling resistance.

3.3.4 Design of the forward osmosis - nanofiltration hybrid system

In section 3.3.2 the results obtained through the high-recovery experiments suggested the potential employment of the hybrid forward osmosis – nanofiltration system to reclaim the contaminated water from site A and B. However, the performance obtained in forward osmosis strongly underlined the differences between treating brackish water sources and wastewater effluents. The FO performance was strongly enhanced when wastewater source, with low level of salinity, is filtered, compared to the system running with brackish water as feed solution. Higher water fluxes across the membrane were obtained, thus suggesting larger recovery rates achievable in real units. Moreover, fouling resistance behaviour was observed by FO, with experiments showing promising results even in the presence of a significant concentration of dissolved organic compounds in solution. Therefore, in this

section we propose a design of the full-scale FO-NF system for the treatment of a low salinity feed water with medium-high content of organics (such as the wastewater samples collected from site B). This analysis wants to represent a step forward toward the implementation of the coupling technology and as a strategy to further evaluate the feasibility of forward osmosis in general.

The system is studied and optimized using a single salt draw solution of sodium sulfate or magnesium chloride. Two are the first critical parameters to select in order to design the full-scale system:

1. The nominal concentration of the draw solution
2. The flow rate of the draw solution entering the FO step

Now, since in real operation the flow rate of the feed solution is usually fixed and related to the site characteristics, the second parameters can be expressed as the ratio between the flow rates of the draw solution and the feed solution, referred to as DS:FS ratio. It is important to keep in mind that an increase of both design parameters would result in higher performance of the FO unit, with higher water fluxes and recovery values (results later). However, on the other hand, a larger flow rate of draw solution characterized by a large final solute concentration would translate into high capital and operational costs for the nanofiltration regeneration stage. Clearly, there is an optimized configuration that ensues from this trade-off.

To study the FO performance in terms of average flux and recovery rate, specific module-scale simulations were performed. Based on mass and volume balances and on the membrane transport properties, a co-current FO configuration was assumed to carry out each simulation. The overall results are presented in Figure 3.7. As expected, the FO performance is enhanced when increasing both the influent draw solution osmotic pressure (π_D) and the DS:FS ratio. Nevertheless, the performance is not significantly improved above certain thresholds. This implies that the optimization procedure would maximize the design parameters up until the magnitude of the first derivative of the curves in Figure 3.7 starts decreasing significantly. For this specific feed water, the best FO configuration seems to be associated to an influent π_D of 15 bar and an influent DS:FS ratio of 1.5:1. In order to have a better understanding of the reason under these selections, the modelling results presented in Figure 3.8a and 3.8b can be observed and discussed. In terms of water productivity or recovery, no significant benefits would be obtained from a DS:FS ratio larger than 1.5. Besides, an influent $\pi_D > 15$ bar would increase the average flux but without improving the overall recovery. In addition, Figure 3.8a and 3.8b show that the utilization of magnesium chloride as draw solution would increase the average fluxes achievable in FO, compared to the employment of sodium sulfate. This may be rationalized considering the higher diffusion coefficient of the magnesium based solute than the sodium based one.

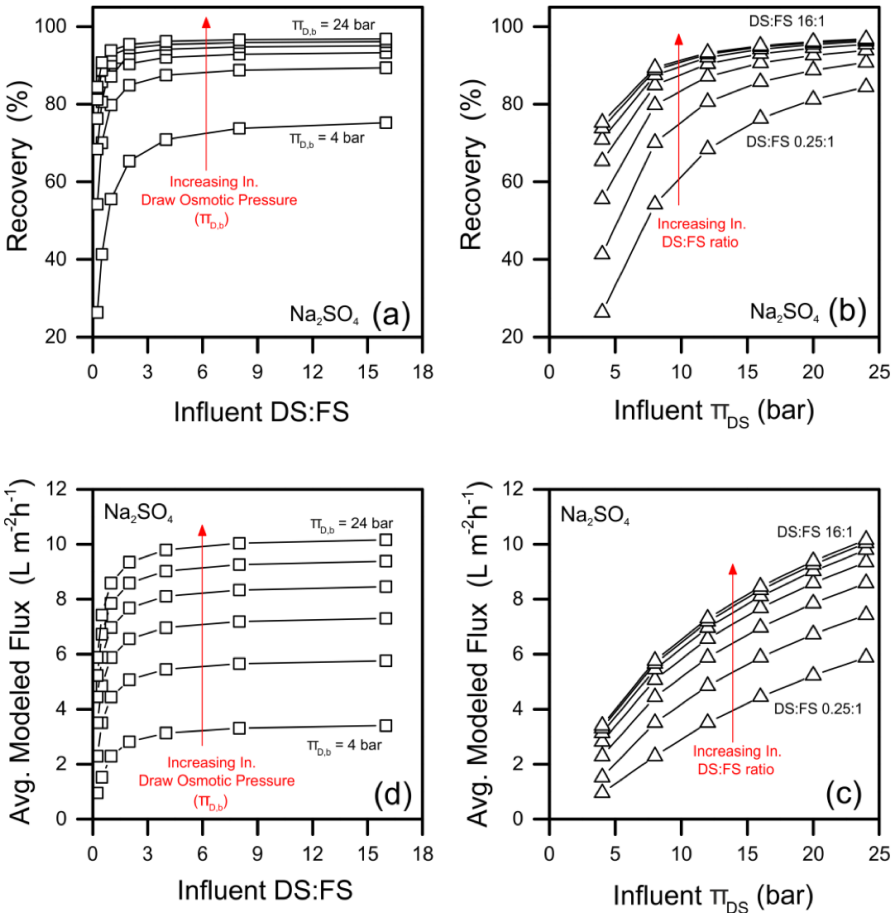

Figure 3.7: *Preliminary simulations performed to select the forward osmosis operational parameters. The FO system was modelled in co-current mode. FO system recovery rates (squares) and average water fluxes (triangles), presented as a function of (a and d) influent DS:FS ratio and (b and c) influent draw osmotic pressure. The results are presented for sodium sulfate as draw solute. Solid lines are intended as guide for the eyes only.*

Once the influent draw osmotic pressure (equal to 15 bar) and the DS:FS ratio (equal to 1.5:1) were selected, the local water fluxes along the hypothetical FO module were calculated. The results are presented for both the $MgCl_2$ and Na_2SO_4 draw solutes (Figure 3.8c). Fluxes are plotted as a function of the recovery rate and of the cumulative permeated volume, both increasing along the modules. The simulations were halted for flux values lower than 5 LMH, as operating below this threshold would not be advantageous, resulting in a large increase of needed membrane area without a significant increase in the overall recovery rate. The recovery values are thus equal to 85% in the case of magnesium chloride and 78% with sodium sulfate as draw solutes.

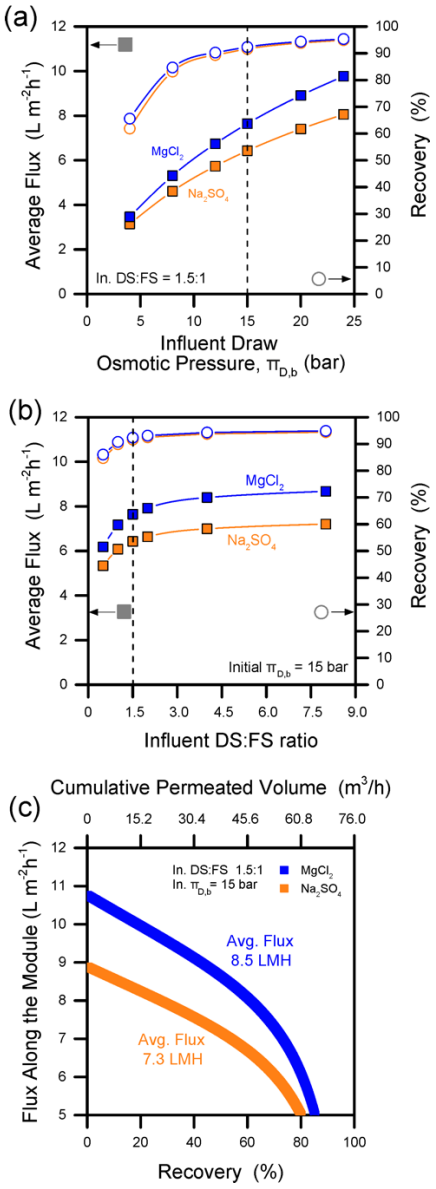

Figure 3.8: *Choice of the forward osmosis operational parameters. The FO system was modelled in co-current mode. FO system recovery values (empty points) and related average modelled fluxes (full square points) as a function of (a) influent DS:FS ratio and (b) of influent draw osmotic pressure. Based on preliminary simulations presented in the Figure 3.7, an influent DS osmotic pressure of 15 bar and an influent DS:FS ratio of 1.5:1 were considered, indicated by dashed lines. The curves in (c) are those modelled for the final FO system, considering the loss of driving force across the FO modules. Blue refers to $MgCl_2$ and red to Na_2SO_4. Solid lines in a) and b) are intended as guide for the eyes only.*

It is important to consider that, while the transport-limiting concentration polarization phenomena are included in the system modelling, these simulations do

not account for the effect of fouling or of membrane degradation in time. Moreover, the system modelling was performed based on a value of the mass transport coefficient representative our lab-scale system, 68 LMH, which is certainly lower than that prevailing in real modules. Therefore, the external concentration polarizations would be reasonably lower in real operation and water fluxes consistently higher.

The feasible configuration of the entire hybrid forward osmosis – nanofiltration system is presented in Figure 3.9. Thanks to the higher average flux achievable in FO with $MgCl_2$, this treatment step would require 10% less membrane area compared to the FO unit operated with Na_2SO_4. The nanofiltration post-treatment stages were designed to regenerate the draw solution to achieve the desired influent osmotic pressure of 15 bar in the FO stage. The NF stage is significantly different depending on the type of DS. The NF270 and NF90 membranes were deployed to recover Na_2SO_4 and $MgCl_2$, respectively. The overall configuration of the two nanofiltration plants is similar, working at almost equivalent applied pressure (i.e., 21.5 bar and 21.2 bar for the NF270 and the NF90, respectively) and comprising both one stage and one pass. However, thanks to the higher permeance of the NF270, the NF system designed to recover the Na_2SO_4 requires less membrane are compared to the NF unit operated with the NF90 to recover the $MgCl_2$. This is visible looking at the set-up of the two nanofiltration units. Despite both are designed to work with seven modules in series for each vessel, the NF plant used to recover the sodium sulfate draw solution requires eleven parallel pressure vessels, while twelve vessels are needed for running the NF90 unit used to recover magnesium chloride DS.

Overall, the simulated quality of the permeates would be very high (not shown), with ions concentration always below the stricter limits imposed for unrestricted irrigation. This is in accordance with our experimental results obtained during the high-recovery tests. In addition, equation 3.2 was used to simulate the loss of the reverse salt fluxes in FO. Results suggested that less than 0.1% of the mass of draw solute may be lost for every hour of operation. Moreover, taking into account a conservative value of 98% for the overall observed solute rejection in nanofiltration, it can be stated that roughly 0.9% of the mass of draw solute passes into the permeate every hour in this stage. These figures yield a total needed replenishment of approximately 0.42/0.21 kg of Na_2SO_4/$MgCl_2$ for each m^3 of recycled draw solution or, equivalently, 48/24 kg of replenishment for every hour of operation, in comparison with a total amount of solutes of 4.9 and 2.4 tonn entering the FO unit every hour.

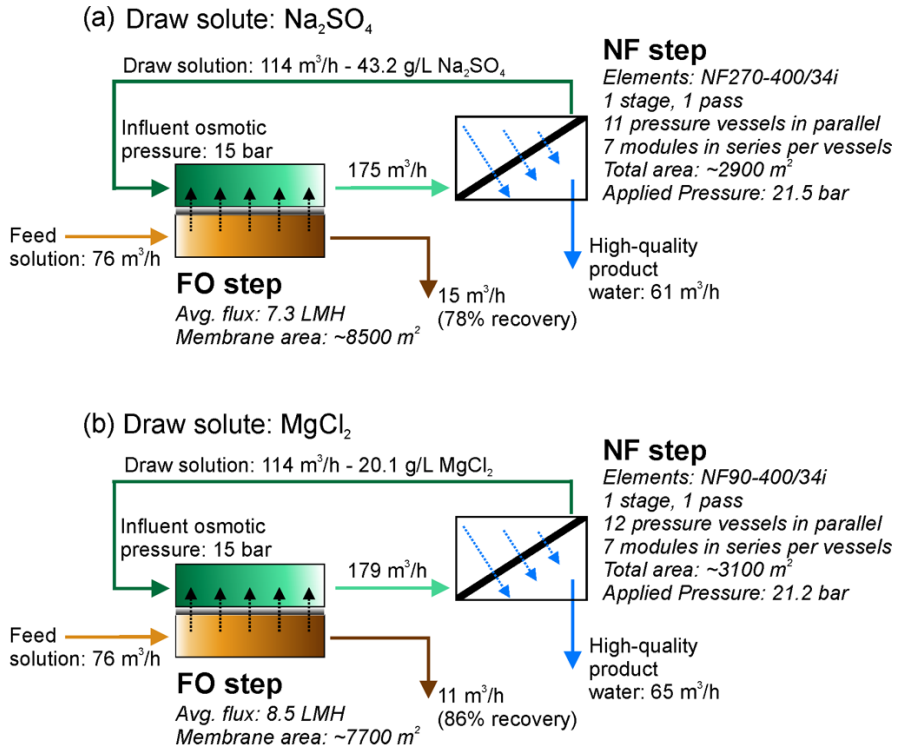

Figure 3.9: *Configurations of the forward osmosis-nanofiltration hybrid system designed to treat the real wastewater with (a) sodium sulfate and (b) magnesium chloride as draw solute. The nanofiltration stage was designed to be operated with the NF270 and NF90 membranes, respectively.*

Co-current vs. counter-current configuration

To further understand the influence of operational parameters and propose better configurations for the full-scale design, FO module-scale simulations were also performed in counter-current configuration. Therefore, the co- and counter-current modes were compared for some chosen configurations. Firstly, the water flux in FO was simulated as a function of the membrane area required in both co-current and counter-current mode. Both the relevant systems were modelled to treat the wastewater investigated in this study, considering the same FO boundary conditions, i.e., the same DS:FS ratio equal to 1.5:1 and the same initial π_D equal to 15 bar, and imposing a recovery of 92%. Results are presented in Figure 3.10a. With a counter-current configuration, higher average fluxes can be achieved in FO with a consequent reduction of the membrane area. This result is in accordance with Deshmukh et al. [75].

Further simulations were performed by varying the influent DS:FS ratio to analyze the differences between a co-current and a counter-current configuration in FO. Results are presented in Figure 3.10c and 3.10d. It can be observed that

the counter-current configuration presents a generally more uniform flux along the membrane module. However, at one end of the system, and in particular where the feed solution is highly concentrated, the flux is much lower than along the rest of the modules. This phenomenon becomes more pronounced as the DS:FS ratio increases. Co-current configuration instead, shows a more linearly flux decline along the modules. We can hence conclude that a lower degree of freedom appears to exist for the DS:FS parameter in the counter-current mode.

These considerations have important implications for a hypothetical treatment plant. Firstly, counter-current configuration does seem generally advantageous in terms of FO performance. Also, the fouling behaviour may be affected by the FO mode of operation. Previous studies suggested less severe fouling in the case of counter-current configuration compared to the co-current mode [187]. This result is sensible given that uniform fluxes more similar to the average value characterize the counter-current configuration. As fouling is somewhat proportional to flux via the permeation drag toward the membrane interface, high flux values at the influent end of the co-current configuration may result in exacerbated fouling at this end of the modules.

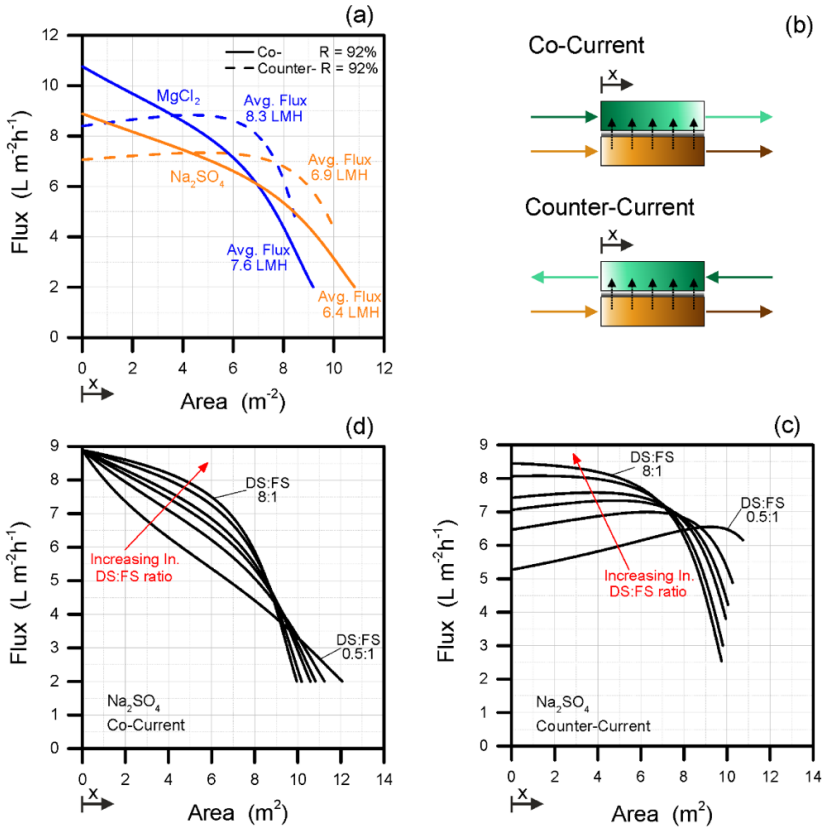

Figure 3.10: *FO stage performance in co- vs. counter-current mode. (a) Water flux along the FO modules in the systems from Figure 3.9, for the (solid lines) co-current and (dashed lines) counter-current configurations. (c-d) Water fluxes along the modules at varying DS:FS ratios with influent π_D equal to 15 bar. The two configurations are schematically depicted in (b).*

3.4 Conclusion

This study represents a second example of the research pathway to follow in order to analyze a specific process/application of a membrane-based separation technology from the "micro" to the "macro" scale (lab-to-full scale approach). In this study, an innovative forward osmosis – nanofiltration system was evaluated as a feasible technology to treat brackish groundwater and a wastewater effluent with the aim to produce high-quality water for beneficial reuse purposes. The study was first performed at the lab scale, with experiments carried out to evaluate the performance of the forward osmosis as feed water treatment step and the nanofiltration as post-recovery process. The system design of the coupling technology was modelled and discussed afterwards together with an in-depth study of the fouling propensity in FO. The overall results suggested the following:

1. The combined technology allows the treatment of the two contaminated liquid streams by producing waters with quality comparable to potable sources and suitable for unrestricted irrigation

2. The forward osmosis – nanofiltration system is more suitable to treat complex water matrices, such as wastewater effluents with high organic content and low salinity levels, compared to brackish groundwater. Indeed, with the former feed solution, average higher water fluxes in FO can be achieved working with a lower osmotic pressure of the draw solution with consequent reduction of membrane area required.

3. Reverse salt flux in FO and incomplete solute rejection in NF of the draw solutions must be accounted for as operational management issues. Experimental results showed non-negligible losses of draw solutes during operation with the stoichiometry of the two ionic species composing the initial draw solution slightly off following regeneration.

4. The sensitivity analysis performed on the forward osmosis step showed the importance of two parameters: (i) the nominal concentration of the draw solution and (ii) its relative flow rate in the process performance. By varying these two parameters, an optimum FO configuration can be designed for each specific application. In the case of the treatment of the wastewater considered in this project, the best FO configuration was associated with an influent DS osmotic pressure of 15 bar and a DS:FS ratio of 1.5:1.

5. Full scale design of the FO-NF system for wastewater treatment showed that an overall 80%/85% recovery can be achieved by the utilization of $Na_2SO_4/MgCl_2$ as draw solutes, with nanofiltration recovery step designed to work with similar energy supply with NF270 and NF90 membrane modules.

6. Module scale analysis of the forward osmosis treatment step showed that, to reduce the overall membrane area, a counter-current configuration should be adopted.

7. Preliminary fouling and cleaning experiments suggested that the flux decline due to fouling may be low and mostly reversible during operation. However, a more in-depth study showed that fouling would be enhanced by using chloride- and magnesium-based draw solutes. Overall, when simulating the performance of a forward osmosis full scale system, in order to account for fouling influence in operating conditions, a safety factor roughly equal to 0.9 may be accounted to estimate average fluxes and recovery ratios at full-scale starting from lab-scale results.

To conclude, the forward-osmosis – nanofiltration system would represent a valuable alternative and innovative technology for the production of high-quality water from complex aqueous streams with high organic matter concentration and low salinity contents, with salinity representing a limitation for the filtration process performance. Thanks to the multi-barrier system, the concentration of the contaminants in the water product would respect the stringent limits applied for water re-use. However, it is fundamental to perform an in-depth study of the membrane process performance depending on the draw solution and system requirements. Higher recovery rates of a smaller system footprint may be achieved with a counter-current configuration. Compared to conventional filtration processes, fouling would also not represent a major issue, if periodical physical cleanings are performed. However, the management of the re-concentrated draw solution and of the concentrated wastewater effluent may have a strong impact in real plant application and maintenance. Due to the intrinsic characteristics of the membranes, the draw solution should be replaced periodically and disposed of. Specific treatment processes should be accounted for the treatment of the exhausted draw solution, possibly with desalination coupled with crystallization technologies, thus potentially recovering the minerals. The correct management of the wastewater effluent may comprise biological and physico-chemical treatments if the salinity is sufficiently low. Otherwise, as specified in previous sections, further desalination steps should be applied for ion removal.

Chapter 4

Final concluding remarks and perspectives

As freshwater demand is increasing worldwide, better management of water and wastewater becomes a critical task for global sustainable development. Among the various water/wastewater treatment processes, membrane-based separation systems represent valuable alternatives to reclaim high-quality water from contaminated streams. Thanks to their high selectivity toward a wide range of contaminants, established technologies such as reverse osmosis and nanofiltration, and innovative processes like forward osmosis and membrane distillation, are continuously studied and analysed with the aim to implement improved engineering water treatment solutions. Within this goal, this thesis presented two innovative processes/applications for membrane separation systems to be employed to extract high-quality water from contaminated/unconventional streams. In the first case, nanofiltration is evaluated as feasible solution to produce drinking water from chromium-contaminated sources. The second case study analysed the implementation of an innovative system where forward osmosis is coupled with nanofiltration to reclaim high-quality water from real brackish groundwater sample and from real wastewater sample.

The results presented in this manuscript refer to specific membrane applications. However, the methodological approach of this dissertation involved the initial evaluation of the processes in lab experimentation; this phase was followed by a streamlined modelling investigation to evaluate the best operating conditions for the upscaling of the processes; a pilot study then followed for one of the two case studies, which were both completed with a proposal for a full-scale design, accompanied with some economic and environmental analyses. One of the key findings of this work was that such lab-to-full scale approach is very valuable and that, when appropriately designed, lab-scale experiments provide reliable key results to inform the subsequent upscaling work.

Furthermore, this approach allowed to draw some interesting conclusions for both the specific systems investigated in this work and for membrane applications in general:

1. Nanofiltration represents a valuable alternative to achieve low contaminant concentrations in potable water, compatible with the increasingly stringent legislative limits (such as the new limit for the hexavalent chromium). Considering the firsy case study, adequate Cr rejection was achieved by employing either loose or tight NF membranes by filtering real water samples of diverse chemical composition. However, the performance of loose NF membranes can be strongly compromised by the presence of ions in solution, mostly divalent cations. Moreover, high concentration of oxidizing agent in solution, such as hexavalent chromium itself, would affect the lifetime of the membranes. Preliminary experimental analyses seem crucial to evaluate the choice of the most promising NF membrane to be applied for each specific application before implementing pilot/large installations.

2. Nanofiltration may represent a robust technology to produce potable water from contaminated drinking water sources (such as groundwater), to be applied as a stand-alone system, easily adjustable depending on the inlet flow rate and with minimal addition of chemical compounds in solution. The results at the pilot scale suggested that periodical chemical cleanings should be performed to avoid irreversible losses in membrane performance. While this topic is not discussed in this thesis, renewable energy sources may be integrated into the energy supply system, thus lowering the overall environmental impact of the NF process.

3. Forward osmosis may represent a valuable technology for the treatment of complex water matrices, such as wastewater with low salinity sources and high organic content. In this latter case, system-scale modelling suggested that an FO system running with either $MgCl_2$ or Na_2SO_4 would be able to achieve large recovery rate (e.g., 85% in the case of the specific wastewater studied in this work). However, preliminary experiments are fundamental to identify the possible membrane performance and to predict the quality of the final product water. Moreover, diverse configurations should be analysed to identify the best operating conditions. The results obtained in this study suggest that a key role in the development of the FO-NF coupled technology is represented by three parameters: the (i) influent draw solution osmotic pressure, (ii) the draw solution to feed solution flow rate ratio, and (iii) the recovery target. Moreover, detailed analysis indicated that the size of the FO unit might be reduced by the employment of a counter-current configuration.

4. Nanofiltration may represent a robust solution as post-treatment system of the diluted draw solution obtained in FO. Choosing the right draw solutes,

NF may guarantee the extraction of high-quality water and the consequent complete re-concentration of the draw solution, to be further re-used in the FO filtration. The results presented in this manuscript suggest that the modular configuration and the size of the NF stage would strongly depend on the type of membranes employed to separate the draw solutes and water. Moreover, periodical change in composition of the draw solutes should be accounted for estimation of maintenance/operational costs.

For both the membrane processes/applications studied, full-scale membrane systems could be potentially realized. Nanofiltration plants can be implemented for the production of drinking water from chromium-contaminated sources. Different membranes can be employed depending on the characteristics of the aqueous solution and NF stand-alone plant may be preferred to other treatment trains based, e.g., ion-exchange resins. Thanks to its modularity and easy maintenance, a nanofiltration plant could be potentially installed also in remote areas. The results obtained from the second case study suggested instead that a full-scale FO-NF system may be employed to improve the performance of a conventional wastewater treatment train. Following the biological section, the FO-NF system would be capable of producing high-quality effluent readily available for further re-use (e.g., suitable for irrigation, livestock production, or for industrial applications). To enhance the process performance, an in-depth study of the possible FO-NF configuration must be performed. A long membrane lifetime may be guaranteed by periodical physical cleaning, with minimized chemical cleanings.

To conclude, the approach presented in this thesis can be generalized, representing a valuable method to evaluate diverse membrane-based treatment solutions. This approach would allow researchers to obtain a complete overview of the membrane process performance, without focusing solely on the "micro" or on the "macro" scale. Advantages and drawbacks of specific membrane applications can be thus evaluated, and important conclusions can be reached for the implementation of potential and innovative full-scale systems.

Bibliography

[1] https://www.who.int/news-room/fact-sheets/detail/drinking water. Drinking-water - world health organization. 2019.

[2] https://www.un.org/sustainabledevelopment/development agenda/. The sustainable development agenda. 2015.

[3] Mark W Rosegrant, Claudia Ringler, and Tingju Zhu. Water for agriculture: maintaining food security under growing scarcity. *Annual review of Environment and resources*, 34:205–222, 2009.

[4] Charlotte De Fraiture, David Molden, and Dennis Wichelns. Investing in water for food, ecosystems, and livelihoods: An overview of the comprehensive assessment of water management in agriculture. *Agricultural Water Management*, 97(4):495–501, 2010.

[5] Robert Alan Holland, Kate A Scott, Martina Flörke, Gareth Brown, Robert M Ewers, Elizabeth Farmer, Valerie Kapos, Ann Muggeridge, Jörn PW Scharlemann, Gail Taylor, et al. Global impacts of energy demand on the freshwater resources of nations. *Proceedings of the National Academy of Sciences*, 112(48):E6707–E6716, 2015.

[6] Karen Hussey, Jamie Pittock, et al. The energy-water nexus: Managing the links between energy and water for a sustainable future. 2012.

[7] Stephan Pfister, Annette Koehler, and Stefanie Hellweg. Assessing the environmental impacts of freshwater consumption in lca. *Environmental science & technology*, 43(11):4098–4104, 2009.

[8] Igor A Shiklomanov. Appraisal and assessment of world water resources. *Water international*, 25(1):11–32, 2000.

[9] MB Pescod. Wastewater treatment and use in agriculture. 1992.

[10] Amit Sonune and Rupali Ghate. Developments in wastewater treatment methods. *Desalination*, 167:55–63, 2004.

[11] P Cornel and B Weber. Water reuse for irrigation from waste water treatment plants with seasonal varied operation modes. *Water Science and Technology*, 50(2):47–53, 2004.

[12] Luciano Basto Oliveira, Andre Luiz Bufoni, Luiz Roberto Martins Pedroso, and Wagner Victer. Waste water treatment plant energy conversion technologies comparison. *International Journal of Innovation and Sustainable Development*, 13(3-4):410–430, 2019.

[13] Smita Raghuvanshi, Vikrant Bhakar, Chelikani Sowmya, and KS Sangwan. Waste water treatment plant life cycle assessment: treatment process to reuse of water. *Procedia CIRP*, 61:761–766, 2017.

[14] ND Tzoupanos and AI Zouboulis. Coagulation-flocculation processes in water/wastewater treatment: the application of new generation of chemical reagents. In *6th IASME/WSEAS International Conference Greece*, 2008.

[15] Gordon J Williams, Bahman Sheikh, Robert B Holden, Tom J Kouretas, and Kara L Nelson. The impact of increased loading rate on granular media, rapid depth filtration of wastewater. *Water research*, 41(19):4535–4545, 2007.

[16] S Rengaraj, Kyeong-Ho Yeon, and Seung-Hyeon Moon. Removal of chromium from water and wastewater by ion exchange resins. *Journal of hazardous materials*, 87(1-3):273–287, 2001.

[17] Reza Haghsheno, Ali Mohebbi, Hassan Hashemipour, and Amir Sarrafi. Study of kinetic and fixed bed operation of removal of sulfate anions from an industrial wastewater by an anion exchange resin. *Journal of hazardous materials*, 166(2-3):961–966, 2009.

[18] Jonas Margot, Luca Rossi, David A Barry, and Christof Holliger. A review of the fate of micropollutants in wastewater treatment plants. *Wiley Interdisciplinary Reviews: Water*, 2(5):457–487, 2015.

[19] Christine Hug, Nadin Ulrich, Tobias Schulze, Werner Brack, and Martin Krauss. Identification of novel micropollutants in wastewater by a combination of suspect and nontarget screening. *Environmental pollution*, 184:25–32, 2014.

[20] Wenfang Lin, Zhisheng Yu, Hongxun Zhang, and Ian P Thompson. Diversity and dynamics of microbial communities at each step of treatment plant for potable water generation. *Water research*, 52:218–230, 2014.

[21] Kaisa Vaaramaa and Jukka Lehto. Removal of metals and anions from drinking water by ion exchange. *Desalination*, 155(2):157–170, 2003.

[22] E Korngold, N Belayev, and L Aronov. Removal of arsenic from drinking water by anion exchangers. *Desalination*, 141(1):81–84, 2001.

[23] Samuel D Faust and Osman M Aly. *Adsorption processes for water treatment*. Elsevier, 2013.

[24] M Al-Shammiri and M Safar. Multi-effect distillation plants: state of the art. *Desalination*, 126(1-3):45–59, 1999.

[25] K Bourouni, MT Chaibi, and Lounes Tadrist. Water desalination by humidification and dehumidification of air: state of the art. *Desalination*, 137(1-3):167–176, 2001.

[26] Paolo Roccaro, Giuseppe Mancini, and Federico GA Vagliasindi. Water intended for human consumption—part i: Compliance with european water quality standards. *Desalination*, 176(1-3):1–11, 2005.

[27] Giuseppe Mancini, Paolo Roccaro, and Federico GA Vagliasindi. Water intended for human consumption—part ii: Treatment alternatives, monitoring issues and resulting costs. *Desalination*, 176(1-3):143–153, 2005.

[28] Amy L Lusher, Valentina Tirelli, Ian O'Connor, and Rick Officer. Microplastics in arctic polar waters: the first reported values of particles in surface and sub-surface samples. *Scientific reports*, 5:14947, 2015.

[29] Janet YM Tang and Beate I Escher. Realistic environmental mixtures of micropollutants in surface, drinking, and recycled water: herbicides dominate the mixture toxicity toward algae. *Environmental toxicology and chemistry*, 33(6):1427–1436, 2014.

[30] Nuri Eshoul, Brian Agnew, Mohammed Al-Weshahi, and Mohanad Atab. Exergy analysis of a two-pass reverse osmosis (ro) desalination unit with and without an energy recovery turbine (ert) and pressure exchanger (px). *Energies*, 8(7):6910–6925, 2015.

[31] Baltasar Peñate and Lourdes García-Rodríguez. Current trends and future prospects in the design of seawater reverse osmosis desalination technology. *Desalination*, 284:1–8, 2012.

[32] Kah Peng Lee, Tom C Arnot, and Davide Mattia. A review of reverse osmosis membrane materials for desalination—development to date and future potential. *Journal of Membrane Science*, 370(1-2):1–22, 2011.

[33] Richard W Baker et al. Overview of membrane science and technology. *Membrane technology and applications*, 3:1–14, 2004.

[34] Andrea Schaefer, Anthony G Fane, and T David Waite. *Nanofiltration: principles and applications*. Elsevier, 2005.

[35] Andriy E Yaroshchuk. Non-steric mechanisms of nanofiltration: superposition of donnan and dielectric exclusion. *Separation and purification Technology*, 22:143–158, 2001.

[36] Daniele Vezzani and Serena Bandini. Donnan equilibrium and dielectric exclusion for characterization of nanofiltration membranes. *Desalination*, 149(1-3):477–483, 2002.

[37] Xiao-Lin Wang, Toshinori Tsuru, Shin-ichi Nakao, and Shoji Kimura. The electrostatic and steric-hindrance model for the transport of charged solutes through nanofiltration membranes. *Journal of membrane science*, 135(1):19–32, 1997.

[38] Jianquan Luo and Yinhua Wan. Effects of ph and salt on nanofiltration—a critical review. *Journal of membrane Science*, 438:18–28, 2013.

[39] Z Beril Gönder, Semiha Arayici, and Hulusi Barlas. Advanced treatment of pulp and paper mill wastewater by nanofiltration process: Effects of operating conditions on membrane fouling. *Separation and Purification Technology*, 76(3):292–302, 2011.

[40] Sharmiza Adnan, Manh Hoang, Haunting Wang, Brian Bolto, Zongli Xie, et al. Recent trends in research, development and application of membrane technology in the pulp and paper industry. *Appita Journal: Journal of the Technical Association of the Australian and New Zealand Pulp and Paper Industry*, 63(3):235, 2010.

[41] C Tang and V Chen. Nanofiltration of textile wastewater for water reuse. *Desalination*, 143(1):11–20, 2002.

[42] JM Gozálvez-Zafrilla, D Sanz-Escribano, J Lora-García, and MC León Hidalgo. Nanofiltration of secondary effluent for wastewater reuse in the textile industry. *Desalination*, 222(1-3):272–279, 2008.

[43] François Zaviska, Patrick Drogui, Alain Grasmick, Antonin Azais, and Marc Héran. Nanofiltration membrane bioreactor for removing pharmaceutical compounds. *Journal of membrane science*, 429:121–129, 2013.

[44] Long D Nghiem, Andrea I Schäfer, and Menachem Elimelech. Removal of natural hormones by nanofiltration membranes: measurement, modeling, and mechanisms. *Environmental science & technology*, 38(6):1888–1896, 2004.

[45] Marco Minella, Nicola De Bellis, Andrea Gallo, Mattia Giagnorio, Claudio Minero, Stefano Bertinetti, Rajandrea Sethi, Alberto Tiraferri, and Davide Vione. Coupling of nanofiltration and thermal fenton reaction for the abatement of carbamazepine in wastewater. *ACS Omega*, 3(8):9407–9418, 2018.

[46] A Bruchet and JM Laine. Efficiency of membrane processes for taste and odor removal. *Water Science and Technology*, 51(6-7):257–265, 2005.

[47] Maryam Haddad, Takashi Ohkame, Pierre R Bérubé, and Benoit Barbeau. Performance of thin-film composite hollow fiber nanofiltration for the removal of dissolved mn, fe and nom from domestic groundwater supplies. *Water research*, 145:408–417, 2018.

[48] Kathleen Moons and Bart Van der Bruggen. Removal of micropollutants during drinking water production from surface water with nanofiltration. *Desalination*, 199(1-3):245–247, 2006.

[49] Akshay Deshmukh, Chanhee Boo, Vasiliki Karanikola, Shihong Lin, Anthony P Straub, Tiezheng Tong, David M Warsinger, and Menachem Elimelech. Membrane distillation at the water-energy nexus: limits, opportunities, and challenges. *Energy & Environmental Science*, 11(5):1177–1196, 2018.

[50] Xiaosheng Ji, Efrem Curcio, Sulaiman Al Obaidani, Gianluca Di Profio, Enrica Fontananova, and Enrico Drioli. Membrane distillation-crystallization of seawater reverse osmosis brines. *Separation and Purification Technology*, 71(1):76–82, 2010.

[51] Gayathri Naidu, Sanghyun Jeong, Youngkwon Choi, and Saravanamuthu Vigneswaran. Membrane distillation for wastewater reverse osmosis concentrate treatment with water reuse potential. *Journal of Membrane Science*, 524:565–575, 2017.

[52] Francesco Ricceri, Mattia Giagnorio, Giulio Farinelli, Giulia Blandini, Marco Minella, Davide Vione, and Alberto Tiraferri. Desalination of produced water by membrane distillation: Effect of the feed components and of a pretreatment by fenton oxidation. *Scientific reports*, 9(1):1–12, 2019.

[53] Zuoyou Zhang, Xuewei Du, Kenneth H Carlson, Cristian A Robbins, and Tiezheng Tong. Effective treatment of shale oil and gas produced water by membrane distillation coupled with precipitative softening and walnut shell filtration. *Desalination*, 454:82–90, 2019.

[54] Kerusha Lutchmiah, ARD Verliefde, Kees Roest, Luuk C Rietveld, and ER Cornelissen. Forward osmosis for application in wastewater treatment: a review. *Water research*, 58:179–197, 2014.

[55] Bryan D Coday, Pei Xu, Edward G Beaudry, Jack Herron, Keith Lampi, Nathan T Hancock, and Tzahi Y Cath. The sweet spot of forward osmosis: Treatment of produced water, drilling wastewater, and other complex and difficult liquid streams. *Desalination*, 333(1):23–35, 2014.

[56] Andrea Achilli, Tzahi Y Cath, Eric A Marchand, and Amy E Childress. The forward osmosis membrane bioreactor: a low fouling alternative to mbr processes. *Desalination*, 239(1-3):10–21, 2009.

[57] Jinsong Zhang, Winson Lay Chee Loong, Shuren Chou, Chuyang Tang, Rong Wang, and Anthony Gordon Fane. Membrane biofouling and scaling in forward osmosis membrane bioreactor. *Journal of membrane science*, 403:8–14, 2012.

[58] Dezhong Xiao, Chuyang Y Tang, Jinsong Zhang, Winson CL Lay, Rong Wang, and Anthony G Fane. Modeling salt accumulation in osmotic membrane bioreactors: implications for fo membrane selection and system operation. *Journal of Membrane Science*, 366(1-2):314–324, 2011.

[59] Wei Jie Yap, Jinsong Zhang, Winson CL Lay, Bin Cao, Anthony G Fane, and Yu Liu. State of the art of osmotic membrane bioreactors for water reclamation. *Bioresource technology*, 122:217–222, 2012.

[60] NT Hancock, MS Nowosielski-Slepowron, and LS Marchewka. Application of forward osmosis based membrane brine concentrators for produced water treatment. In *IDA World Congress, Tianjin, China*, pages 20–25, 2013.

[61] C Riziero Martinetti, Amy E Childress, and Tzahi Y Cath. High recovery of concentrated ro brines using forward osmosis and membrane distillation. *Journal of membrane science*, 331(1-2):31–39, 2009.

[62] Md Shahidul Islam, Sormin Sultana, Jeffrey R McCutcheon, and Md Saifur Rahaman. Treatment of fracking wastewaters via forward osmosis: Evaluation of suitable organic draw solutions. *Desalination*, 452:149–158, 2019.

[63] Mattia Giagnorio, Antonio Amelio, Henrik Grüttner, and Alberto Tiraferri. Environmental impacts of detergents and benefits of their recovery in the laundering industry. *Journal of Cleaner Production*, 154:593–601, 2017.

[64] Guo-dong Kang and Yi-ming Cao. Development of antifouling reverse osmosis membranes for water treatment: a review. *Water research*, 46(3):584–600, 2012.

[65] Nurasyikin Misdan, WJ Lau, and AF Ismail. Seawater reverse osmosis (swro) desalination by thin-film composite membrane—current development, challenges and future prospects. *Desalination*, 287:228–237, 2012.

[66] Shanxue Jiang, Yuening Li, and Bradley P Ladewig. A review of reverse osmosis membrane fouling and control strategies. *Science of the Total Environment*, 595:567–583, 2017.

[67] Guo-Rong Xu, Jiao-Na Wang, and Cong-Ju Li. Strategies for improving the performance of the polyamide thin film composite (pa-tfc) reverse osmosis (ro) membranes: Surface modifications and nanoparticles incorporations. *Desalination*, 328:83–100, 2013.

[68] Qian Yang, Kai Yu Wang, and Tai-Shung Chung. Dual-layer hollow fibers with enhanced flux as novel forward osmosis membranes for water production. *Environmental science & technology*, 43(8):2800–2805, 2009.

[69] Ngai Yin Yip, Alberto Tiraferri, William A Phillip, Jessica D Schiffman, and Menachem Elimelech. High performance thin-film composite forward osmosis membrane. *Environmental science & technology*, 44(10):3812–3818, 2010.

[70] Shihong Lin, Siamak Nejati, Chanhee Boo, Yunxia Hu, Chinedum O Osuji, and Menachem Elimelech. Omniphobic membrane for robust membrane distillation. *Environmental Science & Technology Letters*, 1(11):443–447, 2014.

[71] Zhangxin Wang, Deyin Hou, and Shihong Lin. Composite membrane with underwater-oleophobic surface for anti-oil-fouling membrane distillation. *Environmental science & technology*, 50(7):3866–3874, 2016.

[72] Alberto Tiraferri, Ngai Yin Yip, Anthony P Straub, Santiago Romero-Vargas Castrillon, and Menachem Elimelech. A method for the simultaneous determination of transport and structural parameters of forward osmosis membranes. *Journal of membrane science*, 444:523–538, 2013.

[73] Jirachote Phattaranawik, Ratana Jiraratananon, and Anthony G Fane. Heat transport and membrane distillation coefficients in direct contact membrane distillation. *Journal of membrane science*, 212(1-2):177–193, 2003.

[74] Chanhee Boo, Sangyoup Lee, Menachem Elimelech, Zhiyong Meng, and Seungkwan Hong. Colloidal fouling in forward osmosis: role of reverse salt diffusion. *Journal of Membrane Science*, 390:277–284, 2012.

[75] Akshay Deshmukh, Ngai Yin Yip, Shihong Lin, and Menachem Elimelech. Desalination by forward osmosis: Identifying performance limiting parameters through module-scale modeling. *Journal of membrane science*, 491:159–167, 2015.

[76] Meer AM Khan, S Rehman, and Fahad A Al-Sulaiman. A hybrid renewable energy system as a potential energy source for water desalination using reverse

osmosis: A review. *Renewable and Sustainable Energy Reviews*, 97:456–477, 2018.

[77] Changming Ling, Yifei Wang, Chunhua Min, and Yuwen Zhang. Economic evaluation of reverse osmosis desalination system coupled with tidal energy. *Frontiers in Energy*, 12(2):297–304, 2018.

[78] Andrea Achilli, Tzahi Y Cath, Eric A Marchand, and Amy E Childress. The forward osmosis membrane bioreactor: a low fouling alternative to mbr processes. *Desalination*, 239(1-3):10–21, 2009.

[79] Andrea Achilli, Tzahi Y Cath, Eric A Marchand, and Amy E Childress. The novel osmotic membrane bioreactor for wastewater treatment. *Proceedings of the Water Environment Federation*, 2008(9):6210–6221, 2008.

[80] Gaetan Blandin, Arne RD Verliefde, Chuyang Y Tang, and Pierre Le-Clech. Opportunities to reach economic sustainability in forward osmosis–reverse osmosis hybrids for seawater desalination. *Desalination*, 363:26–36, 2015.

[81] Jung Eun Kim, Sherub Phuntsho, Laura Chekli, Joon Yong Choi, and Ho Kyong Shon. Environmental and economic assessment of hybrid fo-ro/nf system with selected inorganic draw solutes for the treatment of mine impaired water. *Desalination*, 429:96–104, 2018.

[82] Mattia Giagnorio, Barbara Ruffino, Daria Grinic, Sara Steffenino, Lorenza Meucci, Maria Chiara Zanetti, and Alberto Tiraferri. Achieving low concentrations of chromium in drinking water by nanofiltration: membrane performance and selection. *Environmental Science and Pollution Research*, 25(25):25294–25305, 2018.

[83] Mattia Giagnorio, Sara Steffenino, Lorenza Meucci, Maria Chiara Zanetti, and Alberto Tiraferri. Design and performance of a nanofiltration plant for the removal of chromium aimed at the production of safe potable water. *Journal of Environmental Chemical Engineering*, 6(4):4467–4475, 2018.

[84] Max Costa. Potential hazards of hexavalent chromate in our drinking water. *Toxicology and applied pharmacology*, 188(1):1–5, 2003.

[85] International Agency for Research on Cancer et al. Chromium, nickel and welding. *IARC monographs on the evaluation of carcinogenic risks to humans*, 49, 1990.

[86] Fourth Edition. Guidelines for drinking-water quality. *WHO chronicle*, 38(4):104–8, 2011.

[87] Maria Fuerhacker. Eu water framework directive and stockholm convention. *Environmental Science and Pollution Research*, 16(1):92–97, 2009.

[88] Repubblica Italiana. Modifiche all'allegato i del decreto legislativo 2 febbraio 2001, n. 31, attuazione della direttiva 98/83/ce relativa alla qualita' delle acque destinate al consumo umano. 2016.

[89] Mohamed Kheireddine Aroua, Fathiah Mohamed Zuki, and Nik Meriam Sulaiman. Removal of chromium ions from aqueous solutions by polymer-enhanced ultrafiltration. *Journal of hazardous materials*, 147(3):752–758, 2007.

[90] Françoise C Richard and Alain CM Bourg. Aqueous geochemistry of chromium: a review. *Water research*, 25(7):807–816, 1991.

[91] Vinod Kumar Gupta, Imran Ali, Tawfik A Saleh, MN Siddiqui, and Shilpi Agarwal. Chromium removal from water by activated carbon developed from waste rubber tires. *Environmental Science and Pollution Research*, 20(3):1261–1268, 2013.

[92] Gang Qin, Michael J McGuire, Nicole K Blute, Chad Seidel, and Leighton Fong. Hexavalent chromium removal by reduction with ferrous sulfate, coagulation, and filtration: A pilot-scale study. *Environmental science & technology*, 39(16):6321–6327, 2005.

[93] S Rengaraj, Kyeong-Ho Yeon, and Seung-Hyeon Moon. Removal of chromium from water and wastewater by ion exchange resins. *Journal of hazardous materials*, 87(1-3):273–287, 2001.

[94] Cristina-Veronica Gherasim and Gelu Bourceanu. Removal of chromium (vi) from aqueous solutions using a polyvinyl-chloride inclusion membrane: Experimental study and modelling. *Chemical engineering journal*, 220:24–34, 2013.

[95] Aysel Çimen, Fevzi Kılıçel, and Gülşin Arslan. Removal of chromium ions from waste waters using reverse osmosis ag and swhr membranes. *Russian Journal of Physical Chemistry A*, 88(5):845–850, 2014.

[96] Jolanta Bohdziewicz. Removal of chromium ions (vi) from underground water in the hybrid complexation-ultrafiltration process. *Desalination*, 129(3):227–235, 2000.

[97] Irena Korus and Krzysztof Loska. Removal of cr (iii) and cr (vi) ions from aqueous solutions by means of polyelectrolyte-enhanced ultrafiltration. *Desalination*, 247(1-3):390–395, 2009.

[98] Hiroaki Ozaki, Kusumakar Sharma, and Wilasinee Saktaywin. Performance of an ultra-low-pressure reverse osmosis membrane (ulprom) for separating heavy metal: effects of interference parameters. *Desalination*, 144(1-3):287–294, 2002.

[99] BAM Al-Rashdi, DJ Johnson, and Nidal Hilal. Removal of heavy metal ions by nanofiltration. *Desalination*, 315:2–17, 2013.

[100] Young Ku, Shi-Wei Chen, and Wen-Yu Wang. Effect of solution composition on the removal of copper ions by nanofiltration. *Separation and Purification Technology*, 43(2):135–142, 2005.

[101] Cristina-Veronica Gherasim and Petr Mikulášek. Influence of operating variables on the removal of heavy metal ions from aqueous solutions by nanofiltration. *Desalination*, 343:67–74, 2014.

[102] Salomé Gomes, Sofia A Cavaco, Margarida J Quina, and Licínio M Gando-Ferreira. Nanofiltration process for separating cr (iii) from acid solutions: Experimental and modelling analysis. *Desalination*, 254(1-3):80–89, 2010.

[103] P Religa, A Kowalik, and P Gierycz. Effect of membrane properties on chromium (iii) recirculation from concentrate salt mixture solution by nanofiltration. *Desalination*, 274(1-3):164–170, 2011.

[104] Wen-Ping Zhu, Shi-Peng Sun, Jie Gao, Feng-Jiang Fu, and Tai-Shung Chung. Dual-layer polybenzimidazole/polyethersulfone (pbi/pes) nanofiltration (nf) hollow fiber membranes for heavy metals removal from wastewater. *Journal of membrane science*, 456:117–127, 2014.

[105] Andrea Schaefer, Anthony G Fane, and T David Waite. *Nanofiltration: principles and applications*. Elsevier, 2005.

[106] Guo-Dong Kang, Cong-Jie Gao, Wei-Dong Chen, Xing-Ming Jie, Yi-Ming Cao, and Quan Yuan. Study on hypochlorite degradation of aromatic polyamide reverse osmosis membrane. *Journal of membrane science*, 300(1-2):165–171, 2007.

[107] Ho Bum Park, Benny D Freeman, Zhong-Bio Zhang, Mehmet Sankir, and James E McGrath. Highly chlorine-tolerant polymers for desalination. *Angewandte Chemie International Edition*, 47(32):6019–6024, 2008.

[108] Baisali Sarkar, N Venkateswralu, R Nageswara Rao, Chiranjib Bhattacharjee, and Vijay Kale. Treatment of pesticide contaminated surface water for production of potable water by a coagulation-adsorption-nanofiltration approach. *Desalination*, 212(1-3):129–140, 2007.

[109] J Radjenović, M Petrović, F Ventura, and D Barceló. Rejection of pharmaceuticals in nanofiltration and reverse osmosis membrane drinking water treatment. *Water research*, 42(14):3601–3610, 2008.

[110] Krešimir Košutić, Iva Novak, Laszlo Sipos, and Branko Kunst. Removal of sulfates and other inorganics from potable water by nanofiltration membranes of characterized porosity. *Separation and Purification Technology*, 37(3):177–185, 2004.

[111] Bart Van der Bruggen and Carlo Vandecasteele. Removal of pollutants from surface water and groundwater by nanofiltration: overview of possible applications in the drinking water industry. *Environmental pollution*, 122(3):435–445, 2003.

[112] AH Bannoud. Elimination of hardness and sulfate content in water by nanofiltration. *Desalination*, 137(1-3):133–139, 2001.

[113] Francois Vince, Emmanuelle Aoustin, Philippe Bréant, and François Marechal. Lca tool for the environmental evaluation of potable water production. *Desalination*, 220(1-3):37–56, 2008.

[114] Mafalda Pessoa Lopes, Cristina T Matos, Vanessa J Pereira, Maria João Benoliel, Maria Ermelinda Valério, Luís B Bucha, Alexandre Rodrigues, Ana I Penetra, Elisabete Ferreira, Vítor Vale Cardoso, et al. Production of drinking water using a multi-barrier approach integrating nanofiltration: A pilot scale study. *Separation and Purification Technology*, 119:112–122, 2013.

[115] N García-Vaquero, Eunkyung Lee, R Jiménez Castañeda, Jaeweon Cho, and JA López-Ramírez. Comparison of drinking water pollutant removal using a nanofiltration pilot plant powered by renewable energy and a conventional treatment facility. *Desalination*, 347:94–102, 2014.

[116] Ana Rita Costa and Maria Norberta De Pinho. Performance and cost estimation of nanofiltration for surface water treatment in drinking water production. *Desalination*, 196(1-3):55–65, 2006.

[117] Carsten Werner, Heinz Körber, Ralf Zimmermann, Stanislav Dukhin, and Hans-Jörg Jacobasch. Extended electrokinetic characterization of flat solid surfaces. *Journal of colloid and interface science*, 208(1):329–346, 1998.

[118] Long D Nghiem, Andrea I Schäfer, and Menachem Elimelech. Pharmaceutical retention mechanisms by nanofiltration membranes. *Environmental science & technology*, 39(19):7698–7705, 2005.

[119] María José López-Muñoz, Arcadio Sotto, Jesús M Arsuaga, and Bart Van der Bruggen. Influence of membrane, solute and solution properties on the retention of phenolic compounds in aqueous solution by nanofiltration membranes. *Separation and Purification Technology*, 66(1):194–201, 2009.

[120] Alexandre Bonton, Christian Bouchard, Benoit Barbeau, and Stéphane Jedrzejak. Comparative life cycle assessment of water treatment plants. *Desalination*, 284:42–54, 2012.

[121] Luigi Bruni and Serena Bandini. Studies on the role of site-binding and competitive adsorption in determining the charge of nanofiltration membranes. *Desalination*, 241(1-3):315–330, 2009.

[122] T David Waite. Chemical speciation effects in nanofiltration separation. *ChemInform*, 37(5):no–no, 2006.

[123] Maria Diná Afonso. Surface charge on loose nanofiltration membranes. *Desalination*, 191(1-3):262–272, 2006.

[124] Amy E Childress and Menachem Elimelech. Relating nanofiltration membrane performance to membrane charge (electrokinetic) characteristics. *Environmental science & technology*, 34(17):3710–3716, 2000.

[125] Gil Hurwitz, David J Pernitsky, Subir Bhattacharjee, and Eric MV Hoek. Targeted removal of dissolved organic matter in boiler-blowdown wastewater: integrated membrane filtration for produced water reuse. *Industrial & Engineering Chemistry Research*, 54(38):9431–9439, 2015.

[126] Alberto Tiraferri and Menachem Elimelech. Direct quantification of negatively charged functional groups on membrane surfaces. *Journal of Membrane Science*, 389:499–508, 2012.

[127] Razi Epsztein, Wei Cheng, Evyatar Shaulsky, Nadir Dizge, and Menachem Elimelech. Elucidating the mechanisms underlying the difference between chloride and nitrate rejection in nanofiltration. *Journal of Membrane Science*, 548:694–701, 2018.

[128] W Lincoln Hawkins. Polymer degradation. In *Polymer Degradation and Stabilization*, pages 3–34. Springer, 1984.

[129] Zhiwei Thong, Jie Gao, Jia Xi Zoe Lim, Kai-Yu Wang, and Tai-Shung Chung. Fabrication of loose outer-selective nanofiltration (nf) polyethersulfone (pes) hollow fibers via single-step spinning process for dye removal. *Separation and Purification Technology*, 192:483–490, 2018.

[130] Laura A Richards, Marion Vuachère, and Andrea I Schäfer. Impact of ph on the removal of fluoride, nitrate and boron by nanofiltration/reverse osmosis. *Desalination*, 261(3):331–337, 2010.

[131] Nidal Hilal, GJ Kim, and C Somerfield. Boron removal from saline water: a comprehensive review. *Desalination*, 273(1):23–35, 2011.

[132] Naïma Ben Frarès, Samir Taha, and Gerard Dorange. Influence of the operating conditions on the elimination of zinc ions by nanofiltration. *Desalination*, 185(1-3):245–253, 2005.

[133] Razi Epsztein, Evyatar Shaulsky, Nadir Dizge, David M Warsinger, and Menachem Elimelech. Role of ionic charge density in donnan exclusion of monovalent anions by nanofiltration. *Environmental science & technology*, 52(7):4108–4116, 2018.

[134] Eric M Vrijenhoek, Seungkwan Hong, and Menachem Elimelech. Influence of membrane surface properties on initial rate of colloidal fouling of reverse osmosis and nanofiltration membranes. *Journal of membrane science*, 188(1):115–128, 2001.

[135] Benjamin P Espinasse, So-Ryong Chae, Cyril Marconnet, Claire Coulombel, Claire Mizutani, Malik Djafer, Véronique Heim, and Mark R Wiesner. Comparison of chemical cleaning reagents and characterization of foulants of nanofiltration membranes used in surface water treatment. *Desalination*, 296:1–6, 2012.

[136] Wolfgang M Samhaber and Minh Tan Nguyen. Applicability and costs of nanofiltration in combination with photocatalysis for the treatment of dye house effluents. *Beilstein journal of nanotechnology*, 5(1):476–484, 2014.

[137] AI Schäfer, Anthony G Fane, and TD Waite. Cost factors and chemical pretreatment effects in the membrane filtration of waters containing natural organic matter. *Water Research*, 35(6):1509–1517, 2001.

[138] Nathan T Hancock, Nathan D Black, and Tzahi Y Cath. A comparative life cycle assessment of hybrid osmotic dilution desalination and established seawater desalination and wastewater reclamation processes. *Water research*, 46(4):1145–1154, 2012.

[139] Mattia Giagnorio, Francesco Ricceri, and Alberto Tiraferri. Desalination of brackish groundwater and reuse of wastewater by forward osmosis coupled with nanofiltration for draw solution recovery. *Water research*, 153:134–143, 2019.

[140] Mattia Giagnorio, Francesco Ricceri, Marco Tagliabue, Luciano Zaninetta, and Alberto Tiraferri. Hybrid forward osmosis–nanofiltration for wastewater reuse: System design. *Membranes*, 9(5):61, 2019.

[141] Richard G Taylor, Bridget Scanlon, Petra Döll, Matt Rodell, Rens Van Beek, Yoshihide Wada, Laurent Longuevergne, Marc Leblanc, James S Famiglietti, Mike Edmunds, et al. Ground water and climate change. *Nature climate change*, 3(4):322–329, 2013.

[142] Menachem Elimelech and William A Phillip. The future of seawater desalination: energy, technology, and the environment. *science*, 333(6043):712–717, 2011.

[143] Xiaolei Qu, Pedro JJ Alvarez, and Qilin Li. Applications of nanotechnology in water and wastewater treatment. *Water research*, 47(12):3931–3946, 2013.

[144] Yuansong Wei, Renze T Van Houten, Arjan R Borger, Dick H Eikelboom, and Yaobo Fan. Minimization of excess sludge production for biological wastewater treatment. *Water Research*, 37(18):4453–4467, 2003.

[145] Hale Ozgun, Recep Kaan Dereli, Mustafa Evren Ersahin, Cumali Kinaci, Henri Spanjers, and Jules B van Lier. A review of anaerobic membrane bioreactors for municipal wastewater treatment: integration options, limitations and expectations. *Separation and Purification Technology*, 118:89–104, 2013.

[146] George Skouteris, Daphne Hermosilla, Patricio López, Carlos Negro, and Ángeles Blanco. Anaerobic membrane bioreactors for wastewater treatment: a review. *Chemical Engineering Journal*, 198:138–148, 2012.

[147] Charis M Galanakis, Georgios Fountoulis, and Vassilis Gekas. Nanofiltration of brackish groundwater by using a polypiperazine membrane. *Desalination*, 286:277–284, 2012.

[148] Wenshan Guo, Huu-Hao Ngo, and Jianxin Li. A mini-review on membrane fouling. *Bioresource technology*, 122:27–34, 2012.

[149] N Akther, A Sodiq, A Giwa, S Daer, HA Arafat, and SW Hasan. Recent advancements in forward osmosis desalination: a review. *Chemical Engineering Journal*, 281:502–522, 2015.

[150] Bryan D Coday, Bethany GM Yaffe, Pei Xu, and Tzahi Y Cath. Rejection of trace organic compounds by forward osmosis membranes: a literature review. *Environmental science & technology*, 48(7):3612–3624, 2014.

[151] R Valladares Linares, Zhenyu Li, Sarper Sarp, Sz S Bucs, G Amy, and Johannes S Vrouwenvelder. Forward osmosis niches in seawater desalination and wastewater reuse. *Water research*, 66:122–139, 2014.

[152] Laura Chekli, Sherub Phuntsho, Ho Kyong Shon, Saravanamuthu Vigneswaran, Jaya Kandasamy, and Amit Chanan. A review of draw solutes in forward osmosis process and their use in modern applications. *Desalination and Water Treatment*, 43(1-3):167–184, 2012.

[153] Liwei Huang and Jeffrey R McCutcheon. Impact of support layer pore size on performance of thin film composite membranes for forward osmosis. *Journal of Membrane Science*, 483:25–33, 2015.

[154] Devin L Shaffer, Jay R Werber, Humberto Jaramillo, Shihong Lin, and Menachem Elimelech. Forward osmosis: where are we now? *Desalination*, 356:271–284, 2015.

[155] Jian Ren and Jeffrey R McCutcheon. A new commercial biomimetic hollow fiber membrane for forward osmosis. *Desalination*, 442:44–50, 2018.

[156] Dezhong Xiao, Weiyi Li, Shuren Chou, Rong Wang, and Chuyang Y Tang. A modeling investigation on optimizing the design of forward osmosis hollow fiber modules. *Journal of membrane science*, 392:76–87, 2012.

[157] Sherub Phuntsho, Seungkwan Hong, Menachem Elimelech, and Ho Kyong Shon. Forward osmosis desalination of brackish groundwater: Meeting water quality requirements for fertigation by integrating nanofiltration. *Journal of Membrane Science*, 436:1–15, 2013.

[158] Andrea Achilli, Tzahi Y Cath, and Amy E Childress. Selection of inorganic-based draw solutions for forward osmosis applications. *Journal of membrane science*, 364(1-2):233–241, 2010.

[159] Shuaifei Zhao, Linda Zou, and Dennis Mulcahy. Brackish water desalination by a hybrid forward osmosis–nanofiltration system using divalent draw solute. *Desalination*, 284:175–181, 2012.

[160] R Valladares Linares, Z Li, V Yangali-Quintanilla, N Ghaffour, G Amy, T Leiknes, and Johannes S Vrouwenvelder. Life cycle cost of a hybrid forward osmosis–low pressure reverse osmosis system for seawater desalination and wastewater recovery. *Water research*, 88:225–234, 2016.

[161] Beatriz Corzo, Teresa de la Torre, Carmen Sans, Raquel Escorihuela, Susana Navea, and Jorge J Malfeito. Long-term evaluation of a forward osmosis-nanofiltration demonstration plant for wastewater reuse in agriculture. *Chemical Engineering Journal*, 338:383–391, 2018.

[162] Nathan T Hancock, Pei Xu, Molly J Roby, Juan D Gomez, and Tzahi Y Cath. Towards direct potable reuse with forward osmosis: Technical assessment of long-term process performance at the pilot scale. *Journal of Membrane Science*, 445:34–46, 2013.

[163] Gaetan Blandin, Arne RD Verliefde, Joaquim Comas, Ignasi Rodriguez-Roda, and Pierre Le-Clech. Efficiently combining water reuse and desalination through forward osmosis—reverse osmosis (fo-ro) hybrids: a critical review. *Membranes*, 6(3):37, 2016.

[164] R Valladares Linares, Z Li, V Yangali-Quintanilla, N Ghaffour, G Amy, T Leiknes, and Johannes S Vrouwenvelder. Life cycle cost of a hybrid forward osmosis–low pressure reverse osmosis system for seawater desalination and wastewater recovery. *Water research*, 88:225–234, 2016.

[165] Huayong Luo, Qin Wang, Tian C Zhang, Tao Tao, Aijiao Zhou, Lin Chen, and Xufeng Bie. A review on the recovery methods of draw solutes in forward osmosis. *Journal of Water Process Engineering*, 4:212–223, 2014.

[166] Sourav Mondal, Robert W Field, and Jun Jie Wu. Novel approach for sizing forward osmosis membrane systems. *Journal of Membrane Science*, 541:321–328, 2017.

[167] Leonardo D Banchik, Adam M Weiner, Bader Al-Anzi, et al. System scale analytical modeling of forward and assisted forward osmosis mass exchangers with a case study on fertigation. *Journal of Membrane Science*, 510:533–545, 2016.

[168] Dinesh Attarde, Manish Jain, and Sharad Kumar Gupta. Modeling of a forward osmosis and a pressure-retarded osmosis spiral wound module using the spiegler-kedem model and experimental validation. *Separation and Purification Technology*, 164:182–197, 2016.

[169] Syed Muztuza Ali, Jung Eun Kim, Sherub Phuntsho, Am Jang, Joon Young Choi, and Ho Kyong Shon. Forward osmosis system analysis for optimum design and operating conditions. *Water research*, 145:429–441, 2018.

[170] Eric MV Hoek, Albert S Kim, and Menachem Elimelech. Influence of crossflow membrane filter geometry and shear rate on colloidal fouling in reverse osmosis and nanofiltration separations. *Environmental Engineering Science*, 19(6):357–372, 2002.

[171] Laura Chekli, Sherub Phuntsho, Ho Kyong Shon, Saravanamuthu Vigneswaran, Jaya Kandasamy, and Amit Chanan. A review of draw solutes in forward osmosis process and their use in modern applications. *Desalination and Water Treatment*, 43(1-3):167–184, 2012.

[172] Jeffrey R McCutcheon and Menachem Elimelech. Influence of concentrative and dilutive internal concentration polarization on flux behavior in forward osmosis. *Journal of membrane science*, 284(1-2):237–247, 2006.

[173] Ming Xie, Long D Nghiem, William E Price, and Menachem Elimelech. Toward resource recovery from wastewater: extraction of phosphorus from digested sludge using a hybrid forward osmosis–membrane distillation process. *Environmental Science & Technology Letters*, 1(2):191–195, 2014.

[174] Gaetan Blandin, Harm Vervoort, Pierre Le-Clech, and Arne RD Verliefde. Fouling and cleaning of high permeability forward osmosis membranes. *Journal of Water Process Engineering*, 9:161–169, 2016.

[175] Baoxia Mi and Menachem Elimelech. Organic fouling of forward osmosis membranes: fouling reversibility and cleaning without chemical reagents. *Journal of membrane science*, 348(1-2):337–345, 2010.

[176] Qingchun Ge, Mingming Ling, and Tai-Shung Chung. Draw solutions for forward osmosis processes: developments, challenges, and prospects for the future. *Journal of membrane science*, 442:225–237, 2013.

[177] Eric MV Hoek and Menachem Elimelech. Cake-enhanced concentration polarization: a new fouling mechanism for salt-rejecting membranes. *Environmental science & technology*, 37(24):5581–5588, 2003.

[178] Shan Zou, Yangshuo Gu, Dezhong Xiao, and Chuyang Y Tang. The role of physical and chemical parameters on forward osmosis membrane fouling during algae separation. *Journal of Membrane Science*, 366(1-2):356–362, 2011.

[179] Yining Wang, Filicia Wicaksana, Chuyang Y Tang, and Anthony G Fane. Direct microscopic observation of forward osmosis membrane fouling. *Environmental science & technology*, 44(18):7102–7109, 2010.

[180] Huajuan Mo, Kwee Guan Tay, and How Yong Ng. Fouling of reverse osmosis membrane by protein (bsa): effects of ph, calcium, magnesium, ionic strength and temperature. *Journal of Membrane Science*, 315(1-2):28–35, 2008.

[181] XUE Jin, Xiaofei Huang, and Eric MV Hoek. Role of specific ion interactions in seawater ro membrane fouling by alginic acid. *Environmental science & technology*, 43(10):3580–3587, 2009.

[182] Winson CL Lay, Tzyy Haur Chong, Chuyang Y Tang, Anthony G Fane, Jinsong Zhang, and Yu Liu. Fouling propensity of forward osmosis: investigation of the slower flux decline phenomenon. *Water science and technology*, 61(4):927–936, 2010.

[183] Yining Wang, Filicia Wicaksana, Chuyang Y Tang, and Anthony G Fane. Direct microscopic observation of forward osmosis membrane fouling. *Environmental science & technology*, 44(18):7102–7109, 2010.

[184] Shuaifei Zhao, Linda Zou, and Dennis Mulcahy. Effects of membrane orientation on process performance in forward osmosis applications. *Journal of membrane science*, 382(1-2):308–315, 2011.

[185] Ndeye Wemsy Diagne, Murielle Rabiller-Baudry, and Lydie Paugam. On the actual cleanability of polyethersulfone membrane fouled by proteins at critical or limiting flux. *Journal of membrane science*, 425:40–47, 2013.

[186] Robert W Field and Graeme K Pearce. Critical, sustainable and threshold fluxes for membrane filtration with water industry applications. *Advances in colloid and interface science*, 164(1-2):38–44, 2011.

[187] Junseok Lee, Bongchul Kim, and Seungkwan Hong. Fouling distribution in forward osmosis membrane process. *Journal of environmental sciences*, 26(6):1348–1354, 2014.

This Ph.D. thesis has been typeset by means of the TEX-system facilities. The typesetting engine was pdfLATEX. The document class was `toptesi`, by Claudio Beccari, with option `tipotesi=scudo`. This class is available in every up-to-date and complete TEX-system installation.